OPTIMUM DESIGN AND ANALYSIS OF TORSION SPRING USED IN SERIES ELASTIC ACTUATORS FOR REHABILITATION ROBOTS

A Thesis Submitted to
the Graduate School of Engineering and Sciences of
İzmir Institute of Technology
in Partial Fulfilment of the Requirements for the Degree of

MASTER OF SCIENCE

in Mechanical Engineering

by
Hacer İrem ERTEN

December 2021
İZMİR

ACKNOWLEDGMENTS

I would like to thank my thesis advisor, Prof. Hatice Seçil ARTEM for her dedicated support, motherly patience, guidance and encouraging approach through the learning and writing process of my master thesis.

I would like to give my sincere thanks to Associate Prof. Dr. Levent AYDIN, who has always supported me since I started my undergraduate education.

I would like to thank Associate Prof. Dr. Gökhan KİPER for including me in his valuable TÜBİTAK Project 219M483 and thanks to all members of Human-Robot Laboratory for their friendship and support.

I would like to thank my mother Nebahat ERTEN, my father Engin ERTEN and my sister Betül ERTEN, who have always been with me throughout my life, always supporting the decisions I made, encouraging and moralizing me not only during this study process but always. This thesis is dedicated to my family.

I am very thankful to my beloved friend Anıl KAPLAN for his love, caring, support, and motivation.

Last but not least, very special thanks go also to the many others that go unmentioned but have contributed in one way or another to the successful outcome of this study.

ABSTRACT

OPTIMUM DESIGN AND ANALYSIS OF TORSION SPRING USED IN SERIES ELASTIC ACTUATORS FOR REHABILITATION ROBOTS

Along with the developing technology, robotic systems have started to take place in areas where there is one-to-one interaction with people, as well as their use in industrial areas. As the robotic system began to take place in daily life, safety and reliability between humans and robots have become a critical issue. In this context, a series elastic actuator has been developed for the aforementioned robotic systems, which has an elastic element placed in series between the motor output and the mechanical output. In this thesis, the torsion spring, as a critical part for the rotary series elastic actuators of rehabilitation robots, which helps support the extension and flexion of the knee joint during physical therapy of individuals with lower extremity disorders, is discussed. First of all, the data required for modeling was produced by making analyses with the design of experiment and finite element method. In line with the design goal of a light, compact, durable and stiff spring, the torsion spring whose topology was determined was modelled using a hybrid method: Neuro-regression approach and cross-validation technique. To minimize the mass and von Mises stress of the torsion spring, the thickness of the spring and the inner corner radius of the flexible leg are taken as the design variables and multi-objective optimization problems are created. The design and optimization of the torsion spring was done with the help of Differential Evolution, Nelder-Mead, Random Search and Simulated Annealing algorithms. By comparing the obtained optimization results with the finite element method and the results in the literature, it has been seen that the model and optimization methods used in the study are reliable and applicable.

ÖZET

REHABİLİTASYON ROBOTLARI İÇİN SERİ ELASTİK EYLEYİCİLERDE KULLANILAN BURULMA YAYININ OPTİMUM TASARIMI VE ANALİZİ

Gelişen teknolojiyle birlikte robotik sistemler endüstriyel alanlardaki kullanımının yanı sıra insanlar ile birebir etkileşimin olduğu alanlarda da yer almaya başlamıştır. Robotik sistemlerin gündelik hayatımızda yer almaya başlaması ile insan-robot arasındaki güvenlik ve güvenilirlik kritik bir konu haline gelmiştir. Bu bağlamda, bahsi geçen robotik sistemler için motor çıkışı ve mekanik çıkış arasına seri konumlandırılmış bir elastik elemana sahip olan seri elastik eyleyici geliştirilmiştir. Bu tezde, alt ekstremite bozukluğu olan bireylerin fizik tedavisi sırasında diz ekleminin ekstansiyon ve fleksiyonunun desteklemesine yardımcı olan rehabilitasyon robotlarının döner seri elastik eyleyicileri için kritik parça olan burulma yayı ele alınmıştır. Öncelikle deney tasarımı ve sonlu elemanlar metodu ile analizler yapılarak modelleme için gerekli olan veriler üretilmiştir. Hafif, kompakt, dayanıklı ve direngen bir yay tasarım hedefi doğrultusunda, topolojisi belirlenen burulma yayının, hibrit bir yöntem olan Nöro-regresyon yaklaşımı ve çapraz doğruluma tekniği ile modellemesi yapılmıştır. Burulma yayının kütle ve von Mises gerilmesini minimize etme amacıyla, yayın kalınlığı ve esnek bacağın iç köşe yarıçapı tasarım değişkeni olarak alınıp çok amaçlı optimizasyon problemleri oluşturulmuştur. Burulma yayının tasarım ve optimizasyonu Differential Evolution, Nelder-Mead, Random Search ve Simulated Annealing algoritmaları yardımıyla yapılmıştır. Elde edilen optimizasyon sonuçları ile sonlu elemanlar metodu ve literatürdeki sonuçlar kıyaslanarak gerçekleştirilen çalışmada kullanılan modelin ve optimizasyon yöntemlerinin güvenilirliği ve uygulanabilir olduğu görülmüştür.

To My Family…

TABLE OF CONTENTS

LIST OF FIGURES

Figure **Page**

LIST OF TABLES

Table **Page**

CHAPTER 1

INTRODUCTION

1.1. Robots used in Physical Rehabilitation

As technological developments increase, the scope and usage areas of robotic systems are also developing. Although the term robotics reminded industry and production in the past, today it draws attention in the field of medicine with interdisciplinary studies. Since 1985, with the development of technology, robotic treatments have begun to be applied in many fields of medicine from surgery to physical therapy and rehabilitation field [1, 2].

In addition to the undeniable benefits of robotic systems in surgical treatments, this technology has also many conveniences for patients and paramedics in physical therapy and rehabilitation. There are many rehabilitation robots that can treat neurological and physical diseases that impair mobility, especially traumatic brain and spinal cord injuries, stroke and other neurological disorders. The most widely used and still being developed devices are shoulder-arm robots, walking robots, hand-finger robots, non-gravity walking system and vertical passive motion devices combined with current therapy. Apart from these, traditional rehabilitation devices are hardy and expensive, and can only be used under the control of therapists. For patients, motor learning ability is a process that requires skill, experience or practice. For this reason, continuous repetitions should be made for the targeted ability and different types of activities should be used each time. Therefore, it is very difficult to apply this intensive treatment program to every patient in the presence of a physiotherapist. In this context, robotic rehabilitation provides high-intensity, safe and flexible treatments by reducing the workload of physiotherapists. That is, a rehabilitation robot can effectively reduce the errors and shortcomings of classical rehabilitation. For this reason, there are already many studies on the application of robotic technology in therapy, and related researchers have been researching and developing in detail for years [3-7].

A study in 2015, based on the idea of adaptive rehabilitation, a cable-operated robotic glove and sleeve were designed**,** modelled, and then manufactured to assist finger and elbow movements in a way that imitates the biological function of the tendons in

order to transform robotic rehabilitation technology into inherently safe and portable devices [8].

Another study, published the same year, describes several new elements for a soft, easy-to-wear robot designed for the hand. These elements can offer solutions to the problems of the wearable robotic gloves that are desired to be developed. This study was carried out with two subjects, one healthy and one disabled. It has been suggested to improve the study by conducting experiments with more data for a wider range of use [9].

In another study on the subject, the design and evaluation of a soft hand cover with a soft cloth electromyography (EMG) sensor, which is to be used in the rehabilitation of stroke and spinal cord injury patients, was performed. While designing, the criteria of electrical durability, compactness and portability were taken into consideration. Unlike other robotic gloves, it optimizes a bio-inspired fin-ray structure to rehabilitate the hand [10].

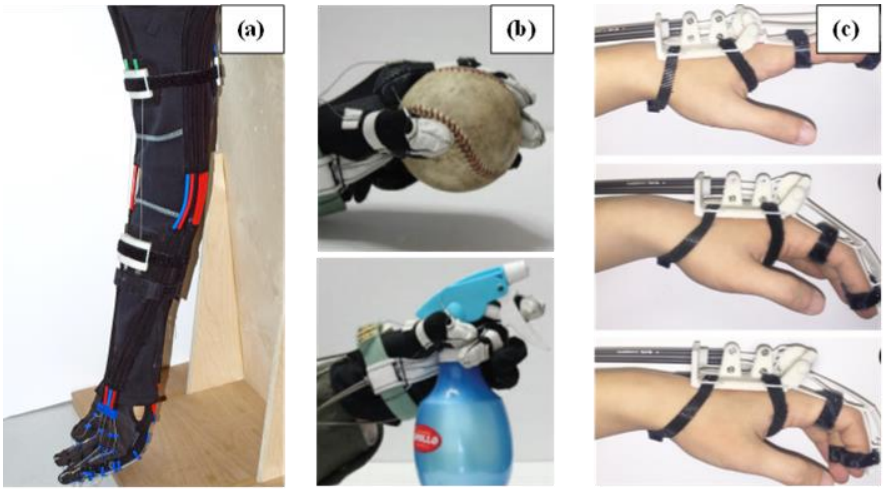

Figure 1.1. Rehabilitation robots for upper and lower limbs. (a-c) is reprinted from [8-10]

1.2. Human - Robot Interaction and Series Elastic Actuator

Due to the fact that robots are too entering the picture in daily life, it is expected that humans and robots work together based on physical cooperation. In this context, with human-robot cooperation based on mutual harmony and complementary working principle, challenging and time-consuming tasks find the opportunity to be performed in the most efficient and cost-effective manner. For robots that perform their tasks in direct contact with humans in industrial production, human-robot cooperation is desired to be safe. However, conventional rigid and high-impedance actuators cannot provide the

desired safety for human joints in parts where human-robot interaction is important. For example, in rehabilitation treatment, a robot with a rigid actuator cannot adequately react to the sudden movements of stroke patients caused by spasm and cannot provide safety. For this reason, actuators that increase interaction safety and contain elastic element have attracted great interest for rehabilitation robots and it has been concluded that they make human-robot interaction more reliable [11-18]. In this context, different studies have been carried out on actuator designs with elastic elements as shown in Figure 1.2.

One of the biggest concerns of the National Aeronautics and Space Administration (NASA) about the health of people going into space is the physical discomfort that can occur due to bone density loss and muscle atrophy. For this reason, exoskeleton designs have started to be developed by NASA. In addition to space applications, the developed X1 exoskeleton robot can be used as a rehabilitation device for walking individuals who have had paralysis, stroke, spinal cord injuries and trauma. using Robonaut 2 [19] and Institute for Human and Machine Cognition Mobility Assist Exoskeleton technologies [20] using a series of elastic actuation schemes, new design has been made that includes elastic actuators and provides force control in hip and knee joints [21].

Mina v2, which is a reinforced lower extremity robotic exoskeleton designed for rehabilitation based on the Mina V1 [22] and X1 exoskeleton, has actuators in the hip and knee parts like its predecessors. Apart from these, Mina V2 includes an actuator for each ankle joint that provides full activation in the sagittal plane. These actuators offer the possibility of obtaining a new exoskeleton that includes reinforced ankle plantar flexion, unlike existing orthotic exoskeletons. Developed with its innovations, Mina V2 gave pretty successful results to set forward, keep walking, going up the ramps and climbing upstairs [23].

In a robot design study, which is also used for rehabilitation purposes, the design and control of an active knee orthosis driven by a rotary series elastic actuator containing a torsion spring was carried out. In order to meet the special requirements for knee joint flexion and extension during physical therapy of people with low motor impairment, the torsion spring was optimized with the help of the Finite Element Method (FEM), considering criteria such as acceptable peak load, flexibility, compact and lightweight design, and optimum design variables were obtained [24].

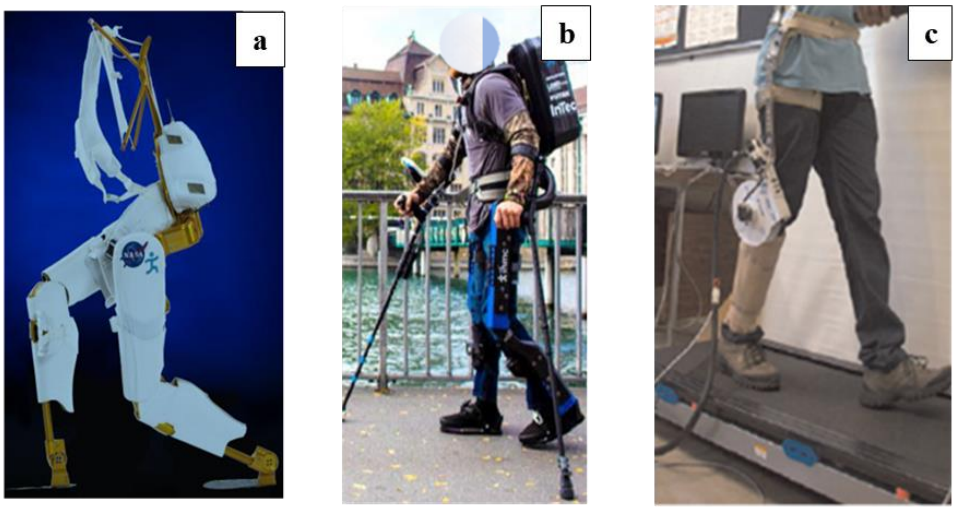

Figure 1.2. Rehabilitation robots with SEA for upper and lower limbs. a is [21] and (b,c) is reprinted from [23–24], respectively

As mentioned above, on the development and improvement of lower and upper extremity rehabilitation robots, many groups have made important studies on devices containing series elastic actuators. The result of the studies is that human-robot interaction is more collaborative and efficient when wearable rehabilitation devices are light, flexible and compact. For this reason, different design and optimization studies have been carried out for elastic elements, which are of great importance for rehabilitation robots to meet these requirements.

Yıldırım et al. designed a compact and lightweight torsion spring that provides rehabilitation and power transfer for the upper limbs embedded in the exoskeleton robot system. After examining the possible types and designs of torsion springs that can be integrated into the series elastic actuator unit, it has been concluded that a torsion spring is suitable for this mechanism. In this context, they concluded that the two-legged topology is more acceptable than the four-legged design. As a result, a spring design has been developed considering the stiffness and load conditions in which the series elastic actuator will be used. In addition, an empirical model for this topology has been obtained and the reliability of the model has been tested by simulation and experimental studies [25].

In order to determine the topology of the torsion spring, a group that started from two rings design connected by flexible elements, performed a study by choosing a suitable topology from the literature samples [24], when this topology did not give sufficient results to calculate the compatible structure of the elastic elements. Study has been done on the

development of the selected torsion spring design for an inexpensive and lightweight series elastic actuator used in an active orthosis. For this, a two-stage optimization study was carried out considering the necessary criteria. In the first step, after the appropriate topology decision was made, two different optimization methods, meta-model and genetic algorithm, were used to minimize the equivalent von Mises stresses, and then FEM-based optimization was performed as the second step [26].

In a study to design a compact monolithic torsion spring to be used as the main component of a modular compatible system for Series Elastic Actuators, the design of the elastic element was carried out by iterative FEM analysis. The main objectives in the study were determined as giving the flexible element the ability to provide the necessary auxiliary torque to support the movement with low stiffness and minimizing the resulting weight and dimensions. After successful analysis, the presented elastic element was included in a SEA operating the knee orthosis to provide knee flexion and extension support for elderly individuals who have motor losses [27].

Due to the kinetic and kinematic requirements for actuators used in robots, undesirable uncertainties occur in the movement of the load. Therefore, Nieto et al. conducted robust optimization studies to account for the uncertainty created during the design of series elastic actuators used in prosthetic robotic ankles. They performed the formulation of a robust-feasible convex optimization program to select the optimum compliance–elongation curve of the torsion spring that minimizes one or more of the factors of spring elongation, motor energy consumption, motor torque or motor speed. The formulas they created ensured that motor torque, winding temperature, and speed were workable despite uncertainty in kinetics, kinematics, or spring production. Simulation case studies help to inform about the selection of different objective functions when evaluating the performance of robust viable designs versus optimal solutions that neglect uncertainty. In this context, the designer aims for reliable robots that reduce overdesign, directly in optimization and showing uncertainty over certain kinetic, kinematic and production parameters [28].

Modeling and torque trajectory control of the rotary series elastic actuator for the humanoid/memetic is critical. In a study on this subject, fuzzy logic torque controller with nonlinear friction compensation was considered and different controllers (PID feed forward controller, fuzzy logic feed forward controller and friction compensated fuzzy torque controller) were used to improve trajectory tracking performance in rotary series

elastic actuator systems. The actuator was designed and necessary tests were carried out. At the end of the study, the trajectory tracking error was minimized by the nonlinear estimation of the frictions occurring in this type of mechanism, and high accuracy trajectory control was achieved by using the fuzzy logic control structure when the system actuators were exposed to nonlinear effects [29].

In a study on a wearable robot designed to improve hip and knee flexion/extension, it is aimed to provide flexibility to the system by operating the series elastic actuator at optimum intervals. In addition, the dynamic properties have been optimized thanks to the smart distribution of the oscillatory masses. In order to be ergonomic, non-anthropomorphic designs have been determined for kinematic synthesis, topology selection and morphological optimization. Afterwards, theoretical and experimental investigations have been made. These theoretical and experimental results show that the proposed design is promising for people in need of rehabilitation [30].

In another study, studies were carried out on the precision of light robot positioning with serial elastic actuators. The modeling uncertainties of these robots negatively affect the precisions gained by approaches such as inversion-based feed-forward. Due to this effect, this work improves the sensitivity of robots around operating points with a multiple-input multiple-output, iterative learning control approach. In this context, an input-weighted complex kernel was defined to predict local multiple-input-multi-output models using complex Gaussian process regression, and Geršgorin theorem-based conditions were developed to ensure precision convergence of iterative learning control based on noise limits. As a result, it was observed that there was an increase in the operating speed of the robot and an improvement of approximately 90% in the positioning accuracy [31].

A group on torsion spring design and optimization examined the spring development and testing stages for long-term use of robots. The main aim of the study is to make a design that meets the actuator weight and dimensional requirements while adjusting the long-term durability, high torque output and the overall weight of the mechanism. After the recursive design and tests, optimal torsion spring geometry was obtained with the SIMP topology optimization method and torsion tests were carried out. They concluded that, through design and testing, series elastic actuators will be successfully adapted to applications where physical human-robot interaction is important

for long-term and continuous use [32]. Figure 1.3 contains the visuals of the studies mentioned above.

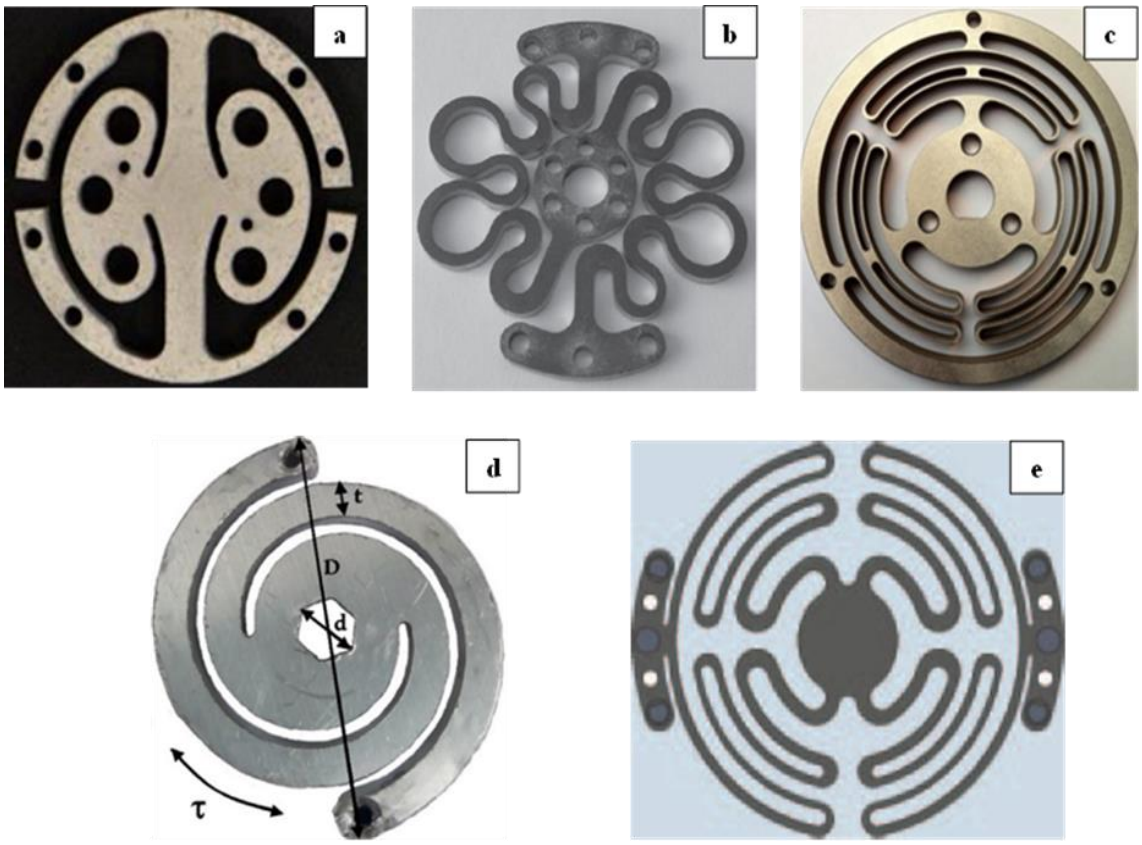

Figure 1.3. Torsion spring topology for SEA (a–c) is reprinted from [25–27], (d,e) is reprinted from [29,30]

1.3. Objectives of Thesis

The main features of the series elastic actuators, which are attached an elastic element to the shaft of the actuators, are as follows: i) being self-elastic ii) measuring the force with the help of Hooke's law by measuring the displacement of the elastic element iii) having high sensitivity and safe human-robot interaction during operation. As it can be understood from the literature studies, the basic element that gives these properties to serial elastic actuators is the elastic element of the actuator. In this context, structural changes in the elastic element directly affect the performance of series elastic actuators.

In this thesis, the design, modeling and optimization of the torsion spring for minimum mass, minimum von Mises stress and maximum stiffness were performed using neuro-Regression approach, cross validation technique and stochastic optimization

methods such as Differential Evolution (DE), Nelder Mead (NM), Simulated Annealing (SA) and Random Search (RS). Torsion springs with constant outer and inner diameter length, different thickness, and different flexible leg inner corner radius were considered.

The aim of this thesis can be listed as follows;

- To obtain torsion spring structural designs using computer technologies and to investigate the capabilities of optimization methods in terms of how better structural design can be obtained by limited design time and limited conditions.
- After deciding on the important factors for the outputs at the design stage, to see the relationship between the design variables and the response variables with the help of mathematical modeling.
- To minimize mass and von Mises stress and maximize stiffness (100-200 N.m/rad) values simultaneously.
- Comparison of the performance of torsion spring designs for different thickness and radius values using DE, NM, SA, RS stochastic methods.
- Comparison of the results of the optimization algorithms used with each other and with the literature outputs.

CHAPTER 2

SERIES ELASTIC ACTUATORS AND TORSION SPRING

2.1. Actuator and Series Elasticity

The robot component that supplies the energy for a mechanism or system to transmit force and motion is called an actuator. Actuators that provide movement can be examined in two groups as linear and rotary actuators. Linear actuators move the mechanism to which they are attached, usually back and forth along a straight line. Rotary actuators, on the other hand, rotate the input of the mechanism to a certain angle limited-infinite. Many rotary actuators are combined with reducers to reduce rotational speed and increase torque [33-35]. In this thesis, rotary series elastic actuators that provide movement are issued.

In robots designed for industrial purposes, actuators that are rigid, with high impedance and safe are made with sensors are used. With the development of technology, human-robot interactions have begun to increase, and research on these robotic systems has focused on the safety of the human-robot interface. This safety emphasized that torque and impedance control algorithms should be applied to robotic systems and that the actuators used should be suitable for this structure. In systems with rigid actuators, safety is usually provided by position/force control. However, delays and sudden shocks caused by the software system reduce the safety of the actuator and transient contact events cannot be tolerated in these cases. These problems are very unsafe for mechanisms interacting with humans and cause noise in the force control of the actuator. Therefore, choosing a compatible actuator is extremely important in human-robot interaction mechanisms where force control and contact dynamics are important. In this context, actuators with compliant elastic elements such as Series Elastic Actuator (SEA) have been proposed as a simple and effective solution for such mechanisms in order to overcome the difficulties and achieve natural compatibility. In this way, unwanted movements can be reduced and damage to the device is prevented while increasing the safety of the user [36-38].

2.2. Series Elastic Actuator

Since the 1990s, numerous studies have been conducted and many scenarios have been created to develop SEAs. While doing these researches, scientists realized that the basis of human-robot mechanisms is based on understanding human muscle tissue. After studies on biomechanics, it was understood that elasticity in muscle tissue is important in terms of energy and efficiency. Studies have shown that muscle work output and stability of the system increase with serial elasticity. SEAs, are very suitable for application to human-robot interactive systems in order to eliminate the mentioned deficiencies [27, 39].

As seen in Figure 2.1, the SEA structure is a simple but impactful solution consisting of a gear motor in series with a spring connected to the load. This structure enables decoupling the output from motor inertia and non-linearity, with benefits in the way of force/torque control fidelity [40]. In addition, the output force of the actuator is dependent on the compression of the spring. Therefore, the spring elements of the SEA are linearized with the Hooke's law given in Equation 2.1. Mathematically, Hooke's law states that the applied force F equals a constant k times the displacement or change in length x. The compression of the spring is calculated with a sensor and, thanks to Hooke's law, the force applied to the load can be calculated automatically by measuring the deflection of the elastic element. According to this calculation, force control is provided by sending a signal to the motor. However, in this case the servo motor operates with low efficiency at low speed and the torque produced is small. This situation is not suitable for collaborative robots with humans. For this reason, small and light motors with gearboxes can be used at low speeds and high torques [40-44].

$$F = kx \tag{2.1}$$

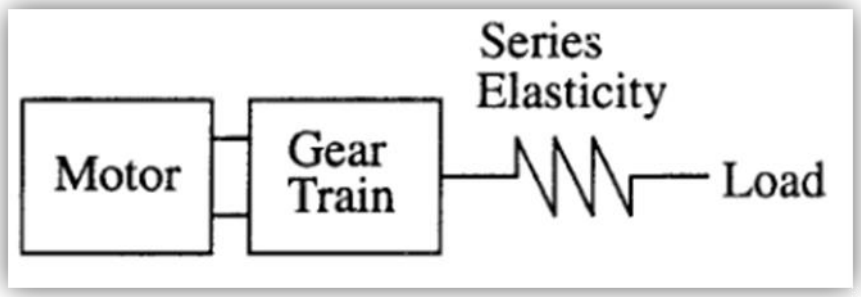

Figure 2.1. Basic Configuration/Block Diagram of Series Elastic Actuator [40]

Unlike a rigid actuator, SEAs contain an elastic element that provides passive mechanical energy storage and low mechanical output, and can filter incoming surges and increase power output. The elastic element, which is the main component of SEA, has a significant influence on the size and mechanical properties of the joint. The design of the elastic element is therefore the key point for SEAs. Two types of elastic elements can be used for SEAs: torsion spring and linear spring [38, 40].

In this study, torsion spring is considered as an elastic element. There are two types of torsion spring designs as linear and planar torsion springs in the literature. The first of these is the designs created as a result of the arrangement of linear springs, which are large in volume and can be adapted to special requirements. An example of linear springs used in SEAs is shown in Figure 2.2. Another design is planar torsion springs, which are specialized to increase performance while minimizing the volume of the torsion spring. These customized springs show better linearity between torque and angle [27, 35]. The design is embedded in the transmission line and directly connected to the load and is specialized to increase performance while minimizing the volume of the torsion spring. These customized springs show better linearity between torque and angle. Also, an example of the second type of springs used in SEA is shown in Figure 2.2 [27, 42].

Figure 2.2. Examples of torsion spring components for rotary SEA.

CHAPTER 3

MODELING

A model is a simplification, reflection, abstraction, and conceptualization of a real-world system or event. Modeling, which, in its most general definition, means copying the truth, is defined as the set of operations made to make an unknown phenomenon clear and understandable by reference to existing sources. In addition, one of the methods used in the concretization process of mathematics, which is an abstract science, is modeling. In this context, mathematical modeling is a dynamic method that makes it easier to see the relationships in the nature of real life problems, to express the relationships between them in mathematical terms, to classify them and to draw conclusions [45-47].

From an engineering perspective, models are smaller-sized structures that are used extensively in engineering problems, reflecting all the features of large-scale systems. These models have details that realistically reflect the features and intended use of the system. Therefore, in the development of optimization technology, researchers have primarily been interested in modeling, and mathematical modeling is the first step in the optimization process of engineering design problems. The expressions in the mathematical models created with experimental or simulation data consist of measurable features of the systems, design variables that determine the performance criteria to be optimized, and constraints that determine their limits [48]. The design process for a system, which starts with the design of experiment and ends with finding the optimal solution, is given in Figure 3.1.

Figure 3.1. Flow diagram for the optimal design [49]

Within the scope of this thesis, simulation data were obtained by using the Design of Experiments (DOE) and Finite Element Method (FEM), which were defined in the next chapters, in order to carry out the modeling phase of the discussed problem.

3.1. Design of Experiments (DOE)

Design of experiment (DOE) is an approach that provides an effective and efficient examination of the cause and effect relationship between inputs and outputs. It is a proactive approach because the conditions that will reveal the error before it occurs are determined in this method. Randomization, blocking, and replication are the basic principles of statistical methods in DOE. Multiplication is the repetition of the simulation in order to obtain a more accurate result and to minimize the experimental error. The randomization defines the random order in which the simulation will be executed. Blocking aims to isolate a known systematic bias and prevent the main effects from being hidden.

There are two important parameters in DOE studies. After these parameters are decided for the problem, the analysis can be started.

1. Factor: Inputs that are thought to have an effect on the output.

2. Level: The ranges of each factor defined in the experiment.

In addition, there are several DOE techniques such as Full Factorial, Randomized Complete Block, Fractional Factorial, Taguchi, Optimal Design (D-Optimal), and Box-Behnken. In this study, it was decided to use the D-optimal design method, since it provides the opportunity to choose different levels for structures that do not have equal effects with each other [49-51].

3.1.1. Full Factorial Design

A full factorial design is the combination of at least two or more parameters and their levels multiplied by each other in experiments. It is more effective than experiments in which one factor at a time is considered. Random blocks are used in full factorial design so that unknown and uncontrollable errors do not affect the experiment. After the experiment, the experiment is repeated at least three times in order to perform the variation analysis, so that it can be interpreted statistically. Also, the effect of the parameter on the experiment can be calculated with this method [50, 51].

3.1.2. Randomized Complete Block Design

On a variable measured in an experiment, besides the factor whose effect is desired to be examined, other factors may also be effective. For this reason, it would be a more accurate approach to create homogeneous structures in terms of these factors and test the desired factor, and experimental errors can be reduced. These homogeneous structures in the technique are called blocks, and the experimental design that emerges when the trials are randomly assigned from each block is called the random block layout. In this most widely used experimental design, it is investigated whether the difference between the groups is statistically significant by comparing the measurement values obtained from randomly selected subjects from two or more groups.

Random block layout is preferred in many different fields, as it provides the opportunity to test the effect of the investigated factor more accurately. In addition, the saving in sample width is another reason for preference. Apart from its advantages, the use of the random block layout is restricted as it is not always possible to run all trials on the same block. But this problem is handled by a method called incomplete random block layout [50, 52].

3.1.3. Fractional Factorial Design

Combinations of the levels of all factors are tried in the full factorial experiment design. Therefore, this experimental design method is quite costly and time consuming. In cases where time and cost are important, the number of experiments is proportionally reduced to obtain a fractional factorial experiment design. This design can be described as a vertical row layout that enables the discovery of significant effects with minimal experimental study [49].

3.1.4. Taguchi Design

The Taguchi method aims to minimize the variability in the design by creating an appropriate combination for the controlled factors against the uncontrollable factors that cause change in the design process.

Orthogonal arrays were created to explain more than one experimental situation in the Taguchi method. Orthogonal arrays, also called design matrices, are determined in two or three stages according to the nature of the problem. This feature allows multiple factors to be tested in small numbers and simultaneously changed factor levels [53, 54].

3.1.5. Optimal Design (D-Optimal)

D-optimal design is a type of computer-aided design that is created during the development phase and complies with the standards or criteria set by the developers at a high level. In this design method, the product prototype represents the best result ever and is often seen as approaching the ideal design for that product. D-optimal designs are straight optimizations based on the chosen optimality criterion and the model that will fit. Unlike standard classical designs such as factorials and fractional factorials, D-optimal design matrices are usually not orthogonal and effect estimates are correlated.

There are several advantages to the D-optimal design regarding the time and cost limitation process. In line with certain criteria, it narrows the focus of the problem and minimizes the expenses incurred in the research process. Different factor allows making different combinations. Ultimately, it ignores certain results while continuing to pursue more promising combinations. Therefore, it is advantageous to use the optimal design method in the following cases [49, 55];

- ✓ If a small number of design work is required,
- ✓ If there are consumables or factor configurations,
- ✓ If unstable experiment structures are available
- ✓ When using the operation and mixing variables in the same design.

3.1.6. Box-Behnken Design

The Box-Behnken method is an effective method for modeling the second-order response surfaces of the trial layouts introduced by Box and Behnken in the 1980. It is a method based on balanced incomplete block trials. Factors to be included in the model must have at least three levels [56].

3.2. Regression Analysis

Regression is one of the most preferred techniques in statistics to determine the cause and effect relationship between two or more variables. In other words, it is examined to what extent one or more of the variables affect other variables. The relationship between these variables is expressed as a mathematical function and this function is called a regression function or a regression model. In the regression model, the dependent variable (response variable) is denoted by Y, while the independent variables (design variables) are denoted by X_i (i=1, 2,..,n). According to the number of variables used and the type of model, regression analysis can be classified as simple linear regression, simple nonlinear regression, multiple linear regression and multiple nonlinear regression [57, 58].

3.2.1. Simple Linear Regression

Simple linear regression; it aims to measure the effect of a one-unit change in the independent variable on the dependent variable. The main purpose is to find the linear function that expresses the relationship between the dependent and independent variable. The simple linear regression equation, which is a stochastic (probabilistic) model and shows the relationship in the population [58], is expressed as Equation 3.1;

$$Y = \beta_0 + \beta_1 X + \in \quad \textbf{(3.1)}$$

Here β_0 is the point where the line intersects the y-axis and is the regression constant. When β_1 is the slope of the line or the regression coefficient, $\in$ is the random error value and it is assumed that this error value has a normal distribution with a mean of zero variance σ_2. This assumption is required for importance checks of coefficients, not parameter estimates. Figure 3.2 graphically describes this formula [59].

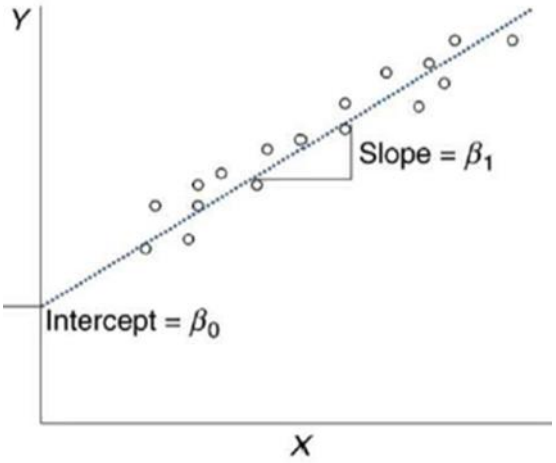

Figure 3.2. Regression Graph for Simple Linear Model

3.2.2. Simple Non-linear Regression

Simple nonlinear regression fits a curve to nonlinear X, Y data. The y is a function of a single x variable: Y = f (X). Depending on the shape of the data, there are different types of curves, resulting from different kinds of functions. Simple nonlinear regression for a model that has only one input variable describes as Equation 3.2 [58]:

$$Y = \beta_0 + \beta_1 X^2 + \in \quad \textbf{(3.2)}$$

3.2.3. Multiple Linear Regression

While there is one dependent and one independent variable in simple linear regression analysis, there is one dependent variable and two or more independent variables in multiple linear regression analysis. In addition, there is a linear relationship between the variables in both analyses. General form of multiple linear regression model is shown in Equation 3.3 [58].

$$Y = \beta_0 + \beta_1 X_1 + \beta_2 X_2 + \cdots + \beta_n X_n + \in \quad \textbf{(3.3)}$$

3.2.4. Multiple Non-linear Regression

The multiple nonlinear regression model is more flexible than simple nonlinear regression models because the function does not have to be linear or linearized. Therefore, it offers a wide choice for fitting the nonlinear regression phenomenon to the data. The form of nonlinear regression models is generally similar to linear regression models. The biggest difference of the nonlinear regression model from the linear regression model is that n - the number of regression parameters is not related to the number of independent variables, which means X, in the model. In this thesis, multiple non-linear regression was used for analysis. General form of multiple nonlinear regression model is shown in Equation 3.4 [58].

$$Y = \beta_0 + \beta_1 X_1 + \beta_2 X_2^2 + \cdots + \beta_n X_n^n + \in \quad \textbf{(3.4)}$$

3.3. Coefficient of Determination (R^2)

The coefficient of determination (R^2), which is widely used in regression analysis, shows the degree of closeness of the data to the accuracy. In other words, it expresses what percentage of the changes in the dependent variable can be explained by the independent variables. This is a good indicator of the explanatory power of the regression model. This value is calculated as the square of the multiple correlation the coefficient in regression models. However, although the R-square value is defined as the square of an expression, it may turn out to be negative in some special cases. This means that the model is not reliable. A coefficient of determination of zero indicates that the independent variables cannot explain the dependent variable at all; being one show that he can explain it fully. A zero here indicates 0% of the model, and a one indicates that the model has 100% explanatory power. It is desirable that this value be close to 1. However, although there is no definite limit, the R-square value is expected to be around 0.90 for good modeling. The formulation of the R-square is given in Equation 3.5 – 3.7.

$$R^2 = 1 - \frac{SSE}{SST} \quad \textbf{(3.5)}$$

$$SSE = \sum_i (\hat{y}_i - \bar{y})^2 \quad \textbf{(3.6)}$$

$$SST = \sum_i (y_i - \bar{y})^2 \quad \textbf{(3.7)}$$

where,

SSE is Sum of Squared Regression also known as variation explained by the model

SST is Total Variation in the data also known as sum of squared total

$\mathbf{y_i}$ is the y value for observation i

$\bar{\mathbf{y}}$ is the mean of y value

$\hat{\mathbf{y}}_\mathbf{i}$ is the predicted value of y for observation i

R-square measures the rate of variation in our dependent variable (+Y) explained by our independent variables (X) for the linear regression model. Apart from that, the adjusted R-square only measures the rate of variation explained by independent variables that actually affect the dependent variable. The R^2 value is always greater than the R^2adjusted values. According to the meaningless variable added to the model, the R^2 adjusted value also changes depending on Equation 3.8.

$$R^2_{adjusted} = 1 - \frac{(1-R^2)(n-1)}{n-k-1} \quad \textbf{(3.8)}$$

In this equation, k denotes the number of independent regressors, which is the number of variables excluding the constant, in the model, while n denotes the number of points in the data sample [58, 60, 61].

3.4. Artificial Neural Network

Artificial neural networks (ANNs) are computer systems developed with the aim of automatically performing the abilities such as deriving, creating and discovering new information through learning by adopting the basic structure of the human brain without any help. These systems have emerged as a result of mathematical modeling of the learning process by taking the human brain as an example. Learning process in artificial neural networks is done using examples. During learning, entry and exit information is given and rules are set. It is used in many fields such as computational finance, image processing and computer vision, computational biology, power generation, automotive, aerospace, manufacturing, and natural language processing. ANN consists of many cells that can work simultaneously and perform complex tasks. They have the ability to learn and learn with different learning algorithms. Missing patterns can be completed by pattern recognition and classification with ANN. Also, the ANN model is generally considered

as a nonlinear statistical modeling algorithm. In this algorithm, the relationships between inputs and outputs are modelled [57, 62].

3.5. Neuro-Regression Modeling

Regression analysis and artificial neural network methods, which are widely used modeling analysis methods, have been examined above. Both have advantages and disadvantages. In this context, a hybrid method combining the strengths of regression analysis and artificial neural networks has been created in order to reduce the disadvantages and make more reliable models and predictions. Since this approach, called Neuro-Regression, is created by taking advantage of the advantages of RA and ANN methods and avoiding their disadvantages, the error rate is much lower than both methods.

The biggest goal of Neuro-regression studies is to create a learning model that accurately predicts previously unknown data items. Therefore, the generated learning model must be generalized very well to ensure correct classification of future data items. Generalization actually means how well our model learns from given data and applies the learned information elsewhere. The most common techniques used to measure generalization are Validation, Training, and Test sets. If model performs well on the data that it has not seen in the training, it can be said that it generalizes well on the given data. [49, 63].

3.5.1. Train and Test Sets

Before performing mathematical modeling, the data set should be divided into training and test sets. This distinction can be approximately 80% training dataset and 20% test dataset. The training set is the dataset on which the model is trained. The test set is a data set used to evaluate the model developed in the training set. First, the model is trained on the training set and predictions are made on the test set. Thus, the predictions are compared with the actual response variable in the test data and the accuracy of the model is evaluated. Also, the larger the training set, the better the model learns. On the other hand, the larger the test set, the more reliable the evaluation metrics and tighter confidence intervals [49, 63].

3.5.2. Validation Set

In the modeling process, since the test set is used in the each iteration for the efficiency of the model, the model may cause the test set to adapt to its unique situations. Therefore, overfitting of the model with the test set occurs. To prevent the model from overfitting, the validation set that has not been trained on the model and is used to set the hyper parameters should be used. After the model is decided at the end of the each training with the validation set, it is tested with the test set and the effectiveness of the model is observed more reliably. In addition, the validation set has no effect on the fit performance of the model. It is just an intermediate step to avoid overfitting the test set. Also, it is the test set that controls whether the model is over fit or under fit. The validation set only checks for over fit to the test set [64].

3.6. Cross Validation

Cross validation is a technique used in model selection to better predict the error of a test performed on a machine learning model. In this technique, sample observation segments known as validation sets are created from the training data set. After placing a model on training data, its performance is measured against each new validation set. Later, when new observations are sought, a better assessment of how the model will perform is obtained.

This technique is examined in three sub-titles as holdout, k-fold cross validation and single-out cross validation method. The details of the k-fold cross validation method used in this thesis are explained below [65, 66].

3.6.1. k-Fold Cross Validation

In this method, the dataset is divided into k subsets and the holding method is repeated k times. Each time, one of the k subsets is used as the test set, while the other k-1 subsets are combined to form a training set. Then the mean error of all k trials is calculated. One of the advantages of this method is that it cares less about how the data is split. Each data point enters the test set exactly once and enters a training set k-1 times. The outcome estimate variance decreases as k increases. The disadvantage of this method is that the training algorithm has to be repeated k times from zero [67].

CHAPTER 4

OPTIMIZATION

Optimization is a mathematical process that aims to find the optimum design by minimizing or maximizing the determined single or multiple objective functions and determining the decision variables of the problem in a system with certain constraints. In other words, it is the process of determining what the inputs or values of this problem will be in order to obtain the desired output. Having a solution to a problem does not mean that the solution gives the best results. Therefore, optimization techniques are used to reveal the best results of the problem to be solved and the solution obtained by these techniques is also called the optimum solution. The aim of optimization in engineering problems is to find the optimum solution regardless of the problem. Therefore, optimization is frequently used for engineering problems such as mass, displacement, strength, time, temperature, buckling, stiffness, vibration, etc [63, 68-70].

In general, the optimization process can be divided into two sub-headings as mathematical modeling and analysis. Mathematical modeling is the transfer of structural features of real-life phenomena to the language of mathematics. On the other hand, analysis is about analysing the mathematical model and knowing the compatibility of the mathematical model with real life. That is, it provides mathematical modeling and analysis, physical interpretation and application of mathematical concepts between design variables and objective functions [71].

The optimization process can be shaped according to the requirements of the problem to be applied. If the decision variables of the problem have a limited, the model is defined as constrained model. If there are no limits, this is defines as the unconstrained model [72]. In addition, if these decision variables have positive real values, it is called continuous optimization, if all decision variables take integer values, it is called discrete optimization problem. In addition, if only the instantaneous relationship is to be examined in the optimization problem, the static model is used, while the dynamic model is used when describing the time-dependent changes in the state of the system. Apart from these, two different optimization problems, single and multi-purpose, can be considered in order to obtain the desired design in the optimization process [49, 73].

4.1. Single Objective Optimization

In an engineering problem that has been mathematically formulated, it is called single-objective optimization to find the parameters that the model will have in order to obtain the most appropriate value for a single design. In other words, problems with a single objective function are called single objective optimization. This approach includes design variables, objective function, constraints and bounds of constraints [71, 74].

The general mathematical definition of a single objective optimization problem is;

Minimize f (x)

where, $x = (x_1, x_2, x_3, \ldots, x_n)^T$

Subject to,

$g_i(x) \leq 0 \qquad i = 1,2,\ldots,m$

$h_j(x) = 0 \qquad j = 1,2,\ldots,k$

Here, the parameter that is desired to be optimized is called the objective function (f(x)), while the parameters that define the physical and functional properties of the system to be designed are called design variable (x). In addition, the ranges determined for the parameters to take values are called constraints (g_i (x) and h_j(x)). The above optimization problem is written as a minimization problem. However, the sign of the objective function can be changed to transform a minimization problem into a maximization problem. That is, as can be seen from Figure 4.1, − f (x) can be maximized to minimize f (x) [71, 74].

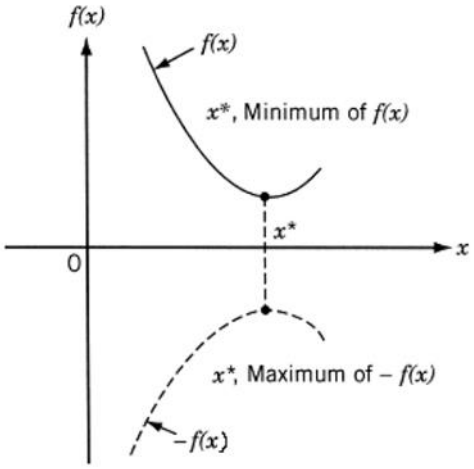

Figure 4.1. The minimum and maximum of the objective function f (x)

Engineering problems that exist in daily life have many purposes. Single-objective optimization algorithms do not give meaningful results due to the conflict, complexity or size of these objectives. For this reason, multi-objective optimization algorithms detailed below have been developed.

4.2. Multi Objective Optimization

Multi-objective optimization can be defined as the simultaneous optimization of more than one objective. Most engineering problems in daily life need simultaneous optimization of multiple and conflicting objectives [70]. For instance; a good design for a spring is expressed as lightness and high stiffness. A good vehicle design needs an optimization model that includes the simultaneous effect of weight, fuel economy and load. In this context, there may not be a single solution that will meet all the requirements in multi-objective optimization. Therefore, these problems can be converted into single-objective problems with constant weight linear functions. However, before the optimization process starts, the weights of the objective functions should be determined in order of importance. In addition, using the algorithms used in single-objective optimization in the solution of these problems may not scan the solution space sufficiently and healthy results may not be obtained. In multi-objective optimization, all objective functions can be optimized simultaneously. But the shortcoming here is that if the objective functions do not all get the best value at the same point, a single best point cannot be found. Therefore, the definition of scalar best cannot be used in multi-objective

optimizations, as in single-objective optimization problems. However, there are several different methods for solving problems using multi-objective optimization, and the most effective one is the Pareto optimal method [75-77]. Pareto analysis has the concept of dominance, which requires choosing between a vector containing all objectives and the resulting solutions. Therefore, the probability of diversifying the solution set with this analysis is quite low compared to other methods. As a result, for the solution of the multi-objective optimization problem, it is necessary to find the Pareto optimal set, which is the set of solutions that represents the best balance between the determined objectives [78, 79].

The general mathematical definition of a multi objective optimization problem can be expressed as follows:

Minimize $f_1(x), f_2(x),\ldots,f_r(x)$

where $x = (x_1, x_2, x_3, \ldots, x_n)^T$

Subject to,

$g_i(x) \leq 0 \qquad i = 1,2,\ldots,m$

$h_j(x) = 0 \qquad j = 1,2,\ldots,k$

Here, the parameter that is desired to be optimized is called the objective function, while the parameters that define the physical and functional properties of the system to be designed are called design variables. In addition, the ranges determined for the parameters to take values are called constraints. The above optimization problem is written as a minimization or maximization problem [74].

4.3. Traditional and Non-Traditional Optimization Methods

The optimization process of engineering problems can be solved with different optimization algorithms. Optimization algorithms can be examined in two groups as traditional (deterministic) and non-traditional (stochastic) optimization methods. Method of analysis, Lagrange multipliers, restricted variation and etc. are traditional optimization methods and are used only in solving problems with continuous and differentiable functions. Years ago, these deterministic methods were used to solve engineering problems. However, with the development of computer technology in recent years,

stochastic methods have become the subject of choice in the fields where most deterministic methods are used. Existing stochastic methods, inspired by the concepts in nature and simulating them in a computer environment, are used in different fields thanks to their features such as producing discrete solutions and obtaining results close to the global optimum without looking at the starting point [49].

Genetic Algorithm (GA), Simulated Annealing (SA), Random Search (RS), Differential Evolution (DE), Particle Swarm Optimization (PSO), Ant Colony Optimization (ACO), Tabu Search (TS), Artificial Bee Colony (ABC), Markov Chain Monte Carlo (MCMC), Harmony Search (HS), Covariance Matrix Adaption (CMA), Grenade Explosion Method (GEM) are stochastic optimization methods. Recently, scientists continue to modify these algorithms and add more efficient methods to the literature. Since the design and optimization problems of torsion springs studied in this thesis have complex and nonlinear functions, stochastic optimization methods were preferred. In this context, in the following sub-headings, Differential Evolution (DE), Simulated Annealing (SA), Random Search (RS) and Nelder-Mead (NM) algorithms, which are preferred stochastic optimization methods for the study, are detailed [63, 74].

4.3.1. Modified Nelder-Mead Algorithm

Conventional Nelder-Mead (NM) derivative optimization technique, also called simplex search, was discovered by John Nelder and Roger Mead Spendley in 1965 and has been used in many fields such as physics, chemistry, medicine, science and technology. This algorithm, which is a traditional local search method, is used to find the local minimum point in multidimensional unconstrained optimization problems. In addition, the simplex is a polyhedron with (n+1) vertex in n-dimensional search space and gradually reaches the optimum point through an iterative process, that is, it is also known as the best point search algorithm [80, 81]. Apart from these, since it is not a global algorithm, it is not suitable for optimization problems with a large local minimum. However, it can give good results in solving optimization problems with a small number of local minimum. The Nelder-Mead algorithm delivers adequate results in less time, thanks to its ability to deliver significant improvements in a few iterations. Nelder Mead, one of the non-linear and non-differentiable direct search algorithms, is an iterative

method with four control parameters. These parameters are reflection factor, expansion factor, construction factor, and shrinkage factor [82].

Since constrained optimization problems cannot be solved with conventional NM, the algorithm can be modified by adding a "penalty function" to the flow of the algorithm to solve the problem. The first step of the algorithm is to make the first working simplex S. Then, minimizing the function moves the search route away from the vertex that is the worst function value. This is achieved by obtaining a reflected and enhanced point. In this improved algorithm, a hybrid form with conjugate gradient and principal axis methods is used [63, 83]. In this thesis, the Modified Nelder-Mead (MNM) algorithm was used because the present optimization problems have nonlinear constraints and continuous design variables [84]. The flowchart of the algorithm is given in Figure 4.2 [85].

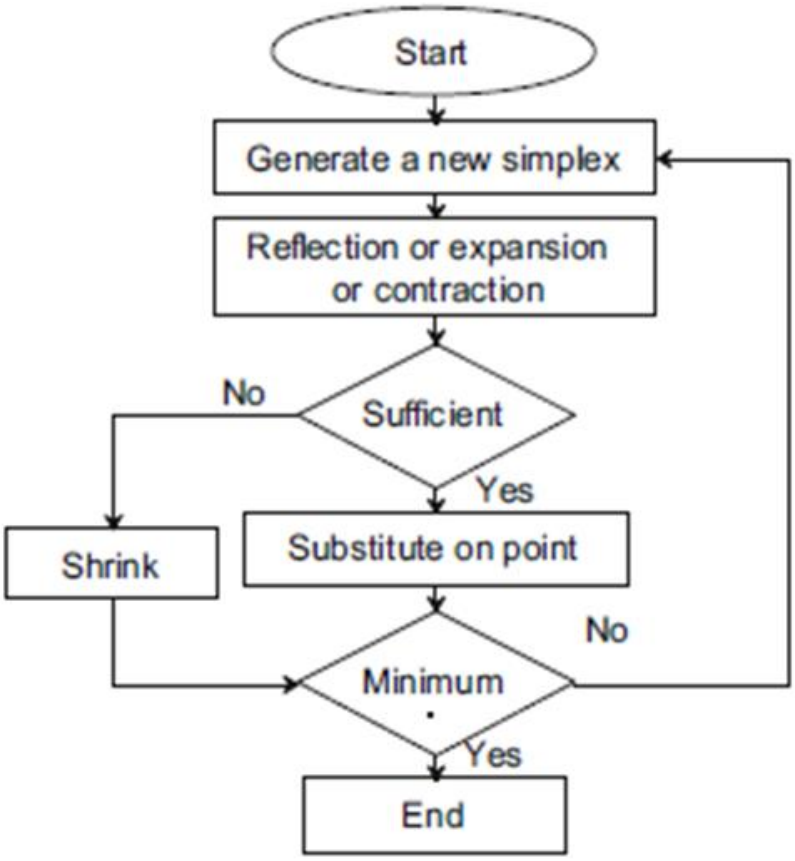

Figure 4.2. Nelder-Mead algorithm flowchart

4.3.2. Modified Differential Evolution Algorithm

Differential Evolution (DE) Algorithm, created by Price and Storn in 1995, is a metaheuristic algorithm which has many variables. In addition, it is a population-based technique based on genetic algorithm, thanks to its operation and operators, as well as giving meaningful results in optimization problems with continuous data. DE, which is generally used in problems with continuous variables, is also used in combinations of discrete variables or continuous-discrete variables. In problems where DE is used, the objective function is used instead of the fitness function and these represent alternative solutions. DE does not work with constraints. It is used to solve problems that are integrated into the objective function of constraints. Compared to other algorithms, DE is one of the most powerful algorithms for real parameter optimization methods. This algorithm has three main control parameters so that each generation obtains new populations with higher quality individuals. These can be listed as differentiation/mutation constant, crossover constant and population size. Other control parameters of this algorithm are: (i) problem size scaling the difficulty of the optimization case, (ii) the maximum number of generations known as the stop condition, (iii) boundary constraint. The evolutionary process consisting of these parameters continues until the stopping condition is met [86, 87].

The Modified Differential Evolution (MDE) algorithm has been developed by making adaptations that can change the scale factor and crossover rate, which allows all solutions in the original DE algorithm to easily get rid of stagnation. Thus, the most obvious advantage of this algorithm is the scale factor and transition speed of each solution. In this thesis, the MDE algorithm was used [88]. The flowchart of the algorithm is given in Figure 4.3 [89].

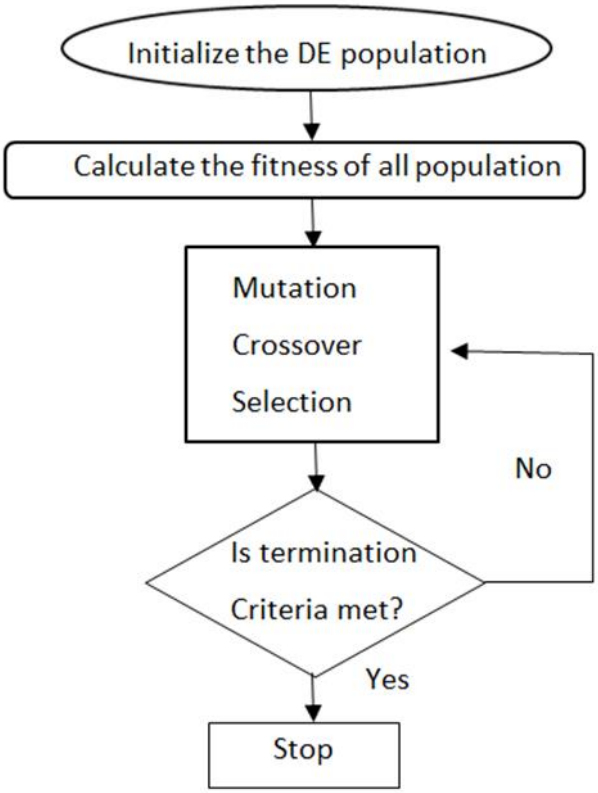

Figure 4.3. Flowchart of Differential Evolution Algorithm

4.3.3. Modified Simulated Annealing Algorithm

Simulated annealing (SA) is one of the most popular stochastic exploration methods that simulate the physical annealing process in which the metal is heated to high temperatures and then slowly cooled until a minimum energy state is achieved. The melting stage of the metal allows it to have a low-energy atomic structure, thus making it a harder material. Simulated annealing moves to neighbouring regions to find the best local optimum as the temperature of the material rises. As the material cools, it tries to stay at its best local optimum. In this context, this process, inspired by the SA algorithm, allows the structure to better discover the global optimum point by moving away from the local minimum point. In other words, it is one of the algorithms used to obtain the best solutions for optimization problems [63, 68, 90].

SA provides solutions for discrete, continuous and mixed-input optimization problems. While doing this solution, a random point is created in each iteration and the algorithm stops when the criteria are met. In this context, the distance of the resting point

from the current point can be explained by Boltzmann's probability distribution function shown in Equation 4.3.

$$P(E) = e^{-E/kT} \quad \textbf{(4.3)}$$

P (E) represents the probability of the energy level, E. k is the Boltzmann constant and T is the temperature. If the temperature is high, the probability of accepting the movements in the objective function will be high, and if the temperature is low, this probability will be low [74].

In addition to these, Modified Simulated Annealing (MSA) is much stronger in finding the global optimum than traditional SA. The reason of this is that it is possible to apply hybrid algorithms and to find the local minimum to speed up the loop simultaneously [91].

The main steps of the SA algorithm are given as flowchart in Figure 4.4 [49].

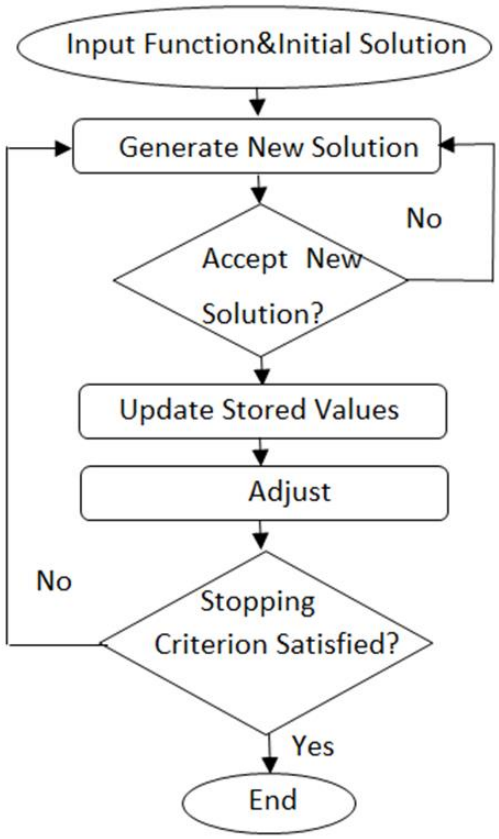

Figure 4.4. Flowchart of Simulated Annealing Algorithm

4.3.4. Modified Random Search Algorithm

The first optimization algorithm based on stochastic processes is the Random Search method, known as the Monte-Carlo method. In the first step of the algorithm, a population with random starting points is created, and then this algorithm examines and evaluates the local minimum convergence of the starting points by local search method. As a solution, the best local minimum point is chosen. Also, there is only one solution in the flow process, and at each iteration step, the solution is changed by adding a random vector. Apart from these, some changes are suggested in the controlled random search algorithm for global optimization. Experiments are one of the stochastic algorithm methods, where modified algorithms give much more meaningful results and offer good alternatives for problems that need direct search methods. In MRS, programs such as conjugate gradient, Quasi-Newton, Newton, Levenberg-Marquardt and non-linear interior point method are used for the placement of all variables in the objective function [92, 93]. A flowchart summarizing the process of Random Search algorithm is shown in Figure 4.5 [94] .

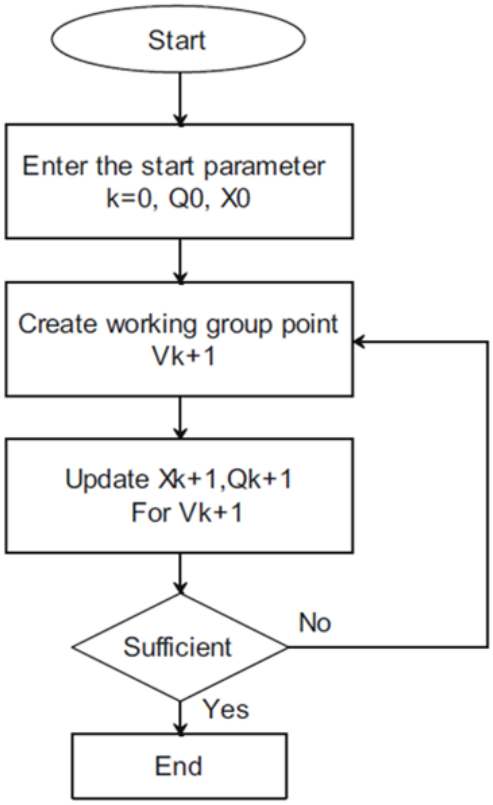

Figure 4.5. Flowchart of Random Search Algorithm

Wolfram MATHEMATICA is one of the frequently used commercial software for optimization of engineering problems. The program software uses DE, NM, RS and SA stochastic optimization algorithms in detailed above, while solving problems. The relevant options in Mathematica for these algorithms are given in Table 4.1.

Table 4.1. Corresponding options for the optimization algorithms MDE, MNM, MRS, and MSA [63]

Options	**MDE**	**MNM**	**MRS**	**MSA**
Crossover fractions	0.5	-	-	-
Random seed	1	5	0	2
Scaling factor	0.6	-	-	-
Tolerance	0.001	0.001	0.001	0.001
Contact ratio	-	0.5	-	-
Expand ratio	-	2.0	-	-
Reflect ratio	-	1.0	-	-
Shrink ratio	-	0.5	-	-
Level iterations	-	-	-	50
Perturbation scale	-	-	-	1.0
Penalty function	-	-	Automatic	-
Search points	-	-	2	-
Method	-	-	Interior point	-

CHAPTER 5

RESULTS AND DISCUSSION

5.1. Problem Definition

In this thesis, an active knee orthosis design operated using a rotary series elastic actuator designed to assist flexion and extension of the knee joint during physical therapy of patients, who have lower extremity injuries, is discussed. The design, modeling and optimization of the compliant torsion spring (elastic element), which is the most critical part of the series elastic actuators, and an actuator system that is frequently encountered and developed in the field of robotics, and helps the force-controlled robot joint drive, has been investigated.

Prior to obtaining the optimum design of torsion spring, verification of finite element analysis for von Mises stress, mass, stiffness has been carried out using specific results from previous study in the literature. In this context, the topology and geometric parameters of the spring, which is aimed to be light, compact, durable and stiff, are shown in Figure 5.1 [24]. The values of these parameters are given in Table 5.1 [24].

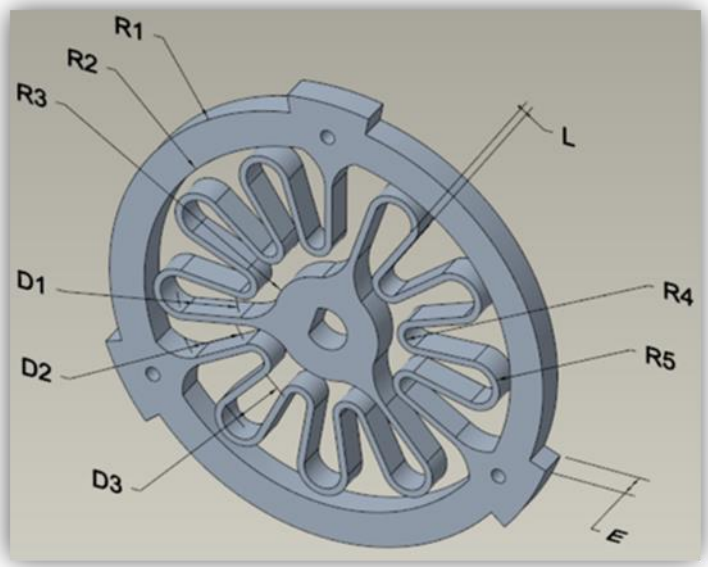

Figure 5.1. Topology of torsion spring

Table 5.1. Torsion spring geometry parameters in millimeter

E	L	D_1	D_2	D_3	R_1	R_2	R_3	R_4	R_5
6,7,8	2	17.6	17	17.1	62.5	52.5	15	2.8	5.3

The material used in the analysis is chromium-vanadium steel (AISI 6150) and its properties are given in Table 5.2 [24]. Although there are better properties on the market for spring designs, the reason for considering AISI 6150 material is its low cost and easy to find. A preliminary analysis was carried out with ANSYS Workbench software and Finite Element Method (FEM) to ensure that the stress and deformation values that will occur when the selected spring is subjected to maximum torque are less than the yield strength of the material and to determine the location of the stress concentration.

Table 5.2. Material properties of Chromium–Vanadium (AISI 6150)

Elastic Modulus	205 GPa
Shear Modulus	73 GPa
Tensile Strength: Ultimate (UTS)	940 MPa
Tensile Strength: Yield Limit	1320 MPa
Poisson's Ratio	0.291
Density	7833 kg/m^3

Meshing is crucial in finite element analysis. The number of elements created in the process of dividing the design into small parts, the element shape and the number of nodes play the main role in the analysis. Therefore, meshing is a process that should be considered in the finite element model. In this study, meshing of the torsion spring, finite element model was performed with the "automatic method" with an element size of 1.5 mm as shown in Figure 5.2, and as a result, 17275 and 25194 elements and nodes were formed on the design, respectively. In addition, the meshing quality control of the pre-analysis design was carried out considering the skewness and orthogonal quality criteria, presented in Table 5.3 [95]**.** The closer the skewness, which is between values of 0-1 and gives the ratio between the current mesh structure and the optimum mesh structure, is to zero, the better our mesh quality. Orthogonal quality, which is the other mesh quality determination criterion, is calculated with vector mechanics and 0 is the worst value and 1 is the best. Apart from these, element quality is another criterion for getting an idea of the overall mesh structure, and the closer to 1, the better the design mesh quality [95]. At the end of the meshing process, based on the above criteria, skewness, orthogonal quality

and element quality values of the design are 0.654, 0.487 0.921, respectively. In addition, these values, which are used as a basis for the evaluation of the mesh quality applied to the design, are graphically shown in Figure 5.3. By looking at the distributions, it can be seen in which region the poor quality elements are concentrated and improvements can be made as much as possible.

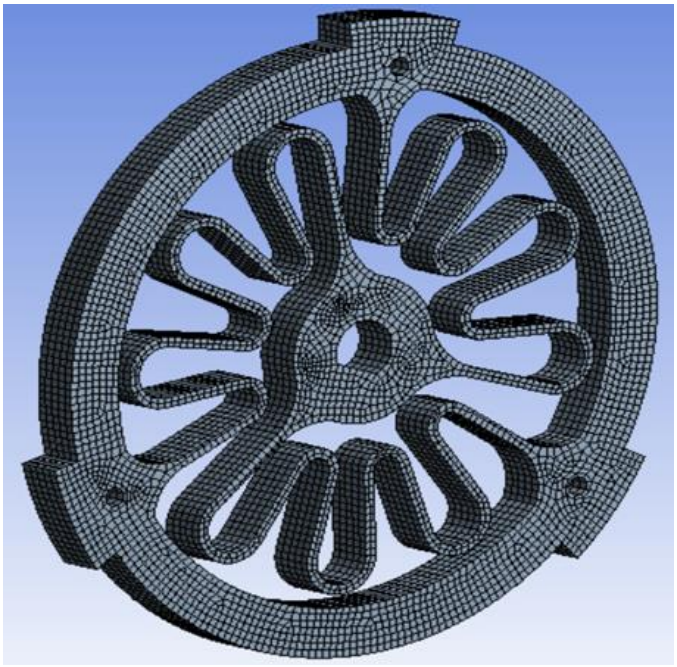

Figure 5.2. Finite element model of the design with automatic mesh elements

Table 5.3. Mesh quality metrics in ANSYS meshing

Skewness mesh metrics spectrum					
Excellent	**Very good**	**Good**	**Acceptable**	**Bad**	**Unacceptable**
0-0.25	0.25-0.50	0.50-0.80	0.80-0.94	0.95-0.97	0.98-1.00
Orthogonal Quality mesh metrics spectrum					
Unacceptable	**Bad**	**Acceptable**	**Good**	**Very good**	**Excellent**
0-0.001	0.001-0.14	0.15-0.20	0.20-0.69	0.70-0.95	0.95-1.00

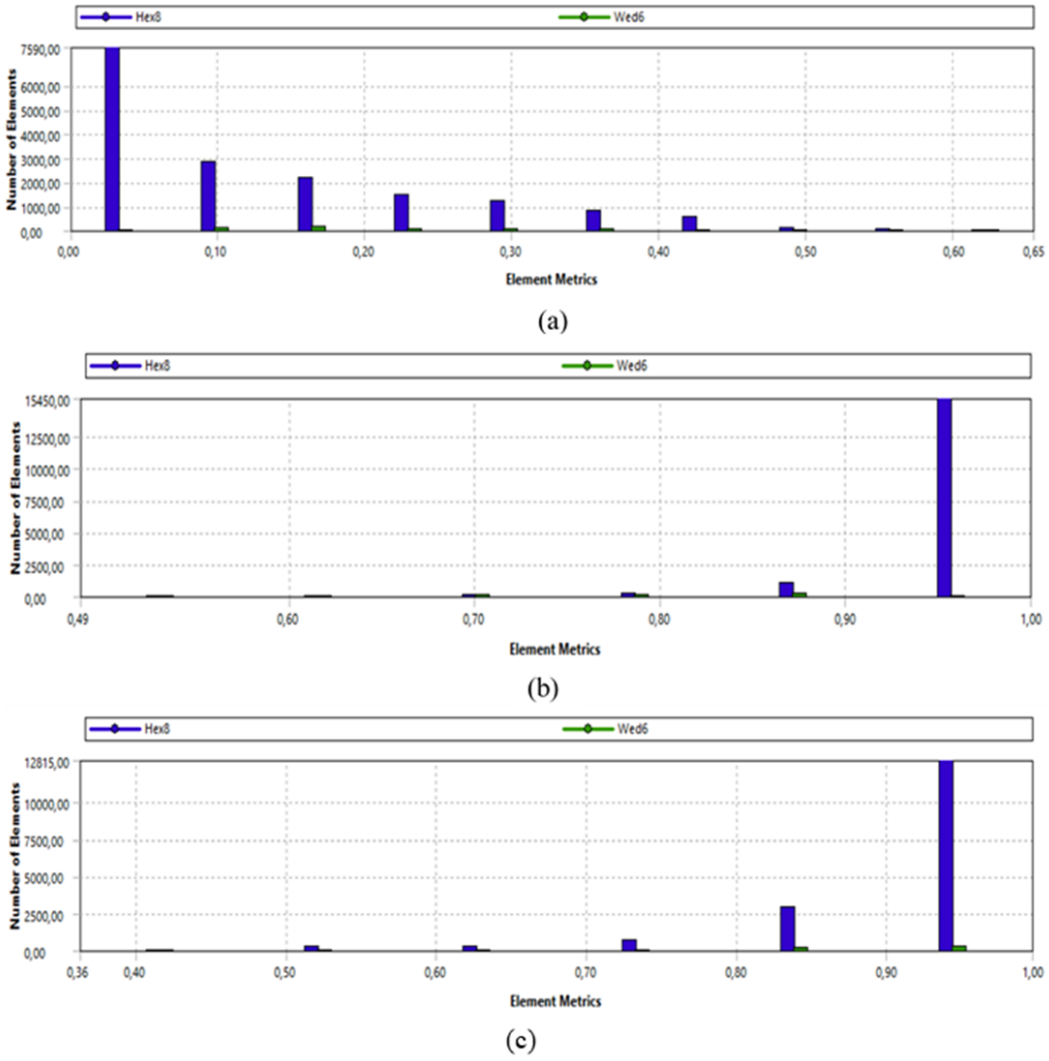

Figure 5.3. Meshing quality parameters (a) Skewness, (b) Orthogonal Quality, (c) Element Quality

After material selection and meshing for analysis, the approximate torque value was calculated according to the body mass normalized data determined for gait cycles [96]. The calculation of the approximate torque value, which is another constraint in the finite element analysis, was done according to the body mass normalized data determined for the gait cycles. It was concluded that the maximum power and torque applied to the orthosis by the knee joint were 0.739 W/kg and 0.365 Nm/kg, respectively, and that the active knee orthosis should provide 60% of the peak torque during a healthy gait [24]. Thus, for a person with a weight of approximately 70 kg, it can be expected that the knee orthosis can support a torque of up to 15 Nm. Therefore, tangential forces equivalent to the input torque of 15 Nm are applied to the outer ring of the torsion spring, while the

inner ring is kept constant, and a finite element analysis is carried out. As a result of the preliminary static analysis, it was observed that the stress concentration occurred at the inner corner radius of R_4, as shown in Figure 5.4 and changes with the thickness (E) of the spring.

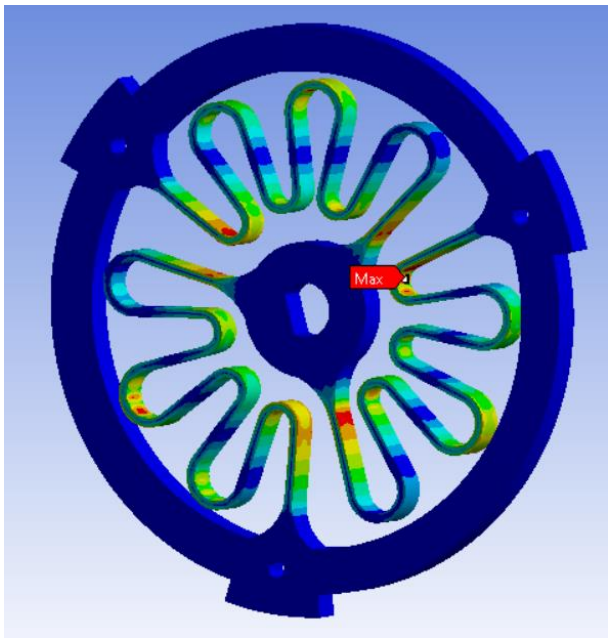

Figure 5.4. Static simulation for stress distribution of torsion spring

As a result of the literature research, it has been concluded that the stiffness value of the springs designed for series elastic actuators can take values between 100-300 N.m/rad [95-97]. In order to find the minimum stress value for these stiffness values, the radius R_4 varied from 2.5 to 3.5 mm with an increment of 0.05 mm, the thickness E was changed from 5 to 8 mm at intervals of 0.5 mm increments. In order not to change the designed topology, D_1, D_2 and D_3 values were changed with R_4 in proportion, while R_1, R_2, R_3, R_5 and L values were kept constant [24].

Considering the aforementioned analysis criteria, finite element preliminary analysis was performed for the three designs discussed in the previous study in the literature. It was decided that the parameters R_4 and E have an effect on the von Mises stress, mass and stiffness. Table 5.4 shows comparison between the present study and the study of Dossantos et al. [24] for von Mises stress, mass and stiffness. In addition, the reason why the same results cannot be obtained may be due to the version of the program used and the mesh criteria being different.

Table 5.4. Verification of response variables

Design	R_4 (mm)	E (mm)	von Mises Stress (MPa) Dossantos et al.	von Mises Stress (MPa) Present Study	Desired Stiffness (Nm/rad)	Stiffness (Nm/rad) Present Study	Mass (kg) Dossantos et al.	Mass (kg) Present Study
1	2.8	6	732	768.44	150	139.7514	0.292	0.292
2	2.8	7	622	656.69	175	163.8864	0.338	0.338
3	2.8	8	541	564.23	200	188.2700	0.384	0.384

After the verification study was completed, the appropriate regression models were created for the problem under consideration by using DOE and FEM. Afterwards, the optimization process was carried out with different optimization algorithms and hence the optimum design was obtained. These are all discussed in the following subsections.

5.2. Design of Experiment Results

Finding the optimum design for a problem experimentally can be expensive and time-consuming. However, using the relationship between the design parameters of the problem and the system responses under certain conditions, the cost and time problems can be minimized even eliminated. In this context, for our problem, first, the desired von Mises stress, mass and stiffness response (output) values of the torsion spring, the parameters (R_4 and E) and the levels that affect them were determined. Afterwards, the design of experiment method, which helps to understand and optimize the effects by changing the levels of the design variables, was applied in the same simulation set. Thus, with the help of experimental design, it is possible to obtain more precise information about the studied system, since the combined effect of all parameters can be evaluated. In order to apply the experimental design method, the levelling process was carried out for the parameters affecting the mechanical properties of the design, based on the previous study [24]. As indicated in Table 5.5, there are 21 levels for R_4 and 7 levels for E.

Table 5.5. Factors and Levels for Design of Experiment

Factors	R_4 (mm)	E (mm)
Level 1	2.50	5
Level 2	2.55	5.5
Level 3	2.60	6
Level 4	2.65	6.5
Level 5	2.70	7
Level 6	2.75	7.5
Level 7	2.80	8
Level 8	2.85	-
Level 9	2.90	-
Level 10	2.95	-
Level 11	3.00	-
Level 12	3.05	-
Level 13	3.10	-
Level 14	3.15	-
Level 15	3.20	-
Level 16	3.25	-
Level 17	3.30	-
Level 18	3.35	-
Level 19	3.40	-
Level 20	3.45	-
Level 21	3.50	-

The next step after a factor and level determination is to choose the appropriate DOE method for the problem. For this study, it is necessary to choose an experimental design method that allows different and controlled selection of the levels of structures that do not have equal effects with each other. For this reason, the D-optimal method, which is optimization-based among the DOE methods mentioned in Chapter 3, was selected. An experimental design was conducted with the Design expert program. The interface steps of Design Expert program is given in Figure 5.5 [98]. The number of factors created for the experimental design in (a) and the levels of these factors in (b), (c) were determined. In (d), the response values are determined and finally in (e), it is shown that input values of 147 simulations were formed based on the main and combined effects (2F1) of the factors.

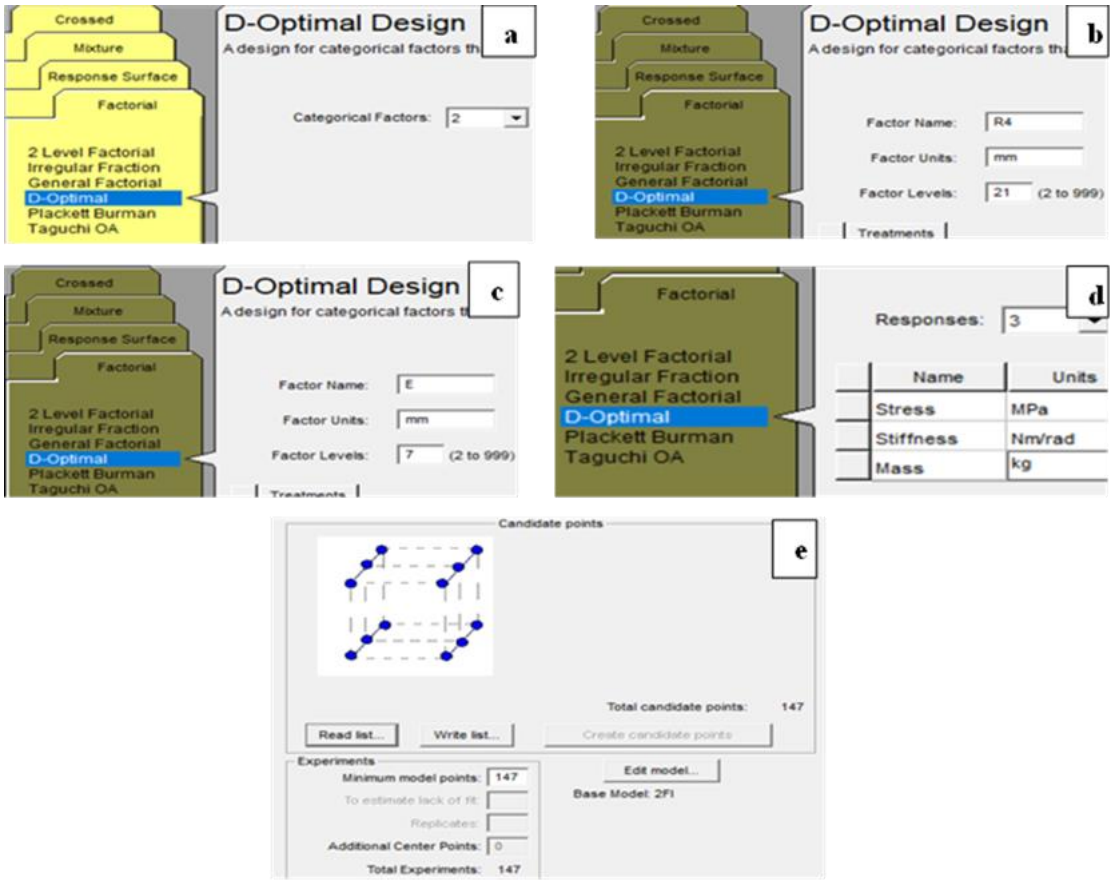

Figure 5.5. Design Expert Environments [98]

According to these obtained 147 input data (R_4 and E) , Finite Element Analysis with the help of ANSYS Software 19.2 was performed for each simulation and the corresponding response variables stress, mass and stiffness were obtained, shown in Table 5.6.

Table 5.6. Simulation data obtained by DOE and FEM

Run	R_4 (mm)	E (mm)	von Mises (MPa)	Mass (kg)	Stiffness (Nm/rad)
1	2.80	7.00	656.70	0.335	163.8864
2	3.40	5.00	925.58	0.240	110.0294
3	2.50	6.50	706.14	0.310	159.7752
4	3.40	6.50	746.29	0.312	143.8114
5	2.95	6.00	791.14	0.287	138.4258
6	2.75	5.00	920.33	0.239	116.4776
7	2.50	5.00	888.90	0.238	120.3282
8	2.85	8.00	563.18	0.383	187.6808
9	3.45	7.00	689.38	0.336	156.9286
10	3.50	6.00	771.73	0.289	124.6784
11	3.25	8.00	565.70	0.384	180.6200
12	2.55	7.50	576.77	0.358	182.9608

(cont. on next page)

Table 5.6. (cont.)

13	3.20	8.00	567.21	0.384	180.2974
14	3.45	6.00	801.93	0.288	133.1316
15	2.95	5.00	896.07	0.239	115.7516
16	3.35	6.50	727.56	0.312	145.5014
17	3.05	7.50	622.02	0.359	172.9914
18	3.35	7.00	662.24	0.336	156.6476
19	2.60	5.50	806.98	0.263	130.2302
20	3.40	8.00	594.38	0.385	179.1174
21	3.30	5.00	930.75	0.240	110.0384
22	2.50	5.50	832.41	0.262	134.3876
23	2.75	5.50	836.18	0.263	128.7752
24	2.55	6.00	725.11	0.287	144.8926
25	3.15	5.00	875.60	0.240	112.3314
26	3.25	6.50	711.84	0.312	145.1746
27	3.35	6.00	771.91	0.288	133.3600
28	2.65	6.00	750.72	0.286	143.9418
29	3.30	5.50	846.70	0.264	122.0708
30	3.25	5.00	940.20	0.240	110.8990
31	3.10	7.00	669.58	0.335	159.6730
32	2.90	7.50	638.09	0.359	174.8248
33	2.70	6.00	749.90	0.286	141.2240
34	3.00	7.50	633.74	0.360	174.3716
35	2.65	7.50	594.36	0.358	181,4718
36	3.10	6.50	693.58	0.312	147.2514
37	3.45	7.50	641.64	0.360	166.1648
38	3.10	8.00	583.50	0.383	183.4468
39	3.00	6.00	793.47	0.287	138.0014
40	3.10	7.50	622.79	0.359	171.5622
41	2.50	7.00	629.84	0.334	170.1458
42	2.55	5.00	871.34	0.238	120.1334
43	2.70	7.00	639.49	0.334	165.5972
44	2.50	6.00	762.25	0.286	145.5800
45	3.05	8.00	582.77	0.383	184.5366
46	2.50	8.00	540.94	0.382	195.5856
47	2.65	5.00	923.91	0.239	118.5552
48	3.00	7.00	681.16	0.335	161.8184
49	2.60	5.00	887.59	0.238	118.6870
50	2.90	6.00	798.88	0.287	138.7382
51	3.35	5.50	842.39	0.264	121.9244
52	3.50	8.00	565.61	0.385	176.1510
53	2.90	6.50	740.36	0.311	150.6446
54	2.80	7.50	610.52	0.359	176.1000
55	2.90	7.00	685.83	0.335	162.6884
56	2.85	5.00	960.24	0.239	116.2382
57	3.05	5.50	793.82	0.263	126.0264
58	2.75	8.00	570.41	0.382	190.7252
59	3.00	8.00	585.05	0.383	185.8890
60	3.15	7.50	624.83	0.360	170.7166
61	3.50	7.00	658.83	0.337	153.3310

(cont. on next page)

Table 5.6. (cont.)

62	2.95	5.50	814.65	0.263	127.4184
63	3.15	8.00	585.42	0.384	182.4752
64	2.75	7.00	664.18	0.334	165.9786
65	3.25	5.50	854.90	0.264	122.0390
66	2.80	6.50	709.46	0.311	151.7436
67	2.65	5.50	820.30	0.262	131.5926
68	2.70	8.00	546.63	0.382	190.2286
69	3.35	5.00	930.13	0.240	110.7192
70	2.80	8.00	564.23	0.382	188.2700
71	3.10	5.50	831.88	0.263	123.9622
72	3.05	5.00	949.97	0.239	113.5320
73	2.90	8.00	589.10	0.383	186.8866
74	2.65	7.00	639.72	0.334	168.7762
75	3.45	8.00	592.74	0.385	179.3320
76	2.60	6.50	683.51	0.310	155.7388
77	3.35	8.00	568.45	0.384	179.6684
78	2.80	5.00	936.57	0.239	117.0556
79	2.60	6.00	750.97	0.286	143.4202
80	3.30	7.50	632.74	0.361	170.2522
81	3.10	5.00	950.84	0.239	112.8802
82	2.85	7.50	609.46	0.359	176.0798
83	3.45	5.50	874.99	0.264	121.6964
84	3.20	7.50	605.81	0.360	169.6968
85	3.40	5.50	842.07	0.264	120.9196
86	3.25	6.00	867.76	0.288	127.4910
87	2.65	8.00	549.98	0.382	193.8756
88	3.20	6.50	708.69	0.312	145.9830
89	3.30	6.50	707.61	0.312	144.1444
90	2.60	7.00	632.60	0.334	168.1842
91	2.50	7.50	585.19	0.358	182.3114
92	2.80	5.50	839.06	0.263	127.7550
93	3.50	7.50	631.00	0.361	166.8786
94	3.25	7.00	659.22	0.336	156.7768
95	2.70	7.50	594.08	0.358	177.9256
96	3.50	5.50	847.45	0.264	119.6324
97	3.25	7.50	613.11	0.360	168.4784
98	2.95	8.00	547.73	0.383	187.7454
99	3.20	7.00	651.55	0.336	157.9402
100	3.30	8.00	592.71	0.384	179.7242
101	3.30	6.00	775.78	0.289	132.7306
102	3.05	6.00	726.61	0.287	137.8424
103	3.00	5.50	855.21	0.263	128.1936
104	2.65	6.50	691.61	0.310	156.2832
105	2.90	5.50	872.15	0.263	126.8298
106	3.45	5.00	961.80	0.240	110.3502
107	2.95	7.00	639.06	0.335	163.4206
108	2.85	6.50	708.15	0.311	151.7378
109	3.40	7.00	691.56	0.336	155.9114
110	3.50	6.50	710.70	0.312	142.1230

(cont. on next page)

Table 5.6 (cont.)

111	2.55	6.50	670.40	0.310	157.3218
112	3.40	7.50	643.57	0.360	167.5320
113	2.70	5.50	819.55	0.263	129.0918
114	3.15	7.00	671.77	0.336	158.8250
115	2.55	5.50	791.97	0.262	132.4640
116	3.45	6.50	743.79	0.312	142.5400
117	2.75	6.00	765.33	0.287	140.5116
118	2.95	7.50	594.09	0.359	175.5990
119	2.55	8.00	531.04	0.382	195.1596
120	3.50	5.00	916.62	0.240	114.6010
121	3.15	6.50	667.42	0.312	148.4546
122	3.20	5.00	926.66	0.240	111.6532
123	2.80	6.00	768.44	0.287	139.7514
124	3.05	7.00	668.79	0.335	160.6122
125	2.55	7.00	620.46	0.334	169.8920
126	2.85	6.00	766.89	0.287	139.7592
127	3.15	6.00	728.40	0.288	135.4476
128	3.10	6.00	761.93	0.287	135.5906
129	3.00	6.50	735.31	0.311	149.7670
130	2.60	7.50	588.19	0.358	182.8158
131	2.90	5.00	870.20	0.239	115.1720
132	2.75	7.50	617.10	0.358	178.3474
133	3.15	5.50	795.67	0.264	123.8326
134	3.20	5.50	847.08	0.264	122.8984
135	3.00	5.00	940.54	0.239	116.2438
136	3.30	7.00	680.26	0.336	158.4448
137	2.70	6.50	691.45	0.310	153.3264
138	2.70	5.00	936.89	0.239	117.9100
139	3.40	6.00	805.09	0.288	132.9708
140	2.95	6.50	733.17	0.311	150.5810
141	3.20	6.00	776.03	0.288	134.4294
142	2.75	6.50	707.95	0.311	152.5750
143	3.05	6.50	665.70	0.312	149.6866
144	2.85	7.00	655.53	0.335	163.8770
145	3.35	7.50	615.99	0.360	168.0420
146	2.60	8.00	550.79	0.382	193.2456
147	2.85	5.50	837.32	0.263	127.7622

5.3. Neuro-Regression Modeling Results

In this thesis, the first step in the optimization process of torsion spring is the mathematical modeling phase. At this stage before the optimization process, the Neuro-Regression analysis mentioned in Section 3.5, which is a combination of the Artificial Neural Network (ANN) and strengths of the traditional regression analysis, was used to increase the accuracy, robustness and reliability of the model predictions. Three output variables were modelled using Neuro-Regression analysis. In this modeling, the data set

given in Table 5.6 was randomly split into three parts. Each group in which the data set will be randomly allocated should contain 80% training data, 20% testing data and 10% of the training data then was selected as the validation data. After this percentage distinction was done. 147 original data sets were divided into five sub-headings including training, testing and validation groups with different k-fold cross validation method (described in Section 3.3) to check whether the empirical model to be selected has quality, reliability, robustness and overfitting problems. These k-folds cross validation groups are presented in Appendix A.

At this stage of the study, it was aimed to use 12 different regression models taken from literature. These models are given in Table 5.7. The coefficients (a_i, a_j, a_n, β_i, β_j, β_n, β_m, γ_j, θ_j) appearing in models have been defined by the use of data given in Appendix A. Then, $R^2_{training}$, $R^2_{trainig\ adjusted}$, $R^2_{testing}$ and $R^2_{validation}$ values were calculated with "Wolfram Mathematica 10" to test the reliability and robustness of the models.

After obtaining suitable models in terms of coefficient of determination (R^2) for each model, it is an important part of model selection that the lower and upper limits of the output, in desired physical range, additionally must be taken into consideration. In this way, the mathematical models developed for the optimization process enabled the estimation of stress, mass and stiffness parameters and the optimum value of the process parameters to obtain the desired values. In order to explain the k-fold cross validation process in detail, only the Neuro-Regression results of the von Mises for 60 models shown in Table 5.8. The results obtained for the other outputs are given in Appendix B and Appendix C**.** The coefficient of determination values for all data groups of the model to be selected from the 60-line Neuro-Regression results produced with 12 different models should be greater than 0.90 [63] and the maximum-minimum values should be in an acceptable range in line with the physical requirements of the problem. In this context, each data group is shown in different colours as seen in Table 5.8. SON2, SON3, SONR, FOTNR, SOTN, SOTNR, SOLN2, SOLN5, SOLNR1, SOLNR4 and SOLNR5 models and groups were not preferred because their $R^2_{testing}$ and maximum-minimum values are so far from data for von Mises. Among the remaining models, the linear rational (LR) model group was chosen for the von Mises output, since the model is not complex and the coefficient of determination and lower-upper limit values for all data groups are better than the others. In addition, the values in all groups are significant and acceptable for the LR model and the desired group can be selected. Therefore, the first group data and model

(LR1) were preferred for von Mises optimization analysis (Eq.5.1). $R^2_{training}$, $R^2_{adjusted}$, $R^2_{testing}$, $R^2_{validation}$ and maximum-minimum values for this model are 0.99857, 0.998436 0.970858, 0.951628, 991.489, 542.919, respectively.

$$\text{von Mises stress} = \frac{-260.1397-27.0545E+674.9903R_4-107.7284R_4^2}{-0.9617+0.0959E+0.8900R_4-0.1427R_4^2} \quad \textbf{(5.1)}$$

Table 5.7. Multiple regression model types including linear, quadratic, trigonometric, logarithmic, and their rational forms

Model Name	Nomenclature	Formula
Multiple linear	L	$Y = \sum_{i=1}^{2}(a_i x_i) + c$
Multiple linear rational	LR	$Y = \frac{\sum_{i=1}^{2}(a_i x_i) + c_1}{\sum_{j=1}^{2}(\beta_j x_j)} + c_2$
Second order multiple non-linear	SON	$Y = \sum_{k=1}^{2}\sum_{j=1}^{2}(a_j x_j x_k) + \sum_{i=1}^{2}(a_i x_i) + c$
Second order multiple non-linear rational	SONR	$Y = \frac{\sum_{k=1}^{2}\sum_{j=1}^{2}(a_j x_j x_k) + \sum_{i=1}^{2}(a_i x_i) + c_1}{\sum_{l=1}^{2}\sum_{m=1}^{2}(\beta_m x_m x_l) + \sum_{n=1}^{2}(\beta_n x_n)} + c_2$
First order trigonometric multiple non-linear	FOTN	$Y = \sum_{i=1}^{2}(a_i Sin[x_i] + a_i Cos[x_i]) + c$
First order trigonometric multiple non-linear rational	FOTNR	$Y = \frac{\sum_{i=1}^{2}(a_i Sin[x_i] + a_i Cos[x_i]) + c_1}{\sum_{j=1}^{2}(\beta_j Sin[x_j] + \gamma_j Cos[x_j])} + c_2$
Second order trigonometric multiple non-linear	SOTN	$Y = \sum_{i=1}^{2}(a_i Sin[x_i] + a_i Cos[x_i]) + \sum_{j=1}^{2}(\beta_j Sin^2[x_j] + \gamma_j Cos^2[x_j]) + c$
Second order trigonometric multiple non-linear rational	SOTNR	$Y = \frac{\sum_{i=1}^{2}(a_i Sin[x_i] + a_i Cos[x_i]) + \sum_{j=1}^{2}(\beta_j Sin^2[x_j] + \gamma_j Cos^2[x_j]) + c_1}{\sum_{k=1}^{2}(\theta_i Sin[x_k] + \theta_i Cos[x_k]) + \sum_{l=1}^{2}(\delta_j Sin^2[x_l] + \delta_j Cos^2[x_l])} + c_2$
First order logarithmic multiple non-linear	FOLN	$Y = \sum_{i=1}^{2}(a_i Log[x_i]) + c$
First order logarithmic multiple non-linear rational	FOLNR	$Y = \frac{\sum_{i=1}^{2}(a_i Log[x_i]) + c_1}{\sum_{j=1}^{2}(\beta_j Log[x_j])} + c_2$
Second order logarithmic multiple non-linear	SOLN	$Y = \sum_{k=1}^{2}\sum_{j=1}^{2}(a_j Log[x_j x_k]) + \sum_{i=1}^{2}(a_i Log[x_i]) + c$
Second order logarithmic multiple non-linear rational	SOLNR	$Y = \frac{\sum_{k=1}^{2}\sum_{j=1}^{2}(a_j Log[x_j x_k]) + \sum_{i=1}^{2}(a_i Log[x_i]) + c_1}{\sum_{m=1}^{2}\sum_{l=1}^{2}(a_l Log[x_l x_m]) + \sum_{n=1}^{2}(a_n Log[x_n])} + c_2$

Table 5.8. K-folds cross validation results of the Neuro-regression model for von Mises stress

Models	R^2 training	R^2 training Adjusted	R^2 testing	R^2 Validation	Maximum	Minimum
L1	0.998322	0.998165	0.967253	0.914878	929.849	506.065
L2	0.998414	0.998266	0.946181	0.935766	925.348	510.525
L3	0.998969	0.998873	0.944572	0.973644	935.036	495.629
L4	0.998301	0.998142	0.957456	0.932683	927.194	503.393
L5	0.998464	0.998324	0.954542	0.979779	914.453	525.281
LR1	0.998570	0.998436	0.970858	0.951628	991.489	542.919
LR2	0.998625	0.998496	0.958261	0.960475	969.587	542.608
LR3	0.999305	0.999241	0.965591	0.985722	1054.65	544.095
LR4	0.998537	0.998400	0.967307	0.953570	972.024	543.780
LR5	0.998615	0.998489	0.970128	0.972393	955.552	538.473
SON1	0.998610	0.998131	0.969204	0.956884	1190.45	250.589
~~SON2~~	~~0.998650~~	~~0.998184~~	~~0.957816~~	~~0.959428~~	~~1168.67~~	~~68.3836~~
SON3	0.999318	0.999083	0.966352	0.986512	1304.03	496.596
~~SON4~~	~~0.998575~~	~~0.998084~~	~~0.96516~~	~~0.950112~~	~~1175.48~~	~~186.863~~
SON5	0.998664	0.998219	0.516195	0.97491	3037.24	471.095
~~SONR1~~	~~0.998710~~	~~0.998265~~	~~0.967058~~	~~0.952673~~	~~$9.00268*10^{13}$~~	~~76988.9~~
~~SONR2~~	~~0.999443~~	~~0.999251~~	~~0.73424~~	~~0.962098~~	~~$4.9693*10^{10}$~~	~~537.996~~
~~SONR3~~	~~0.999421~~	~~0.999222~~	~~0.944464~~	~~0.98996~~	~~$2.14987*10^{9}$~~	~~$-2.96196*10^{9}$~~
~~SONR4~~	~~0.998692~~	~~0.998241~~	~~-1.65196~~	~~0.947681~~	~~$8.02573*10^{11}$~~	~~512.922~~
~~SONR5~~	~~0.998842~~	~~0.998455~~	~~0.712011~~	~~0.962581~~	~~$2.94548*10^{13}$~~	~~507.891~~
FOTN1	0.998148	0.997811	0.946076	0.932844	988.649	494.448
FOTN2	0.998065	0.997713	0.94996	0.919469	965.079	485.667
FOTN3	0.998661	0.998418	0.940032	0.95741	940.751	540.174
FOTN4	0.998116	0.997774	0.927802	0.906991	1002.99	481.895
FOTN5	0.998261	0.997954	0.905169	0.979354	1034.56	430.330
~~FOTNR1~~	~~0.997974~~	~~0.997606~~	~~0.933368~~	~~0.934451~~	~~$2.08191*10^{12}$~~	~~546.545~~
~~FOTNR2~~	~~0.999381~~	~~0.999268~~	~~0.956876~~	~~0.960459~~	~~$9.58283*10^{9}$~~	~~520.903~~
~~FOTNR3~~	~~0.999353~~	~~0.999236~~	~~0.964425~~	~~0.987335~~	~~1101.63~~	~~$-6.82961*10^{8}$~~
~~FOTNR4~~	~~0.998704~~	~~0.998468~~	~~0.951684~~	~~0.955103~~	~~$2.82691*10^{10}$~~	~~467.953~~
~~FOTNR5~~	~~0.980106~~	~~0.976595~~	~~0.202376~~	~~0.012695~~	~~$4.18687*10^{8}$~~	~~-115986~~
~~SOTN1~~	~~0.999041~~	~~0.995846~~	~~0.489547~~	~~0.973693~~	~~476111~~	~~$-1.06428*10^{6}$~~
~~SOTN2~~	~~0.999250~~	~~0.996751~~	~~0.924087~~	~~0.573408~~	~~236257~~	~~-549685~~
~~SOTN3~~	~~0.999618~~	~~0.998346~~	~~0.965597~~	~~0.996924~~	~~72149~~	~~-272313~~
~~SOTN4~~	~~0.999177~~	~~0.996434~~	~~0.916569~~	~~0.976491~~	~~250003~~	~~-569484~~
~~SOTN5~~	~~0.999166~~	~~0.996664~~	~~-820.991~~	~~0.989228~~	~~243302~~	~~-533436~~
~~SOTNR1~~	~~0.999473~~	~~0.997718~~	~~0.896958~~	~~0.953532~~	~~$2.85064*10^{8}$~~	~~$-3.4501*10^{10}$~~
~~SOTNR2~~	~~0.998924~~	~~0.995336~~	~~0.931642~~	~~0.990271~~	~~$1.75413*10^{14}$~~	~~$-1.3891*10^{10}$~~
~~SOTNR3~~	~~0.999675~~	~~0.998594~~	~~0.753212~~	~~0.993411~~	~~$2.16133*10^{8}$~~	~~$-4.0312*10^{11}$~~
~~SOTNR4~~	~~0.999679~~	~~0.998608~~	~~0.966562~~	~~0.992389~~	~~$1.93875*10^{12}$~~	~~$-8.92886*10^{9}$~~
~~SOTNR5~~	~~0.998794~~	~~0.995175~~	~~0.87008~~	~~0.97235~~	~~992.057~~	~~$-2.3526*10^{12}$~~
FOLN1	0.998525	0.998387	0.97387	0.941694	943.667	511.140
FOLN2	0.998592	0.99846	0.958165	0.954576	934.685	521.710
FOLN3	0.999232	0.99916	0.960789	0.984189	945.371	510.629
FOLN4	0.998505	0.998365	0.966358	0.950355	941.639	509.466
FOLN5	0.998599	0.998472	0.969512	0.9759	928.657	531.815
FOLNR1	0.998569	0.998435	0.971837	0.950839	989.868	543.810
FOLNR2	0.998627	0.998499	0.958604	0.961086	967.81	533.681
FOLNR3	0.999309	0.999245	0.965633	0.985541	1064.66	533.94
FOLNR4	0.998540	0.998403	0.967367	0.953485	984.372	543.502
FOLNR5	0.998615	0.998489	0.970757	0.972519	956.847	538.390
SOLN1	0.998607	0.998126	0.970714	0.955282	1190.17	158.995
~~SOLN2~~	~~0.998660~~	~~0.998198~~	~~0.957051~~	~~0.960282~~	~~1207.61~~	~~-124.174~~

(cont. on next page)

Table 5.8 (cont.)

SOLN3	0.999332	0.999102	0.967513	0.987526	1333.09	526.771
SOLN4	0.998577	0.998086	0.965957	0.952349	1156.41	314.571
~~SOLN5~~	~~0.998664~~	~~0.998219~~	~~-0.170716~~	~~0.973618~~	~~3277.91~~	~~451.397~~
~~SOLNR1~~	~~0.998820~~	~~0.998414~~	~~0.971126~~	~~0.949918~~	~~$1.98799*10^9$~~	~~509.993~~
SOLNR2	0.999376	0.999161	0.888161	0.962731	1004.21	543.866
SOLNR3	0.999338	0.999109	0.963842	0.986834	1023.16	528.676
~~SOLNR4~~	~~0.998655~~	~~0.998192~~	~~0.939537~~	~~0.950081~~	~~$6.04575*10^{10}$~~	~~7.74106~~
~~SOLNR5~~	~~0.999257~~	~~0.99901~~	~~0.920979~~	~~0.964228~~	~~$2.0161*10^9$~~	~~543.064~~

According to the model chosen for von Mises stress, the effect of R_4 and E values on the von Mises stress value is shown by the three-dimensional plot in Figure 5.6. In addition contour plot is used to see how the output value related to input values (See Figure 5.7.a). Each colour shows a different von Mises value and this colour distribution is separated by the contour line. The sharp contour lines show the sudden rise and fall of the von Mises value according to the data. High stress values are indicated by light colours, while low ones are identified by darker colours. Figure 5.7b shows the results obtained by combining the data and the model in colour. As seen in the figure, it is seen that a linear model is captured with the data with nonlinear distribution.

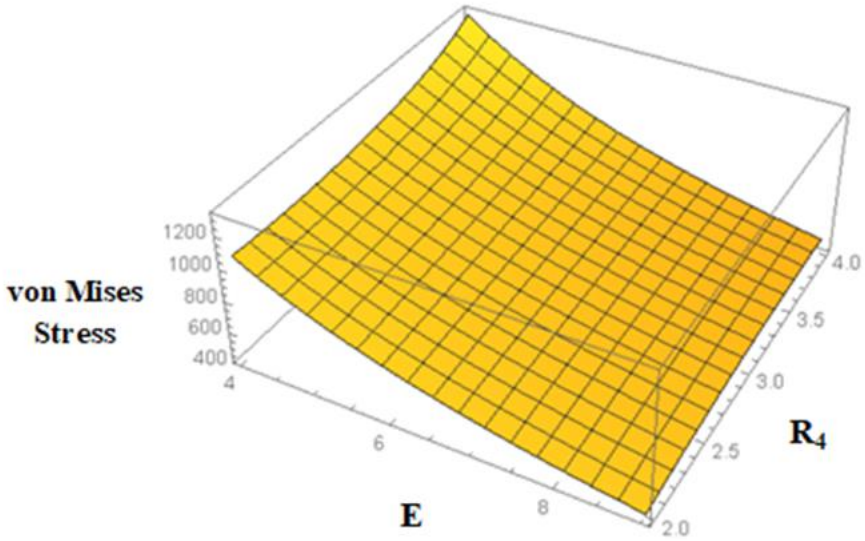

Figure 5.6. Effect of R_4 and E for von Mises stress

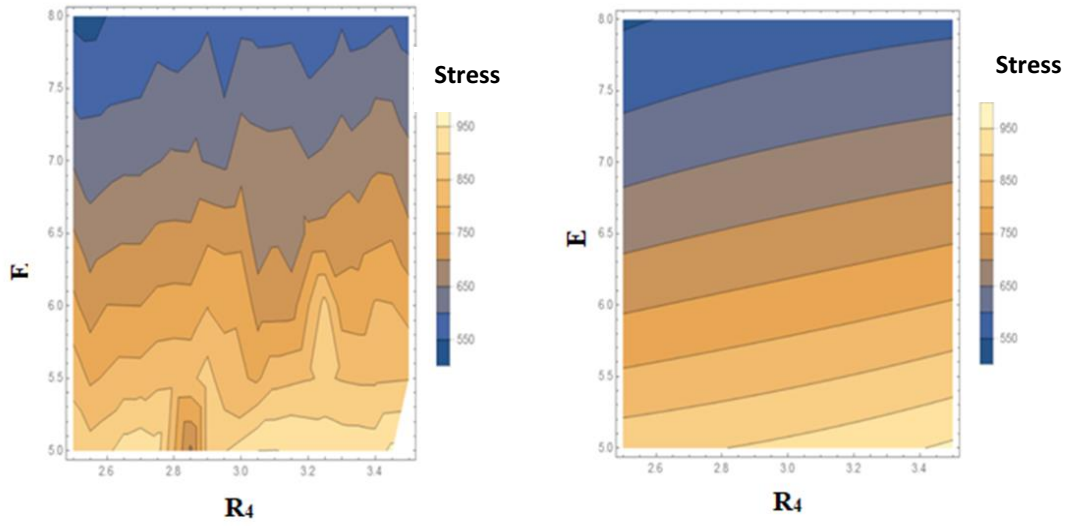

(a) Effect of data distribution on von Mises (b) Effect of data and model on von Mises

Figure 5.7. Contour Plots for von Mises stress

For mass output, a model was selected by considering the same criteria. Among the 12 models and 60 groups in Appendix B, SONR2, SONR3, SONR4, SONR5, FOTNR3, SOTN, SOTNR models and groups could not be preferred because the R_2testing value was negative and the maximum-minimum limits did not match the mass values in Table 5.6. Among the remaining models after elimination, the model group with the highest correlation values and an uncomplicated one was selected. The model group selected for Mass is shown in Table 5.9. As can be seen in the table, the first group and the model (L) were chosen randomly for the optimization analysis of the mass (Eq.5.2), since the values of all groups are very significant. R^2 training, R^2 adjusted, R^2 testing and R^2 validation maximum-minimum values for this model are 0.999999, 0.999999, 0.999942, 0.999927, 0.384793, 0.237745, respectively.

$$\text{Mass} = -0.00893 + 0.04799\text{E} + 0.00299\text{R}_4 - 0.000088\text{R}_4^2 \quad \textbf{(5.2)}$$

Table 5.9. Cross Validation Results of the Selected Neuro-Regression Models for Mass

Models	R^2 training	R^2 training Adjusted	R^2 testing	R^2 validation	Maximum	Minimum
L1	0.999999	0.999999	0.999942	0.999927	0.384793	0.237745
L2	0.999999	0.999999	0.999933	0.999941	0.385148	0.237448
L3	0.999999	0.999999	0.999942	0.999938	0.384804	0.237737
L4	0.999999	0.999999	0.999950	0.999926	0.385172	0.237456
L5	0.999999	0.999999	0.999944	0.999968	0.384796	0.237731

The effect of R_4 and E values for the model chosen for mass is shown in the three-dimensional graph in Figure 5.8. Then it is detailed with contour plot in Figure 5.9. Contrary to the effect of the data on the von Mises stress output, the data used for the mass showed small deviations in between and slightly wavy, near-linear contour lines were formed (Figure 5.9a). This is because the R_4 input change has little effect on the mass, while the changes in the E input have a large effect on the mass, as can be seen from the sudden colour transitions. The graphic in Figure 5.9b, which is formed by fitting the data to the model, has almost completely horizontal contour lines. In other words, when the data is fitted to the model, the fluctuations are considerably reduced. This shows that the effect of the R_4 change is gradually decreasing when considered in terms of the model for the mass.

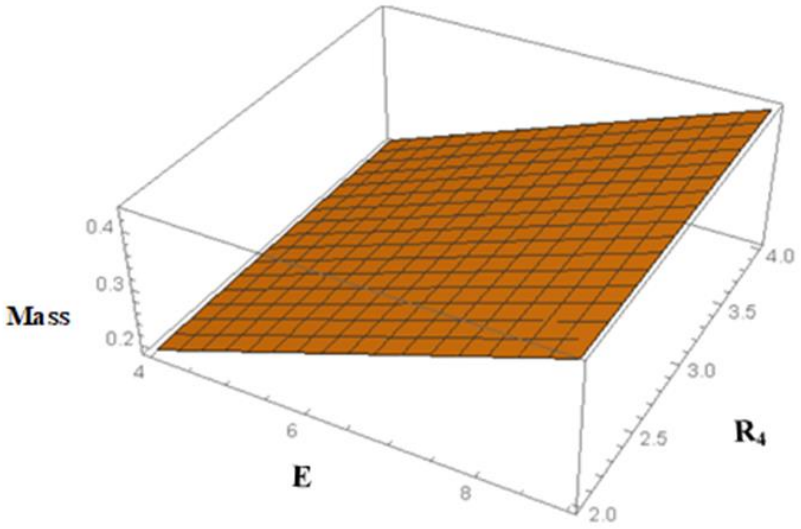

Figure 5.8. Effect of R_4 and E for mass

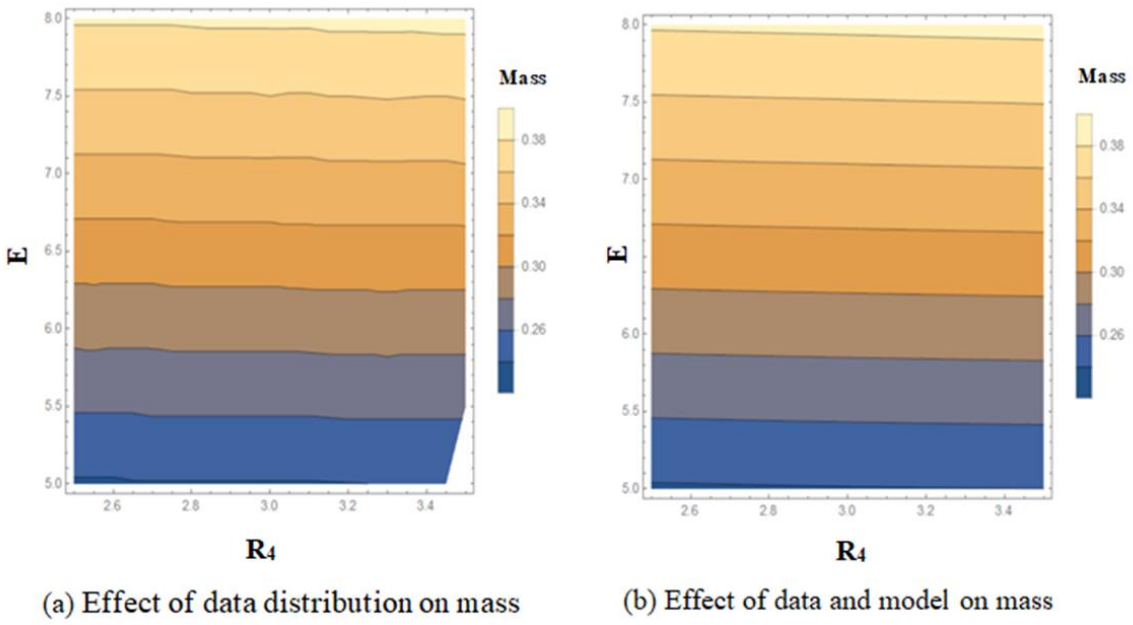

(a) Effect of data distribution on mass (b) Effect of data and model on mass

Figure 5.9. Contour Plots for Mass

The analysis results for the stiffness parameter, which is the last output, are included in Appendix C. Among the models and groups created, SONR, SOTN, SONTR2, SOTNR3, SOTNR4, SOTNR5, SOLNR models were eliminated because the R^2testing value was less than 0.90 and the maximum-minimum values for this design variable were in the physical ranges. In Appendix C Afterwards, the model group with the highest correlation value and the simplest one (Linear equation) was selected for the stiffness output. Table 5.10 shows the model group selected for the stiffness output. As seen in the table, the first group and the model (L) were randomly chosen for the optimization analysis of the stiffness (Eq.5.3). $R^2_{training}$, $R^2_{adjusted}$, $R^2_{testing}$ and $R^2_{validation}$ maximum-minimum values for this model are 0.999937, 0.999931, 0.992763, 0.997713, 194.749, and 106.052, respectively.

$$\text{Stiffness} = 60.49094 + 23.92919\ \text{E} - 28.61375\ \text{R4} + 2.15705\ \text{R4}^2 \qquad \textbf{(5.3)}$$

Table 5.10. Cross Validation Results of the Selected Neuro-Regression Models for Stiffness

Models	R^2 training	R^2 training Adjusted	R^2 testing	R^2 validation	Maximum	Minimum
L1	0.999937	0.999931	0.992763	0.997713	194.749	106.052
L2	0.999912	0.999904	0.995187	0.991430	193.979	106.807
L3	0.999900	0.999891	0.997358	0.998608	193.933	106.689
L4	0.999894	0.999884	0.998327	0.997175	194.122	106.833
L5	0.999907	0.999899	0.996349	0.990546	196.138	105.961

In Figure 5.10, it is shown in the form of a three-dimensional graphic that the stiffness value changes between about 100 N.m/rad and 200 N.m/rad according to the change of R_4 and E. The relationship between inputs, model and output is shown in Figure 5.11 in more detail. Figure 5.11a shows the interaction of R_4, E and output values obtained as a result of data analysis. Sharp contour lines represent sudden shifts in stiffness values ranging from about 110 to 200. In other words, it is understood that the input values that create the sharp lines are more effective than the others. Apart from these, Figure 5.11b shows the relationship between the data and the model to which the data is fitted. As can be seen, the data created a linear effect on the model selected for stiffness.

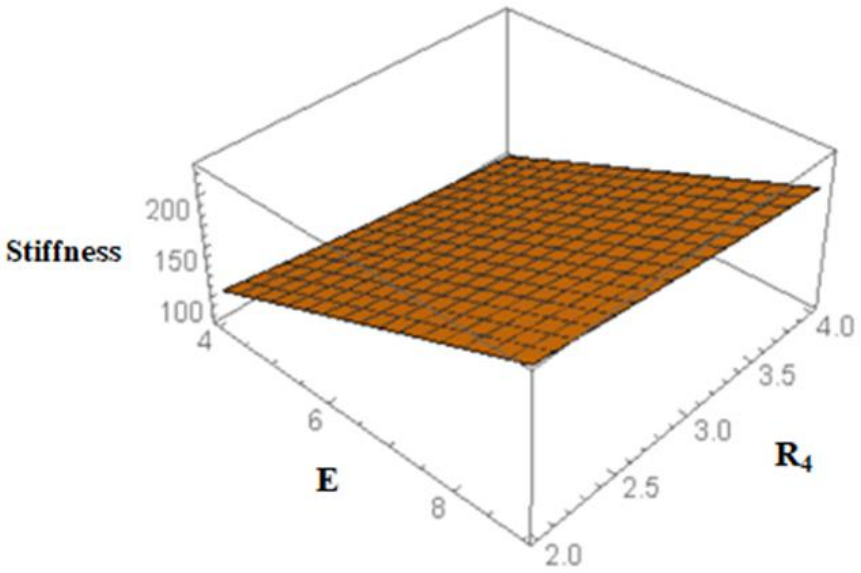

Figure 5.10. Effects of R_4 and E for Stiffness

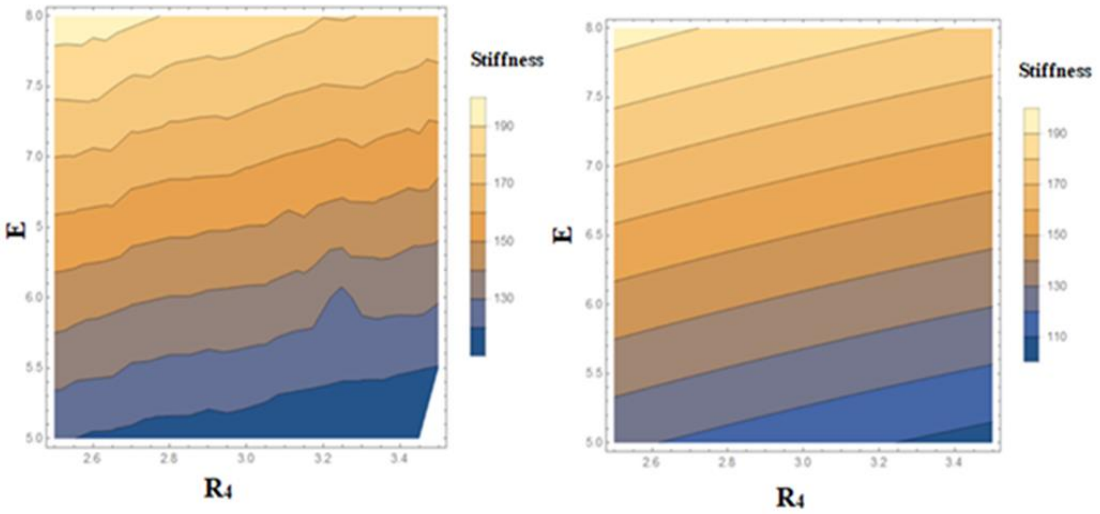

Figure 5.11. Contour Plots for the Stiffness

5.4. Optimization Results

The purpose of regression analysis and optimization studies is to investigate whether classical regression analysis and optimization applications provide the desired results, and whether more stable and more optimum results can be obtained by using the same design parameters. In this context, as a result of the R^2 values examined in Section 5.3, three different models (Eq.5.1, Eq.5.2 and Eq.5.3) that correctly express the physical problem were selected for the three response variables.

In this part of the thesis, it is aimed to determine the optimal values of the system parameters that minimize the stress and mass values of the torsion spring of the SEA used for rehabilitation robots. Regression models were created for each output. The mathematical models with which the output data converged the most were determined as objective functions. As shown in Table 5.11, two optimization problems for von Mises stress and mass, and five sub-scenarios for each problem were determined for the optimization processes. The stiffness, which is an important factor for torsion springs, was considered as a constraint. In addition, the defined problems and sub-scenarios given in detailed below. These optimization processes were carried out using the stochastic methods “Differential Evolution”, “Simulated Annealing”, “Random Search” and “Nelder-Mead” algorithms with the help of “NMinimize” tool in "Wolfram MATHEMATICA 10" program. Options for the used stochastic methods are shown in

Table 4.1. In addition, the related optimization study performed with the "Wolfram Mathematica 10" program.

Table 5.11. Optimization scenarios for each problem

Scenario	Optimization Problem 1 (von Mises stress)	Scenario	Optimization Problem 2 (Mass)
1a	$2.5 \leq R_4 \leq 3.5$ $5 \leq E \leq 8$ $16.987 \leq D_2 \leq 17.014$ $17.064 \leq D_3 \leq 17.12$	2a	$2.5 \leq R_4 \leq 3.5$ $5 \leq E \leq 8$ $16.987 \leq D_2 \leq 17.014$ $17.064 \leq D_3 \leq 17.12$
1b	$2.5 \leq R_4 \leq 3.5$ $5 \leq E \leq 8$	2b	$2.5 \leq R_4 \leq 3.5$ $5 \leq E \leq 8$
1c	**Stiffness** ≥ 197.5 $2.5 \leq R4 \leq 3.5$ $5 \leq E \leq 8$	2c	**Stiffness** ≥ 146.021 $2.5 \leq R_4 \leq 3.5$ $5 \leq E \leq 8$
1d	**Mass** ≤ 0.299 $2.5 \leq R_4 \leq 3.5$ $5 \leq E \leq 8$	2d	**Stress** ≤ 747.01 $2.5 \leq R_4 \leq 3.5$ $5 \leq E \leq 8$
1e	**Stiffness** ≥ 146.1 **Mass** ≤ 0.299 $2.5 \leq R_4 \leq 3.5$ $5 \leq E \leq 8$	2e	**Stiffness** ≥ 157.9785 **Stress** ≤ 684.317 $2.5 \leq R_4 \leq 3.5$ $5 \leq E \leq 8$

In scenarios 1a and 2a, it is aimed to examine the theoretical limits of the physical phenomenon [24] discussed. For this reason, an optimization study has been carried out by specifying the upper and lower limits where the input values are constant in the range, without any extra constraints. With these scenarios, the minimum stress and mass values in the range of input parameters were investigated without any strength restrictions for the torsion spring.

In scenarios 1b and 2b for both objective functions, input values that directly affect the response values obtained as a result of the Finite Element analysis are considered. In this context, since the parameters R_4 and E were decided as the independent input variables, the optimization process was carried out by expressing the parameters D_2 and D_3 in terms of R_4 and E in Scenario 1. Depending on the tolerance related to the mesh density created with finite elements, the increased levels of the R_4 and E constraints were determined as 0.5 and 0.05, respectively. This scenario offers safer solutions for designing a lighter spring by not exceeding the yield strength limit of used material.

Unlike scenario 1b, in scenario 1c, the active stiffness constraint for the von Mises stress model is given as greater than or equal to 197.5 Nm/rad. The purpose of this scenario is to obtain a more durable spring design above a certain stiffness value in order

to obtain the minimum stress value when the input parameters are defined in certain ranges.

In scenario 2c, which was conducted for mass minimization, after many optimization attempts, it was decided that the active stiffness constraint for this model was 146.021 Nm/rad. In this scenario, it was aimed to minimize the mass of designs with stiffness equal to or greater than 146.021 Nm/rad by defining the input parameters at continuous intervals with certain increments as in Scenario 2b.

Within the scope of this thesis, since a light, compact, durable and stiff torsion spring design is aimed, it was decided that the mass should be equal to or less than 0.299 kilograms as another constraint in scenario 1d. As in other scenarios, in addition to this constraint, input parameters are defined at certain incremental and continuous intervals. Thanks to this scenario, it is possible to obtain lightweight spring designs with low stresses.

Scenario 2d can be thought of as an optimization problem, which is a validation of scenario 1d. In this scenario, a stress constraint of 747.01 MPa is considered in addition to defining the input values as continuous intervals when the objective function is mass. The aim here is to obtain a torsion spring with low stresses while planning a lightweight spring design, as in scenario 1d. In other words, the main purpose of scenarios 1d and 2d is to find out what the minimum mass or stress limit of the spring is so that there is no yield [24, 99] at the stress value to which the spring material is exposed.

In scenario 1e, combination of Scenario 1c and 1d, hybrid effects of stiffness and mass parameters on the objective function was examined. In this problem, while the constraint for mass was 0.299 kg, the stiffness parameter was active at 146.1 Nm/rad for the model, and the scenario was created with these nonlinear constraints. The aim here is to observe how much the optimum result changes if the variables must be under certain constraints.

In Scenario 2e, similar situations were checked as in Scenario 1e. Scenario 2e was constructed to examine the impact of hybrid effects of scenarios 1c and 1d on the response variable. In this context, the stiffness value was accepted as 157.9785 Nm/rad as the nonlinear constraint, while the stress value was considered as 684.317 MPa. The purpose of this scenario is to examine how much mass can be minimized under hybrid nonlinear constraints.

5.4.1. Optimization Results for von Mises Stress Output

Table 5.12 shows the results of optimization problems for von Mises stress model. According to these results;

In Scenario 1a, stress value, which is the objective function for all optimization algorithms, is found to be 542.919 Mpa and the suggested input parameters are given. In addition, mass and stiffness values, which are other corresponding output values for the result, were found to be 0.382126 kg and 194.749 Nm/rad, respectively. That is, the maximum stress value that the torsion spring can withstand without yielding is 542.919 MPa within the given constraints.

For Scenario 1b, the minimum von Mises stress values in all optimization algorithms were obtained as 543.674 MPa, while the other compatible output values, the mass and stiffness values, and were found to be 0.381703 kg and 193.872 Nm/rad, respectively. The suggested input parameters for these outputs are defined as R_4=2.5 and E=8. In this case, the material will be able to work reliably up to a stress value of 543.674 MPa within the constraints determined before reaching the yield limit.

As a result of the analyses made in scenario 1b, it was decided that the stiffness parameter was inactive for this problem with a value of 197.4362 Nm/rad. Therefore, Scenario 1c is proposed. While 197.4362 Nm/rad is still an inactive constraint in the solutions produced by the MNM and MRS algorithms, as can be seen from the result of the MSA algorithm, this problem is active in the stiffness value of 239.969 Nm/rad and gave the best result of the minimum von Mises stress. However, it could not produce values in the relevant range within the tolerances for the E parameter. On the other hand, in the solution of the MDE algorithm, it is seen that the change in the digits after the comma of the von Mises value changes the structure and gives a better stiffness value.

When the 1d scenario is solved with the MNM and MSA optimization algorithms, the obtained 0.381703 kg value does not match with the nonlinear constraint mass $\leq$ 0.299, so the obtained solutions with these algorithms are not considered. While the minimum von Mises stress value was found to be 742.487 MPa within the constraints of the MDE algorithm, the corresponding outputs of mass and stiffness values were found to be 0.285957 kg and 146.013 Nm/rad, respectively. In the part of the scenario 1dsolved with the MRS algorithm, the results obtained are 757.644 MPa, 0.286647 kg and 141.691 Nm/rad values for stress, mass and stiffness, respectively. As a result, in this scenario, according to the comparison of optimization results, it is concluded that the computational

performance of MDE is better than other algorithms to find the global optimum of torsion spring design problems.

In scenario 1e, the design analysis is performed with the stiffness value above 146.1 Nm/rad, provided that the mass constraint is the same as scenario 1d. But better results than the previous scenario could not be obtained. For this reason, it is clearly seen that there is no benefit from both the stiffness value and the mass simultaneously within the given constraints. In such cases, instead of investigating the hybrid effect, as a different optimization scenario, it is decided which constraint is more important and if the constraints are allowed within certain tolerances, optimum results can be obtained.

Table 5.12. Results of the optimization problem for von Mises Stress Model

Scenario No	Constraints	Optimization Algorithms	Output1 vonMises (MPa)	Output2 Weight (kg)	Output3 Stiffness (Nm/rad)	Suggested Design
1a	$2.5 \leq R_4 \leq 3.5$ $5 \leq E \leq 8$ $16.987 \leq D_2 \leq 17.014$ $17.064 \leq D_3 \leq 17.12$	MNM	542.919	0.382126	194.749	R_4=2.5, E=8, D_2=17.014, D_3=17.064
		MDE	542.919	0.382126	194.749	R_4=2.5, E=8, D_2=17.014, D_3=17.064
		MSA	542.919	0.382126	194.749	R_4=2.5, E=8, D_2=17.014, D_3=17.064
		MRS	542.919	0.382126	194.749	R_4=2.5, E=8, D_2=17.014, D_3=17.064
1b	$2.5 \leq R_4 \leq 3.5$ $5 \leq E \leq 8$	MNM	543.674	0.381703	193.872	R_4=2.5, E=8
		MDE	543.674	0.381703	193.872	R_4=2.5, E=8
		MSA	543.674	0.381703	193.872	R_4=2.5, E=8
		MRS	543.674	0.381703	193.872	R_4=2.5, E=8
1c	Stiffness $\geq$ 197.4362 $2.5 \leq R_4 \leq 3.5$ $5 \leq E \leq 8$	MNM	543.674	0.381703	193.872	R_4=2.5, E=8
		MDE	543.2312	0.381751	197.43623	R_4=2.51, E=7.58
		~~MSA~~	~~416.522~~	~~0.477560~~	~~239.969~~	~~R_4=2.6, E=10~~
		MRS	543.674	0.381703	193.872	R_4=2.5, E=8
1d	Mass $\leq$ 0.299 $2.5 \leq R_4 \leq 3.5$ $5 \leq E \leq 8$	~~MNM~~	~~543.674~~	~~0.381703~~	~~193.872~~	~~R_4=2.5, E=8~~
		MDE	742.487	0.285957	146.013	R_4=2.5, E=6
		~~MSA~~	~~543.674~~	~~0.381703~~	~~193.872~~	~~R_4=2.5, E=8~~
		MRS	757.644	0.286647	141.691	R_4=2.75, E=6
1e	Stiffness $\geq$ 146.1 Mass $\leq$ 0.299 $2.5 \leq R_4 \leq 3.5$ $5 \leq E \leq 8$	MNM	543.674	0.381703	193.872	R_4=2.5, E=8
		MDE	684.317	0.309908	157.978	R_4=2.5, E=6.5
		MSA	543.674	0.381703	193.872	R_4=2.5, E=8
		MRS	684.317	0.309908	157.978	R_4=2.5, E=6.5

5.4.2. Optimization Results for Mass Output

Table 5.13 contains the minimum optimization results for the mass of the torsion spring. According to these results ;

In Scenario 2a, the mass value, which is the objective function for all optimization algorithms, was found to be 0.238027 kg. The suggested input parameters R_4, E, D_2 and D_3 for this result were calculated as 2.5 mm, 5 mm, 16.987 mm and 17.12 mm, respectively. In addition, stress and stiffness values, which are other corresponding output values for the result, were found to be 917.622 MPa and 193.872 Nm/rad, respectively. In other words, regardless of the optimization algorithm selection, within the given constraints, the lightest design of the torsion spring is 0.238027 kg.

For Scenario 2b, the mass value is the same and 0.238027 kg in MNM, MDE and MSA optimization algorithms, while the corresponding outputs stress and stiffness values are 882.712 MPa and 122.084 Nm/rad. On the other hand, when the same problem was solved with the MRS algorithm, the mass, stress and stiffness values were calculated as 0.239623 kg, 928.353 MPa and 110.661 Nm/rad, respectively. Among these different results, the result that is suitable for the study and engineering limits can be selected. Since our problem is mass minimization, MNM, MDE and MSA optimization algorithms gave more meaningful results.

When scenario 2c, created with the stiffness constraint added to Scenario 2b, is examined, it is seen in the table that there are improvements in the stress and stiffness values for output values for all optimization algorithms. When this problem was solved with MNM, MDE and MSA algorithms, the stress, mass and stiffness values were found to be 684.317 MPa, 0.309908 kg and 157.978 N.m/rad, respectively, while 702.909 MPa, 0.310731 kg, 152.824 N.m/rad were found with the MRS algorithm. Considering the engineering limits of the problem, it has been observed that MNM, MDE and MSA algorithms give more realistic results. According to these results, it is seen that the maximum stress value that the spring with a stiffness of 152.824 N.m/rad and a weight of 0.309908 kg can withstand without yielding is 684.317 MPa.

In scenario 2d, which has a stress constraint, it is seen that the first three optimization algorithms give the same results (stress, mass and stiffness values are 742.487 MPa, 0.285957 kg, 146.013 Nm/rad) for this scenario respectively. Unlike these, in the MRS algorithm, the values of 705.776 MPa, 0.310861 kg and 152.002 Nm/rad were obtained for these outputs, respectively. From these different results, a suitable result for the engineering limits of the problem can be selected. If the results of MNM, MDE and MSA algorithms are chosen, we will choose a lighter but softer spring than the other algorithm. If we consider the results of the MRS algorithm, we get a heavier but stiffer

spring with a lower stress value. In other words, analysing with different algorithms gives the chance to choose according to the requirements, taking into account such effects.

In scenario 2e, which includes the hybrid effects of scenario 2c and 2d, it is seen that the values closest to the engineering limits of the problem are obtained. While MNM, MSA and MRS gave the same results for this problem, MDE offered different solutions.

Table 5.13. Results of optimization problem for Mass Model

Scenario No	**Constraints**	**Optimization Algorithms**	**Output1 vonMises (MPa)**	**Output2 Mass (kg)**	**Output3 Stiffness (Nm/rad)**	**Suggested Design**
2a	$2.5 \leq R_4 \leq 3.5$ $5 \leq E \leq 8$ $16.987 \leq D_2 \leq 17.01$ $17.064 \leq D_3 \leq 17.12$	MNM	917.622	0.238027	193.872	R_4=2.5, E=5, D_2=16.987, D_3=17.12
		MDE	917.622	0.238027	193.872	R_4=2.5, E=5, D_2=16.987, D_3=17.12
		MSA	917.622	0.238027	193.872	R_4=2.5, E=5, D_2=16.987, D_3=17.12
		MRS	917.622	0.238027	193.872	R_4=2.5, E=5, D_2=16.987, D_3=17.12
2b	$2.5 \leq R_4 \leq 3.5$ $5 \leq E \leq 8$	MNM	882.712	0.238027	122.084	R_4=2.5, E=5
		MDE	882.712	0.238027	122.084	R_4=2.5, E=5
		MSA	882.712	0.238027	122.084	R_4=2.5, E=5
		MRS	928.353	0.239623	110.661	R_4=3.2, E=5
2c	Stiffness ≥146.021 $2.5 \leq R_4 \leq 3.5$ $5 \leq E \leq 8$	MNM	684.317	0.309908	157.978	R_4=2.5, E=6.5
		MDE	684.317	0.309908	157.978	R_4=2.5, E=6.5
		MSA	684.317	0.309908	157.978	R_4=2.5, E=6.5
		MRS	702.909	0.310731	152.824	R_4=2.5, E=7.5
2d	Stress ≤ 747.01 $2.5 \leq R_4 \leq 3.5$ $5 \leq E \leq 8$	MNM	742.487	0.285957	146.013	R_4=2.5, E=6
		MDE	742.487	0.285957	146.013	R_4=2.5, E=6
		MSA	745.596	0.286101	145.127	R_4=2.55, E=6
		MRS	705.776	0.310861	152.002	R_4=2.85, E=6.5
2e	Stiffness≥157.9785 Stress ≤ 684.317 $2.5 \leq R_4 \leq 3.5$ $5 \leq E \leq 8$	MNM	632.398	0.333849	169.943	R_4=2.5, E=7
		MDE	684.317	0.309908	157.978	R_4=2.5, E=7
		MSA	632.398	0.333849	169.943	R_4=2.5, E=7.5
		MRS	632.398	0.333849	169.943	R_4=2.5, E=7.5

In Figures 5.12 and 5.13, convergence graphs of the minimization results obtained with four different search algorithms for von Mises and mass objective functions are given. The production number specifies when to stop the algorithms and has different values for each design. In addition, it is seen that there is stability after 40 iterations for MDE and MNM optimization algorithms. On the other hand, in the solutions of the MSA algorithm, the reason for jumping after about 100 iterations and coming back to the same value is that there is no improvement in successive iterations, confirming that the optimum result is after about 40 iterations.

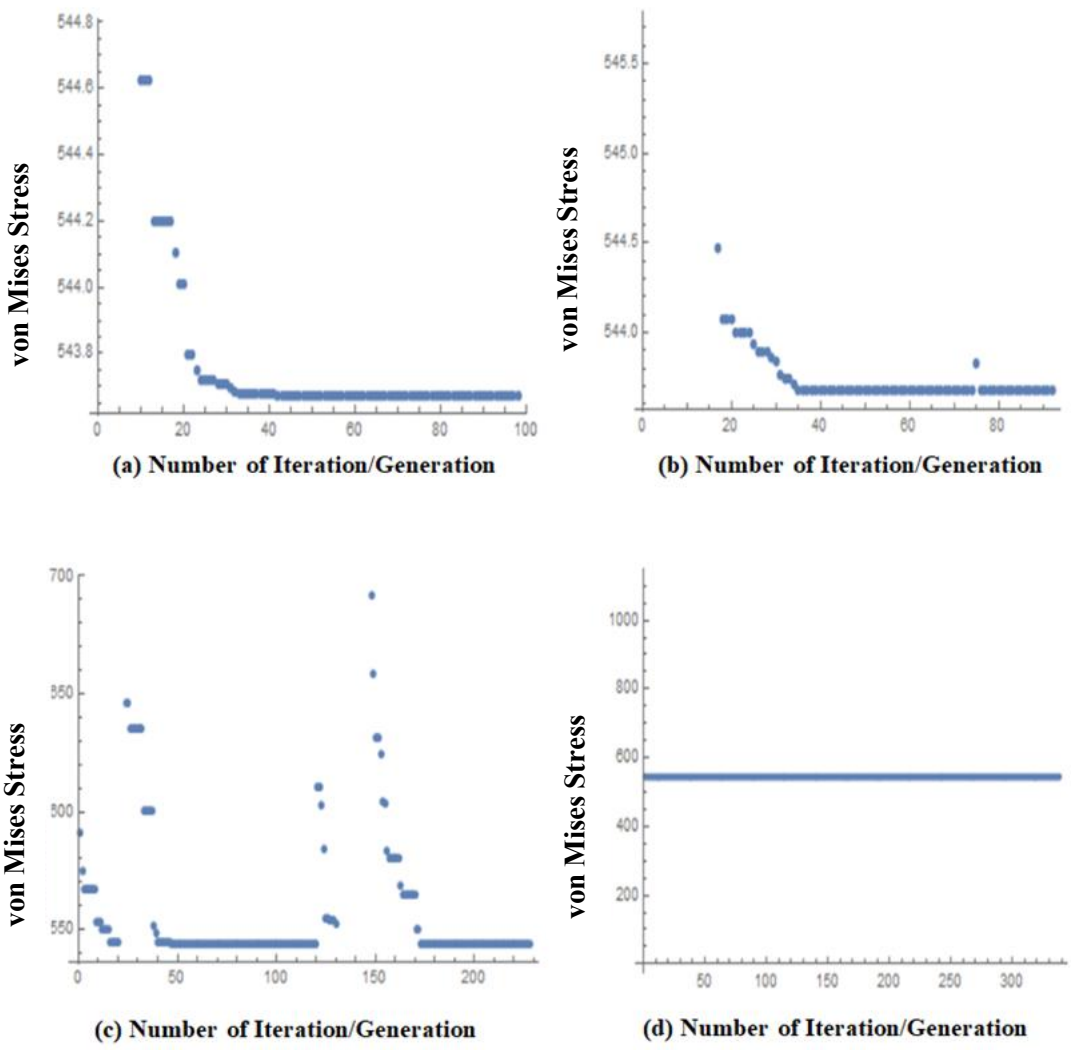

Figure 5.12. Convergence graphic representations of the stochastic algorithms for von Mises Stress (a) MDE, (b) MNM, (c) MSA, and (d) MRS

The linear answer of the random search algorithm shows that it uses the minimum and maximum values of the constraints of the independent variable as an initial guess in the solution steps. When the value of the von Mises objective function is generated for the case where R_4 is minimum and E is maximum, no iterative progression has taken place after the values used as an initial guess.

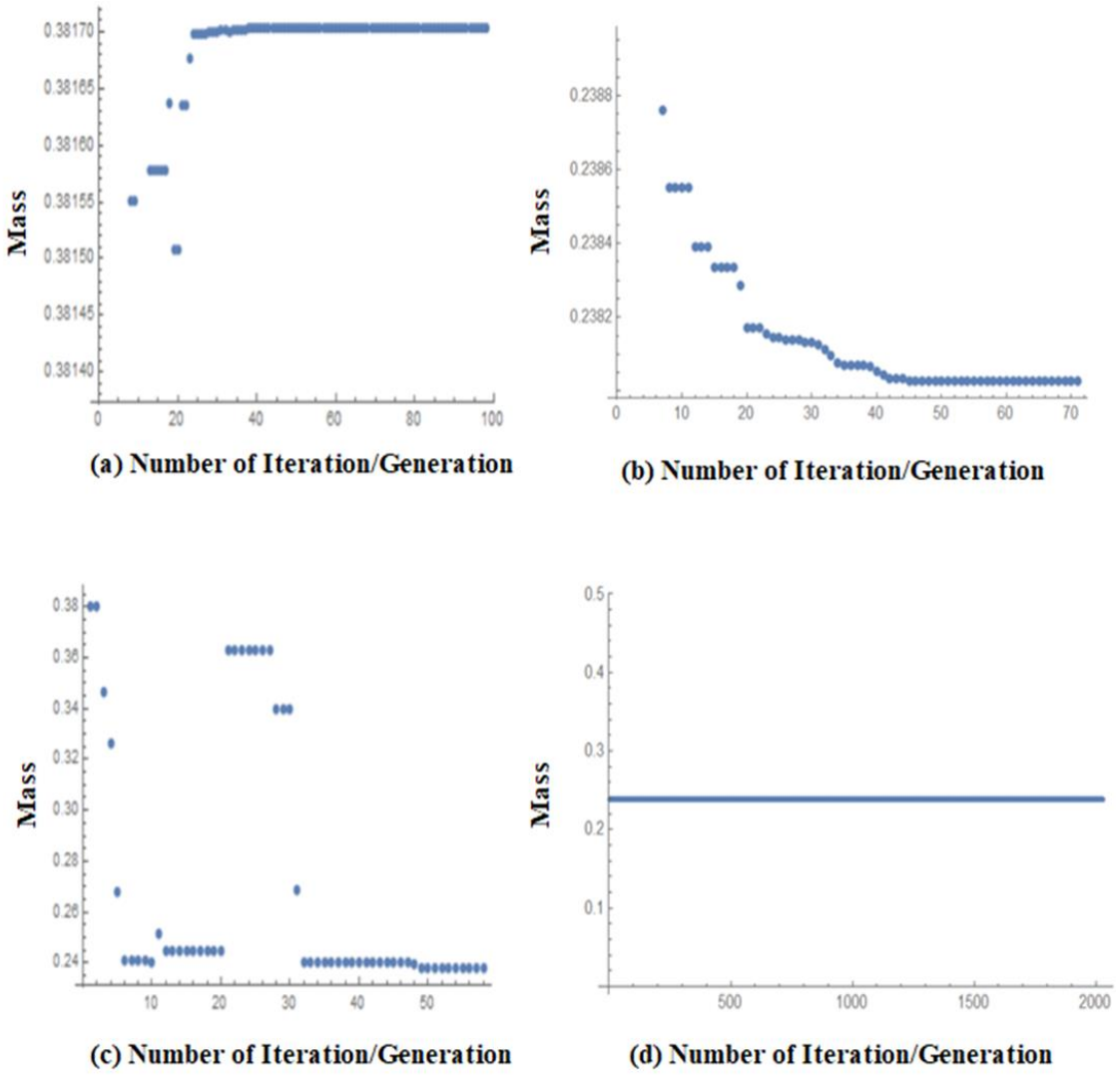

Figure 5.13. Convergence graphic representations of the stochastic algorithms for Mass (a) MDE, (b) MNM, (c) MSA, and (d) MRS

CHAPTER 6

CONCLUSION

In this thesis, the design, modeling and optimization studies of the torsion spring, which is the most critical and important part of the rotary series elastic actuator used in the rehabilitation robots of individuals with lower extremity damage, were carried out. First, by using the specific results given in the previous study in the literature, the von Mises stress, mass and stiffness values of the torsion spring were verified with the help of FEM. Then, using torsion spring topology parameters, 147 data sets were created with the help of the D-Optimal method, which is an experimental design method, in order to develop a new process and present new solution methods. Afterwards, a suitable three-dimensional design space was created using SolidWorks® 2019 and finite element analyses were made with the ANSYS® 19.2. The Neuro-Regression approach and cross-validation technique, which combines the strengths of artificial neural network and traditional regression, were used to obtain the mathematical model of the FEM simulations. Among the models proposed and analysed for the problem with two inputs (thickness and inner corner radius) and three outputs (von Mises stress, mass, stiffness), the model selection was made with Wolfram MATHEMATICA software for each output, according to the training, testing and validation determination of coefficients. In line with the selected models, ten different optimization scenarios were defined by selecting the mass and von Mises stress as an objective function. A light, compact, durable and stiff spring design is aimed by minimizing the mass and von Mises stress within various constraints. Optimization processes were performed using stochastic search techniques such as Differential Evolution, Nelder Mead, Random Search and Simulated Annealing. When the results obtained with these methods are compared, it can be clearly said that all algorithms give very similar results for the mass objective function. On the other hand, for the von Mises stress objective function, Nelder Mead and Simulated Annealing could not give results in the given ranges for some optimization problems.

When the results of optimization studies, finite element analysis results and the results in the literature are compared, it is seen that some results based on various radii

and thicknesses are similar, while some results solved with different scenarios and algorithms are better than the literature.

In conclusion, with this study, it has been revealed that the optimal design can be found in a shorter time, reliable and closer to reality by optimizing the conceptual models that will shed light on the final design with various mathematical models, optimization algorithms, scenarios and constraints in the early stages of the design process of the torsion spring. This study, with its comprehensive content, is a resource that will undoubtedly be useful to scientists working on torsion spring design.

REFERENCES

1. Davies, B., A review of robotics in surgery. *Proceedings of the Institution of Mechanical Engineers, Part H: Journal of Engineering in Medicine* 2000, *214* (1), 129-140.

2. Pugin, F.; Bucher, P.; Morel, P., History of robotic surgery: from AESOP® and ZEUS® to da Vinci®. *Journal of visceral surgery* 2011, *5* (148), e3-e8.

3. Peng, Z.; Huang, J., Soft rehabilitation and nursing-care robots: A review and future outlook. *Applied Sciences* 2019, *9* (15), 3102.

4. Siciliano, B.; Khatib, O.; Kröger, T., *Springer handbook of robotics*. Springer: 2008; Vol. 200.

5. Valero-Cuevas, F. J.; Klamroth-Marganska, V.; Winstein, C. J.; Riener, R., Robot-assisted and conventional therapies produce distinct rehabilitative trends in stroke survivors. *Journal of neuroengineering and rehabilitation* 2016, *13* (1), 1-10.

6. Shi, D.; Zhang, W.; Zhang, W.; Ju, L.; Ding, X., Human-centred adaptive control of lower limb rehabilitation robot based on human–robot interaction dynamic model. *Mechanism and Machine Theory* 2021, *162*, 104340.

7. Shi, D.; Zhang, W.; Zhang, W.; Ding, X., A review on lower limb rehabilitation exoskeleton robots. *Chinese Journal of Mechanical Engineering* 2019, *32* (1), 1-11.

8. Nycz, C. J.; Delph, M. A.; Fischer, G. S. In *Modeling and design of a tendon actuated soft robotic exoskeleton for hemiparetic upper limb rehabilitation*, 2015 37th Annual International Conference of the IEEE Engineering in Medicine and Biology Society (EMBC), IEEE: 2015; pp 3889-3892.

9. In, H.; Kang, B. B.; Sin, M.; Cho, K.-J., Exo-glove: A wearable robot for the hand with a soft tendon routing system. *IEEE Robotics & Automation Magazine* 2015, *22* (1), 97-105.

10. Guo, J.; Yu, S.; Li, Y.; Huang, T.-H.; Wang, J.; Lynn, B.; Fidock, J.; Shen, C.-L.; Edwards, D.; Su, H. In *A soft robotic exo-sheath using fabric EMG sensing for*

hand rehabilitation and assistance, 2018 IEEE international conference on soft robotics (RoboSoft), IEEE: 2018; pp 497-503.

11. Dollar, A. M.; Herr, H. In *Active orthoses for the lower-limbs: challenges and state of the art*, 2007 IEEE 10th International Conference on Rehabilitation Robotics, IEEE: 2007; pp 968-977.

12. Aydın, Y. A Multi Criteria Optimization Framework for Interaction Controller Design for Physical Human-robot Interaction. Koç University, 2019.

13. Şabanoviç, A.; Yannier, S., Robotlar: Sosyal etkileşimli makineler. *TÜBİTAK Bilim Teknik Dergisi* 2003.

14. Nof, S. Y., *Handbook of industrial robotics*. John Wiley & Sons: 1999.

15. Secil, S.; Ozkan, M., Minimum distance calculation using skeletal tracking for safe human-robot interaction. *Robotics and Computer-Integrated Manufacturing* 2022, *73*, 102253.

16. Ajoudani, A.; Zanchettin, A. M.; Ivaldi, S.; Albu-Schäffer, A.; Kosuge, K.; Khatib, O., Progress and prospects of the human–robot collaboration. *Autonomous Robots* 2018, *42* (5), 957-975.

17. Accoto, D.; Carpino, G.; Sergi, F.; Tagliamonte, N. L.; Zollo, L.; Guglielmelli, E., Design and characterization of a novel high-power series elastic actuator for a lower limb robotic orthosis. *International Journal of Advanced Robotic Systems* 2013, *10* (10), 359.

18. Ates, S.; Sluiter, V. I.; Lammertse, P.; Stienen, A. H. In *Servosea concept: cheap, miniature series-elastic actuators for orthotic, prosthetic and robotic hands*, 5th IEEE RAS/EMBS International Conference on Biomedical Robotics and Biomechatronics, IEEE: 2014; pp 752-757.

19. Fong, T.; Provencher, C.; Micire, M.; Diftler, M.; Berka, R.; Bluethmann, B.; Mittman, D. In *The Human Exploration Telerobotics project: objectives, approach, and testing*, 2012 IEEE Aerospace Conference, IEEE: 2012; pp 1-9.

20. Kwa, H. K.; Noorden, J. H.; Missel, M.; Craig, T.; Pratt, J. E.; Neuhaus, P. D. In *Development of the IHMC mobility assist exoskeleton*, 2009 IEEE international conference on robotics and automation, IEEE: 2009; pp 2556-2562.

21. Rea, R.; Beck, C.; Rovekamp, R.; Neuhaus, P.; Diftler, M. In *X1: A robotic exoskeleton for in-space countermeasures and dynamometry*, AIAA space 2013 conference and exposition, 2013; p 5510.

22. Neuhaus, P. D.; Noorden, J. H.; Craig, T. J.; Torres, T.; Kirschbaum, J.; Pratt, J. E. In *Design and evaluation of Mina: A robotic orthosis for paraplegics*, 2011 IEEE international conference on rehabilitation robotics, IEEE: 2011; pp 1-8.

23. Griffin, R.; Cobb, T.; Craig, T.; Daniel, M.; van Dijk, N.; Gines, J.; Kramer, K.; Shah, S.; Siebinga, O.; Smith, J., Stepping forward with exoskeletons: Team IHMC? s design and approach in the 2016 cybathlon. *IEEE Robotics & Automation Magazine* 2017, *24* (4), 66-74.

24. dos Santos, W. M.; Caurin, G. A.; Siqueira, A. A., Design and control of an active knee orthosis driven by a rotary series elastic actuator. *Control Engineering Practice* 2017, *58*, 307-318.

25. Yıldırım, M. C.; Şendur, P.; Uğurlu, B., Mechanical Design Procedures for Series Elastic Actuators. *Pamukkale University Journal of Engineering Sciences 25* (1), 34-42.

26. Irmscher, C.; Woschke, E.; May, E.; Daniel, C., Design, optimisation and testing of a compact, inexpensive elastic element for series elastic actuators. *Medical engineering & physics* 2018, *52*, 84-89.

27. Carpino, G.; Accoto, D.; Sergi, F.; Luigi Tagliamonte, N.; Guglielmelli, E., A novel compact torsional spring for series elastic actuators for assistive wearable robots. *Journal of Mechanical Design* 2012, *134* (12), 121002.

28. Bolívar-Nieto, E. A.; Summers, T.; Gregg, R. D.; Rezazadeh, S., A convex optimization framework for robust-feasible series elastic actuators. *Mechatronics* 2021, *79*, 102635.

29. Fotuhi, M. J.; Bingul, Z., Fuzzy torque trajectory control of a rotary series elastic actuator with nonlinear friction compensation. *ISA transactions* 2021.

30. Accoto, D.; Sergi, F.; Tagliamonte, N. L.; Carpino, G.; Sudano, A.; Guglielmelli, E., Robomorphism: a nonanthropomorphic wearable robot. *IEEE Robotics & Automation Magazine* 2014, *21* (4), 45-55.

31. Yan, L. L.; Banka, N.; Owan, P.; Piaskowy, W. T.; Garbini, J. L.; Devasia, S., MIMO ILC using complex-kernel regression and application to Precision SEA robots. *Automatica* 2021, *127*, 109550.

32. Yildirim, M. C.; Sendur, P.; Kansizoglu, A. T.; Uras, U.; Bilgin, O.; Emre, S.; Yapici, G. G.; Arik, M.; Ugurlu, B., Design and development of a durable series elastic actuator with an optimized spring topology. *Proceedings of the Institution of Mechanical Engineers, Part C: Journal of Mechanical Engineering Science* 2021, 09544062211020337.

33. Murat, R., Robotik Uygulamalar İçin Prizmatik Kesitli Millerin Burulması Esasına Dayanan Elastik Eyleyici Tasarımı. *Avrupa Bilim ve Teknoloji Dergisi*, 146-151.

34. Robinson, D. W.; Pratt, J. E.; Paluska, D. J.; Pratt, G. A. In *Series elastic actuator development for a biomimetic walking robot*, 1999 IEEE/ASME International Conference on Advanced Intelligent Mechatronics (Cat. No. 99TH8399), IEEE: 1999; pp 561-568.

35. Chironis, N. P., *Spring design and application*. McGraw-Hill New York: 1961; Vol. 276.

36. Dilibal, S.; Şahin, H., İşbirlikçi endüstriyel robotlar ve dijital endüstri. *International Journal of 3D Printing Technologies and Digital Industry* 2018, *2* (1), 86-96.

37. Kılıç, E.; Şekerci, B.; Kizilhan, H.; Başer, Ö., Evaluation of position tracking control performance of a variable stiffness ankle exoskeleton robot with various controller types. *Journal of the Faculty of Engineering and Architecture of Gazi University* 2020, *35* (3), 1551-1563.

38. Elftman, H., Biomechanics of muscle: with particular application to studies of gait. *JBJS* 1966, *48* (2), 363-377.

39. Martins, L. T.; de Mendonça Pretto, R.; Gerndt, R.; da Silva Guerra, R. In *Design of a modular series elastic upgrade to a robotics actuator*, Robot Soccer World Cup, Springer: 2014; pp 701-708.

40. Pratt, G. A.; Williamson, M. M. In *Series elastic actuators*, Proceedings 1995 IEEE/RSJ International Conference on Intelligent Robots and Systems. Human Robot Interaction and Cooperative Robots, IEEE: 1995; pp 399-406.

41. Chen, B.; Zhao, X.; Ma, H.; Qin, L.; Liao, W.-H., Design and characterization of a magneto-rheological series elastic actuator for a lower extremity exoskeleton. *Smart Materials and Structures* 2017, *26* (10), 105008.

42. Liu, H.; Cui, S.; Liu, Y.; Ren, Y.; Sun, Y., Design and vibration suppression control of a modular elastic joint. *Sensors* 2018, *18* (6), 1869.

43. Veneman, J. F.; Ekkelenkamp, R.; Kruidhof, R.; van der Helm, F. C.; van der Kooij, H., A series elastic-and bowden-cable-based actuation system for use as torque actuator in exoskeleton-type robots. *The international journal of robotics research* 2006, *25* (3), 261-281.

44. Pekdur, Ö.; Akdaş, D., Yay katsayısı sürekli değiştirilebilen seri elastik aktüatör tasarımı ve imalatı. *Balıkesir Üniversitesi Fen Bilimleri Enstitüsü Dergisi* 2019, *21* (2), 724-738.

45. Richard Lesh, G. H., Problem Solving, Modeling, and Local Conceptual Development. *Mathematical Thinking And Learning* 2003, *5*, 33.

46. Lesh, R.; Lehrer, R., Models and modeling perspectives on the development of students and teachers. *Mathematical thinking and learning* 2003, *5* (2-3), 109-129.

47. Sriraman, B., Are giftedness and creativity synonyms in mathematics? *Journal of Secondary Gifted Education* 2005, *17* (1), 20-36.

48. Tutak, T.; Güder, Y., Matematiksel modellemenin tanımı, kapsamı ve önemi. *Turkish Journal of Educational Studies* 2014, *1* (1).

49. Erten, H. I.; Deveci, H. A.; Artem, H. S., *Stochastic optimization methods*. CRC Press: 2020.

50. Antony, J., *Design of experiments for engineers and scientists*. Elsevier: 2014.

51. Ramírez, J. G., Understanding Design of Experiments: A Primer for Technologists. Taylor & Francis: 1999.

52. Karaağaoğlu, E., Bir Deney Tasarımı Türü: Rasgele Blok Düzeni. *Turkish Journal of Biochemistry/Turk Biyokimya Dergisi* 2013, *38* (1).

53. Caniyilmaz, E.; Kutay, F., Taguchi Metodunda Varyans Analizine Alternatif Bir Yaklaşim. *Gazi Üniversitesi Mühendislik Mimarlık Fakültesi Dergisi* 2003, *18* (3).

54. Karna, S. K.; Sahai, R., An overview on Taguchi method. *International journal of engineering and mathematical sciences* 2012, *1* (1), 1-7.

55. Pukelsheim, F., *Optimal design of experiments*. SIAM: 2006.

56. Olawale, O., Bamboo leaves as an alternative source for silica in ceramics using Box Benhken design. *Scientific African* 2020, *8*, e00418.

57. Tolon, M.; Tosunoğlu, N. G., Tüketici tatmini verilerinin analizi: yapay sinir ağlari ve regresyon analizi karşilaştirmasi. *Gazi Üniversitesi İktisadi ve İdari Bilimler Fakültesi Dergisi* 2008, *10* (2), 247-259.

58. Devore, J. L., *Probability and Statistics for Engineering and the Sciences*. Cengage Learning: 2015.

59. Pinder, J. P., *Introduction to business analytics using simulation*. Academic Press: 2016.

60. Miles, J., R-squared, adjusted R-squared. *Encyclopedia of statistics in behavioral science* 2005.

61. Sun, M.-f.; Yang, J.-y.; Cao, W.; Shao, J.-y.; Wang, G.-x.; Qu, H.-b.; Huang, W.-h.; Gong, X.-c., Critical process parameter identification of manufacturing processes

of Astragali Radix extract with a weighted determination coefficient method. *Chinese Herbal Medicines* 2020, *12* (2), 125-132.

62. Polatoğlu, İ.; Aydin, L., A new design strategy with stochastic optimization on the preparation of magnetite cross-linked tyrosinase aggregates (MCLTA). *Process Biochemistry* 2020, *99*, 131-138.

63. Ceylan, A. B.; Aydın, L.; Nil, M.; Mamur, H.; Polatoğlu, İ.; Sözen, H., A new hybrid approach in selection of optimum establishment location of the biogas energy production plant. *Biomass Conversion and Biorefinery* 2021, 1-16.

64. Jerez, T.; Kristjanpoller, W., Effects of the validation set on stock returns forecasting. *Expert Systems with Applications* 2020, *150*, 113271.

65. Dang, D. Z.; Stern, E. C.; Boyd, I. D., Inferring thermal conductivity of a dual-layer woven thermal protection system using cross-validation. *Thermal Science and Engineering Progress* 2021, *23*, 100904.

66. Bartel, F.; Hielscher, R.; Potts, D., Fast cross-validation in harmonic approximation. *Applied and Computational Harmonic Analysis* 2020, *49* (2), 415-437.

67. Wei, J.; Chen, H., Determining the number of factors in approximate factor models by twice K-fold cross validation. *Economics Letters* 2020, *191*, 109149.

68. Polatoğlu, İ.; Aydın, L.; Nevruz, B. Ç.; Özer, S., A novel approach for the optimal design of a biosensor. *Analytical Letters* 2020, *53* (9), 1428-1445.

69. Ombach, J., A short introduction to stochastic optimization. *Schedae Informaticae* 2014, *23*.

70. Aydin, L.; Artem, H. S., Comparison of stochastic search optimization algorithms for the laminated composites under mechanical and hygrothermal loadings. *Journal of reinforced plastics and composites* 2011, *30* (14), 1197-1212.

71. Xu, J.; Yang, P.; Liu, G.; Bai, Z.; Li, W., Constraint handling in constrained optimization of a storage ring multi-bend-achromat lattice. *Nuclear Instruments and Methods in Physics Research Section A: Accelerators, Spectrometers, Detectors and Associated Equipment* 2021, *988*, 164890.

72. Yang, X.-S., *Engineering optimization: an introduction with metaheuristic applications*. John Wiley & Sons: 2010.

73. Aydin, L.; Aydin, O.; Artem, H. S.; Mert, A., Design of dimensionally stable composites using efficient global optimization method. *Proceedings of the Institution of Mechanical Engineers, Part L: Journal of Materials: Design and Applications* 2019, *233* (2), 156-168.

74. Rao, R. V.; Savsani, V. J., Mechanical design optimization using advanced optimization techniques. 2012.

75. Serkan, K.; FIĞLALI, N., Çok Amaçlı Optimizasyon Problemlerinde Pareto Optimal Kullanımı. *Sosyal Bilimler Araştırma Dergisi* 2016, *5* (2), 9-18.

76. Pelletier, J. L.; Vel, S. S., Multi-objective optimization of fiber reinforced composite laminates for strength, stiffness and minimal mass. *Computers & structures* 2006, *84* (29-30), 2065-2080.

77. Eröz, E.; Tanyildizi, E. In *Çok Amaçlı Metasezgisel Optimizasyon Algoritmalarının Performans Karşılaştırması*, 2019 International Artificial Intelligence and Data Processing Symposium (IDAP), IEEE: 2019; pp 1-11.

78. Irisarri, F.-X.; Bassir, D. H.; Carrere, N.; Maire, J.-F., Multiobjective stacking sequence optimization for laminated composite structures. *Composites Science and Technology* 2009, *69* (7-8), 983-990.

79. Hasanoglu, M. S.; Dolen, M., Comparison of multi-objective and single-objective approaches in feasibility enhanced particle swarm optimization. *Journal of the Faculty of Engineering and Architecture of Gazi University* 2020, *35* (2), 887-900.

80. Nelder, J. A.; Mead, R., A simplex method for function minimization. *The computer journal* 1965, *7* (4), 308-313.

81. Rajan, A.; Malakar, T., Optimal reactive power dispatch using hybrid Nelder–Mead simplex based firefly algorithm. *International Journal of Electrical Power & Energy Systems* 2015, *66*, 9-24.

82. Xu, S.; Wang, Y.; Wang, Z., Parameter estimation of proton exchange membrane fuel cells using eagle strategy based on JAYA algorithm and Nelder-Mead simplex method. *Energy* 2019, *173*, 457-467.

83. Ozturk, S.; Aydin, L.; Celik, E., A comprehensive study on slicing processes optimization of silicon ingot for photovoltaic applications. *Solar Energy* 2018, *161*, 109-124.

84. Agrawal, S.; Singh, D., Modified Nelder-Mead self organizing migrating algorithm for function optimization and its application. *Applied Soft Computing* 2017, *51*, 341-350.

85. Barati, R., Parameter estimation of nonlinear Muskingum models using Nelder-Mead simplex algorithm. *Journal of Hydrologic Engineering* 2011, *16* (11), 946-954.

86. Storn, R.; Price, K., Differential evolution–a simple and efficient heuristic for global optimization over continuous spaces. *Journal of global optimization* 1997, *11* (4), 341-359.

87. Das, S.; Suganthan, P. N., Differential evolution: A survey of the state-of-the-art. *IEEE transactions on evolutionary computation* 2010, *15* (1), 4-31.

88. Ali, M.; Pant, M.; Abraham, A. In *A modified differential evolution algorithm and its application to engineering problems*, 2009 International Conference of Soft Computing and Pattern Recognition, IEEE: 2009; pp 196-201.

89. Satya Eswari, J.; Venkateswarlu, C., Dynamic modeling and metabolic flux analysis for optimized production of rhamnolipids. *Chemical engineering communications* 2016, *203* (3), 326-338.

90. Akçair, M.; Savran, M.; Aydın, L.; Ayakdas, O.; Öztürk, S.; Küçükdogan, N., Optimum design of anti-buckling behavior of graphite/epoxy laminated composites by differential evolution and simulated annealing method. *Res Eng Struct Mat* 2019, *5* (2), 175-188.

91. Haghverdi, A.; Baniassadi, M.; Baghani, M.; Sahraei, A. A.; Garmestani, H.; Safdari, M., A modified simulated annealing algorithm for hybrid statistical

reconstruction of heterogeneous microstructures. *Computational Materials Science* 2021**,** *197*, 110636.

92. Aydin, L.; Savran, M., Geliştirilmiş Benzetilmiş Tavlama Algoritması Kullanılarak Minimum Fiyat, Minimum Ağırlık ve Maksimum Doğal Frekans Açısından Hibrit Grafit-Keten/Epoksi Tabakalı Kompozitlerin Optimum Tasarımı. *Dokuz Eylül Üniversitesi Mühendislik Fakültesi Fen ve Mühendislik Dergisi 21* (63), 833-844.

93. Abakarov, A.; Sushkov, Y.; Almonacid, S.; Simpson, R., Thermal processing optimization through a modified adaptive random search. *Journal of Food Engineering* 2009**,** *93* (2), 200-209.

94. Zakouni, A.; Luo, J.; Kharroubi, F. In *Random optimization algorithm for solving the static manycast RWA problem in optical WDM networks*, 2016 International Conference on Information and Communication Technology Convergence (ICTC), IEEE: 2016; pp 640-645.

95. Ansys Meshing User's Guide. 2010.

96. Kirtley, C., *Clinical gait analysis: theory and practice*. Elsevier Health Sciences: 2006.

97. Kong, K.; Bae, J.; Tomizuka, M. In *A compact rotary series elastic actuator for knee joint assistive system*, 2010 IEEE International Conference on Robotics and Automation, IEEE: 2010; pp 2940-2945.

98. Design Expert 6.0.8.

99. Walsh, R. A., *Electromechanical design handbook*. McGraw-Hill Professional: 2000.

APPENDIX A

REGRESSION AND CROSS VALIDATION GROUPS

Testing Data 1					
Run	**R_4**	**E**	**Mass**	**Stiffness**	**von Mises stress**
3	2.5	6.5	0.310	159.7752	706.14
12	2.55	7.5	0.358	182.9608	576.77
19	2.6	5.5	0.263	130.2302	806.98
28	2.65	6	0.286	143.9418	750.72
68	2.7	8	0.382	190.2286	547.63
64	2.75	7	0.334	165.9786	664.18
78	2.8	5	0.239	117.0556	936.57
82	2.85	7.5	0.359	176.0798	609.46
55	2.9	7	0.335	162.6884	685.83
98	2.95	8	0.383	187.7454	547.73
103	3	5.5	0.263	128.1936	855.21
124	3.05	7	0.335	160.6122	668.79
128	3.1	6	0.287	135.5906	761.93
133	3.15	5.5	0.264	123.8326	795.67
141	3.2	6	0.288	134.4294	776.03
97	3.25	7.5	0.360	168.4784	613.11
89	3.3	6.5	0.312	144.1444	707.61
145	3.35	7.5	0.360	168.0420	615.99
4	3.4	6.5	0.312	143.8114	746.29
83	3.45	5.5	0.264	121.6964	874.99
120	3.5	5	0.240	114.6010	916.62
41	2.5	7	0.334	170.1458	629.84
76	2.6	6.5	0.310	155.7388	683.51
70	2.8	8	0.382	188.2700	564.23
135	3	5	0.239	116.2438	940.54
122	3.2	5	0.240	111.6532	926.66
20	3.4	8	0.385	179.1174	594.38
10	3.5	6	0.289	124.6784	771.73
25	3.15	5	0.240	112.3314	875.60
35	2.65	7.5	0.358	181.4718	594.36

Training Data 1					
Run	**R_4**	**E**	**Mass**	**Stiffness**	**von Mises stress**
1	2.8	7	0.335	163.8864	656.70
2	3.4	5	0.240	110.0294	925.58
5	2.95	6	0.287	138.4258	791.14
6	2.75	5	0.239	116.4776	920.33
7	2.5	5	0.238	120.3282	888.90
8	2.85	8	0.383	187.6808	563.18
9	3.45	7	0.336	156.9286	689.38
11	3.25	8	0.384	180.6200	565.70
13	3.2	8	0.384	180.2974	567.21
14	3.45	6	0.288	133.1316	801.93
15	2.95	5	0.239	115.7516	896.07
16	3.35	6.5	0.312	145.5014	727.56

17	3.05	7.5	0.359	172.9914	622.02
18	3.35	7	0.336	156.6476	662.24
21	3.3	5	0.240	110.0384	930.75
22	2.5	5.5	0.262	134.3876	832.41
23	2.75	5.5	0.263	128.7752	836.18
24	2.55	6	0.287	144.8926	725.11
26	3.25	6.5	0.312	145.1746	711.84
27	3.35	6	0.288	133.3600	771.91
29	3.3	5.5	0.264	122.0708	846.70
30	3.25	5	0.240	110.8990	940.20
31	3.1	7	0.335	159.6730	669.58
32	2.9	7.5	0.359	174.8248	638.09
33	2.7	6	0.286	141.2240	749.90
34	3	7.5	0.360	174.3716	633.74
36	3.1	6.5	0.312	147.2514	693.58
37	3.45	7.5	0.360	166.1648	641.64
38	3.1	8	0.383	183.4468	583.50
39	3	6	0.287	138.0014	793.47
40	3.1	7.5	0.359	171.5622	622.79
42	2.55	5	0.238	120.1334	871.34
43	2.7	7	0.334	165.5972	639.49
44	2.5	6	0.286	145.5800	762.25
45	3.05	8	0.383	184.5366	582.77
46	2.5	8	0.382	195.5856	540.94
47	2.65	5	0.239	118.5552	923.91
48	3	7	0.335	161.8184	681.16
49	2.6	5	0.238	118.6870	887.59
50	2.9	6	0.287	138.7382	798.88
51	3.35	5.5	0.264	121.9244	842.39
52	3.5	8	0.385	176.1510	565.61
53	2.9	6.5	0.311	150.6446	740.36
54	2.8	7.5	0.359	176.1000	610.52
56	2.85	5	0.239	116.2382	960.24
57	3.05	5.5	0.263	126.0264	793.82
58	2.75	8	0.382	190.7252	570.41
59	3	8	0.383	185.8890	585.05
60	3.15	7.5	0.360	170.7166	624.83
61	3.5	7	0.337	153.3310	658.83
62	2.95	5.5	0.263	127.4184	814.65
63	3.15	8	0.384	182.4752	585.42
65	3.25	5.5	0.264	122.0390	854.90
66	2.8	6.5	0.311	151.7436	709.46
67	2.65	5.5	0.262	131.5926	820.30
69	3.35	5	0.240	110.7192	930.13
71	3.1	5.5	0.263	123.9622	831.88
72	3.05	5	0.239	113.5320	949.97
73	2.9	8	0.383	186.8866	589.10
74	2.65	7	0.334	168.7762	639.72
75	3.45	8	0.385	179.3320	592.74
77	3.35	8	0.384	179.6684	568.45
79	2.6	6	0.286	143.4202	750.97
80	3.3	7.5	0.361	170.2522	632.74
81	3.1	5	0.239	112.8802	950.84
84	3.2	7.5	0.360	169.6968	605.81
85	3.4	5.5	0.264	120.9196	842.07
86	3.25	6	0.288	127.4910	867.76
87	2.65	8	0.382	193.8756	549.98
88	3.2	6.5	0.312	145.9830	708.69
90	2.6	7	0.334	168.1842	632.60
91	2.5	7.5	0.358	182.3114	585.19
92	2.8	5.5	0.263	127.7550	839.06
93	3.5	7.5	0.361	166.8786	631.00
94	3.25	7	0.336	156.7768	659.22
95	2.7	7.5	0.358	177.9256	594.08

96	3.5	5.5	0.264	119.6324	847.45
99	3.2	7	0.336	157.9402	651.55
100	3.3	8	0.384	179.7242	592.71
101	3.3	6	0.289	132.7306	775.78
102	3.05	6	0.287	137.8424	726.61
104	2.65	6.5	0.310	156.2832	691.61
105	2.9	5.5	0.263	126.8298	872.15
106	3.45	5	0.240	110.3502	961.8
107	2.95	7	0.335	163.4206	639.06
108	2.85	6.5	0.311	151.7378	708.15
109	3.4	7	0.336	155.9114	691.56
110	3.5	6.5	0.312	142.1230	710.70
111	2.55	6.5	0.310	157.3218	670.40
112	3.4	7.5	0.360	167.5320	643.57
113	2.7	5.5	0.263	129.0918	819.55
114	3.15	7	0.336	158.8250	671.77
115	2.55	5.5	0.262	132.4640	791.97
116	3.45	6.5	0.312	142.5400	743.79
117	2.75	6	0.287	140.5116	765.33
118	2.95	7.5	0.359	175.5990	594.09
119	2.55	8	0.382	195.1596	531.04
121	3.15	6.5	0.312	148.4546	667.42
123	2.8	6	0.287	139.7514	768.44
125	2.55	7	0.334	169.8920	620.46
126	2.85	6	0.287	139.7592	766.89
127	3.15	6	0.288	135.4476	728.40
129	3	6.5	0.311	149.7670	735.31
130	2.6	7.5	0.358	182.8158	588.19
131	2.9	5	0.239	115.1720	870.20
132	2.75	7.5	0.358	178.3474	617.10
134	3.2	5.5	0.264	122.8984	847.08
136	3.3	7	0.336	158.4448	680.26
137	2.7	6.5	0.310	153.3264	691.45
138	2.7	5	0.239	117.9100	936.89
139	3.4	6	0.288	132.9708	805.09
140	2.95	6.5	0.311	150.5810	733.17
142	2.75	6.5	0.311	152.5750	707.95
143	3.05	6.5	0.312	149.6866	665.70
144	2.85	7	0.335	163.8770	655.53
146	2.6	8	0.382	193.2456	550.79
147	2.85	5.5	0.263	127.7622	837.32

Validation Data 1					
Run	**R_4**	**E**	**Mass**	**Stiffness**	**von Mises stress**
7	2.5	5	0.238	120.3282	888.90
79	2.6	6	0.286	143.4202	750.97
113	2.7	5.5	0.263	129.0918	819.55
1	2.8	7	0.335	163.8864	656.70
73	2.9	8	0.383	186.8866	589.10
34	3	7.5	0.360	174.3716	633.74
143	3.05	6.5	0.312	149.6866	665.70
31	3.1	7	0.335	159.6730	669.58
84	3.2	7.5	0.360	169.6968	605.81
100	3.3	8	0.384	179.7242	592.71
139	3.4	6	0.288	132.9708	805.09
110	3.5	6.5	0.312	142.1230	710.70

Testing Data 2					
Run	**R_4**	**E**	**Mass**	**Stiffness**	**von Mises stress**
7	2.5	5	0.238	120.3282	888.90
24	2.55	6	0.287	144.8926	725.11
79	2.6	6	0.286	143.4202	750.97
74	2.65	7	0.334	168.7762	639.72
113	2.7	5.5	0.263	129.0918	819.55
132	2.75	7.5	0.358	178.3474	617.10
66	2.8	6.5	0.311	151.7436	709.46
8	2.85	8	0.383	187.6808	563.18
32	2.9	7.5	0.359	174.8248	638.09
15	2.95	5	0.239	115.7516	896.07
34	3	7.5	0.360	174.3716	633.74
45	3.05	8	0.383	184.5366	582.77
81	3.1	5	0.239	112.8802	950.84
63	3.15	8	0.384	182.4752	585.42
84	3.2	7.5	0.360	169.6968	605.81
86	3.25	6	0.288	127.4910	867.76
100	3.3	8	0.384	179.7242	592.71
51	3.35	5.5	0.264	121.9244	842.39
139	3.4	6	0.288	132.9708	805.09
116	3.45	6.5	0.312	142.5400	743.79
93	3.5	7.5	0.361	166.8786	631.00
69	3.35	5	0.240	110.7192	930.13
90	2.6	7	0.334	168.1842	632.60
94	3.25	7	0.336	156.7768	659.22
88	3.2	6.5	0.312	145.9830	708.69
105	2.9	5.5	0.263	126.8298	872.15
99	3.2	7	0.336	157.9402	651.55
111	2.55	6.5	0.310	157.3218	670.40
147	2.85	5.5	0.263	127.7622	837.32
142	2.75	6.5	0.311	152.5750	707.95

Training Data 2					
Run	**R_4**	**E**	**Mass**	**Stiffness**	**von Mises stress**
1	2.8	7	0.335	163.8864	656.70
2	3.4	5	0.240	110.0294	925.58
3	2.5	6.5	0.310	159.7752	706.14
4	3.4	6.5	0.312	143.8114	746.29
5	2.95	6	0.287	138.4258	791.14
6	2.75	5	0.239	116.4776	920.33
9	3.45	7	0.336	156.9286	689.38
10	3.5	6	0.289	124.6784	771.73
11	3.25	8	0.384	180.6200	565.70
12	2.55	7.5	0.358	182.9608	576.77
13	3.2	8	0.384	180.2974	567.21
14	3.45	6	0.288	133.1316	801.93
16	3.35	6.5	0.312	145.5014	727.56
17	3.05	7.5	0.359	172.9914	622.02
18	3.35	7	0.336	156.6476	662.24
19	2.6	5.5	0.263	130.2302	806.98
20	3.4	8	0.385	179.1174	594.38
21	3.3	5	0.240	110.0384	930.75
22	2.5	5.5	0.262	134.3876	832.41
23	2.75	5.5	0.263	128.7752	836.18
25	3.15	5	0.240	112.3314	875.60
26	3.25	6.5	0.312	145.1746	711.84

27	3.35	6	0.288	133.3600	771.91
28	2.65	6	0.286	143.9418	750.72
29	3.3	5.5	0.264	122.0708	846.70
30	3.25	5	0.240	110.8990	940.20
31	3.1	7	0.335	159.6730	669.58
33	2.7	6	0.286	141.2240	749.90
35	2.65	7.5	0.358	181.4718	594.36
36	3.1	6.5	0.312	147.2514	693.58
37	3.45	7.5	0.360	166.1648	641.64
38	3.1	8	0.383	183.4468	583.50
39	3	6	0.287	138.0014	793.47
40	3.1	7.5	0.359	171.5622	622.79
41	2.5	7	0.334	170.1458	629.84
42	2.55	5	0.238	120.1334	871.34
43	2.7	7	0.334	165.5972	639.49
44	2.5	6	0.286	145.5800	762.25
46	2.5	8	0.382	195.5856	540.94
47	2.65	5	0.239	118.5552	923.91
48	3	7	0.335	161.8184	681.16
49	2.6	5	0.238	118.6870	887.59
50	2.9	6	0.287	138.7382	798.88
52	3.5	8	0.385	176.1510	565.61
53	2.9	6.5	0.311	150.6446	740.36
54	2.8	7.5	0.359	176.1000	610.52
55	2.9	7	0.335	162.6884	685.83
56	2.85	5	0.239	116.2382	690.24
57	3.05	5.5	0.263	126.0264	793.82
58	2.75	8	0.382	190.7252	570.41
59	3	8	0.383	185.8890	585.05
60	3.15	7.5	0.360	170.7166	624.83
61	3.5	7	0.337	153.3310	658.83
62	2.95	5.5	0.263	127.4184	814.65
64	2.75	7	0.334	165.9786	664.18
65	3.25	5.5	0.264	122.0390	854.9
67	2.65	5.5	0.262	131.5926	820.3
68	2.7	8	0.382	190.2286	547.63
70	2.8	8	0.382	188.2700	564.23
71	3.1	5.5	0.263	123.9622	831.88
72	3.05	5	0.239	113.5320	949.97
73	2.9	8	0.383	186.8866	589.1
75	3.45	8	0.385	179.3320	592.74
76	2.6	6.5	0.310	155.7388	683.51
77	3.35	8	0.384	179.6684	568.45
78	2.8	5	0.239	117.0556	936.57
80	3.3	7.5	0.361	170.2522	632.74
82	2.85	7.5	0.359	176.0798	609.46
83	3.45	5.5	0.264	121.6964	874.99
85	3.4	5.5	0.264	120.9196	842.07
87	2.65	8	0.382	193.8756	549.98
89	3.3	6.5	0.312	144.1444	707.61
91	2.5	7.5	0.358	182.3114	585.19
92	2.8	5.5	0.263	127.7550	839.06
95	2.7	7.5	0.358	177.9256	594.08
96	3.5	5.5	0.264	119.6324	847.45
97	3.25	7.5	0.360	168.4784	613.11
98	2.95	8	0.383	187.7454	547.73
101	3.3	6	0.289	132.7306	775.78
102	3.05	6	0.287	137.8424	726.61
103	3	5.5	0.263	128.1936	855.21
104	2.65	6.5	0.310	156.2832	691.61
106	3.45	5	0.240	110.3502	961.8
107	2.95	7	0.335	163.4206	639.06
108	2.85	6.5	0.311	151.7378	708.15
109	3.4	7	0.336	155.9114	691.56

110	3.5	6.5	0.312	142.1230	710.7
112	3.4	7.5	0.360	167.5320	643.57
114	3.15	7	0.336	158.8250	671.77
115	2.55	5.5	0.262	132.4640	791.97
117	2.75	6	0.287	140.5116	765.33
118	2.95	7.5	0.359	175.5990	594.09
119	2.55	8	0.382	195.1596	531.04
120	3.5	5	0.240	114.6010	916.62
121	3.15	6.5	0.312	148.4546	667.42
122	3.2	5	0.240	111.6532	926.66
123	2.8	6	0.287	139.7514	768.44
124	3.05	7	0.335	160.6122	668.79
125	2.55	7	0.334	169.8920	620.46
126	2.85	6	0.287	139.7592	766.89
127	3.15	6	0.288	135.4476	728.4
128	3.1	6	0.287	135.5906	761.93
129	3	6.5	0.311	149.7670	735.31
130	2.6	7.5	0.358	182.8158	588.19
131	2.9	5	0.239	115.1720	870.2
133	3.15	5.5	0.264	123.8326	795.67
134	3.2	5.5	0.264	122.8984	847.08
135	3	5	0.239	116.2438	940.54
136	3.3	7	0.336	158.4448	680.26
137	2.7	6.5	0.310	153.3264	691.45
138	2.7	5	0.239	117.9100	936.89
140	2.95	6.5	0.311	150.5810	733.17
141	3.2	6	0.288	134.4294	776.03
143	3.05	6.5	0.312	149.6866	665.7
144	2.85	7	0.335	163.8770	655.53
145	3.35	7.5	0.360	168.0420	615.99
146	2.6	8	0.382	193.2456	550.79

Validation Data 2					
Run	**R_4**	**E**	**Mass**	**Stiffness**	**von Mises stress**
10	3.5	6	0.289	124.6784	771.73
11	3.25	8	0.384	180.6200	565.70
12	2.55	7.5	0.358	182.9608	576.77
23	2.75	5.5	0.263	128.7752	836.18
27	3.35	6	0.288	133.3600	771.91
28	2.65	6	0.286	143.9418	750.72
37	3.45	7.5	0.360	166.1648	641.64
54	2.8	7.5	0.359	176.1000	610.52
59	3	8	0.383	185.8890	585.05
62	2.95	5.5	0.263	127.4184	814.65
121	3.15	6.5	0.312	148.4546	667.42
124	3.05	7	0.335	160.6122	668.79

Testing Data 3					
Run	**R_4**	**E**	**Mass**	**Stiffness**	**von Mises stress**
22	2.5	5.5	0.262	134.3876	832.41
42	2.55	5	0.238	120.1334	871.34
130	2.6	7.5	0.358	182.8158	588.19
87	2.65	8	0.382	193.8756	549.98
137	2.7	6.5	0.310	153.3264	691.45
117	2.75	6	0.287	140.5116	765.33
1	2.8	7	0.335	163.8864	656.70
56	2.85	5	0.239	116.2382	960.24
50	2.9	6	0.287	138.7382	798.88

62	2.95	5.5	0.263	127.4184	814.65
129	3	6.5	0.311	149.7670	735.31
102	3.05	6	0.287	137.8424	726.61
31	3.1	7	0.335	159.6730	669.58
60	3.15	7.5	0.360	170.7166	624.83
13	3.2	8	0.384	180.2974	567.21
65	3.25	5.5	0.264	122.0390	854.90
80	3.3	7.5	0.361	170.2522	632.74
27	3.35	6	0.288	133.3600	771.91
2	3.4	5	0.240	110.0294	925.58
9	3.45	7	0.336	156.9286	689.38
110	3.5	6.5	0.312	142.1230	710.70
46	2.5	8	0.382	195.5856	540.94
73	2.9	8	0.383	186.8866	589.10
107	2.95	7	0.335	163.4206	639.06
123	2.8	6	0.287	139.7514	768.44
143	3.05	6.5	0.312	149.6866	665.70
95	2.7	7.5	0.358	177.9256	594.08
39	3	6	0.287	138.0014	793.47
134	3.2	5.5	0.264	122.8984	847.08
37	3.45	7.5	0.360	166.1648	641.64

Training Data 3					
Run	**R4**	**E**	**Mass**	**Stiffness**	**von Mises stress**
3	2.5	6.5	0.310	159.7752	706.14
4	3.4	6.5	0.312	143.8114	746.29
5	2.95	6	0.287	138.4258	791.14
6	2.75	5	0.239	116.4776	920.33
7	2.5	5	0.238	120.3282	888.90
8	2.85	8	0.383	187.6808	563.18
10	3.5	6	0.289	124.6784	771.73
11	3.25	8	0.384	180.6200	565.70
12	2.55	7.5	0.358	182.9608	576.77
14	3.45	6	0.288	133.1316	801.93
15	2.95	5	0.239	115.7516	896.07
16	3.35	6.5	0.312	145.5014	727.56
17	3.05	7.5	0.359	172.9914	622.02
18	3.35	7	0.336	156.6476	662.24
19	2.6	5.5	0.263	130.2302	806.98
20	3.4	8	0.385	179.1174	594.38
21	3.3	5	0.240	110.0384	930.75
23	2.75	5.5	0.263	128.7752	836.18
24	2.55	6	0.287	144.8926	725.11
25	3.15	5	0.240	112.3314	875.60
26	3.25	6.5	0.312	145.1746	711.84
28	2.65	6	0.286	143.9418	750.72
29	3.3	5.5	0.264	122.0708	846.70
30	3.25	5	0.240	110.8990	940.20
32	2.9	7.5	0.359	174.8248	638.09
33	2.7	6	0.286	141.2240	749.90
34	3	7.5	0.360	174.3716	633.74
35	2.65	7.5	0.358	181.4718	594.36
36	3.1	6.5	0.312	147.2514	693.58
38	3.1	8	0.383	183.4468	583.50
40	3.1	7.5	0.359	171.5622	622.79
41	2.5	7	0.334	170.1458	629.84
43	2.7	7	0.334	165.5972	639.49
44	2.5	6	0.286	145.5800	762.25
45	3.05	8	0.383	184.5366	582.77
47	2.65	5	0.239	118.5552	923.91
48	3	7	0.335	161.8184	681.16

49	2.6	5	0.238	118.6870	887.59
51	3.35	5.5	0.264	121.9244	842.39
52	3.5	8	0.385	176.1510	565.61
53	2.9	6.5	0.311	150.6446	740.36
54	2.8	7.5	0.359	176.1000	610.52
55	2.9	7	0.335	162.6884	685.83
57	3.05	5.5	0.263	126.0264	793.82
58	2.75	8	0.382	190.7252	570.41
59	3	8	0.383	185.8890	585.05
61	3.5	7	0.337	153.3310	658.83
63	3.15	8	0.384	182.4752	585.42
64	2.75	7	0.334	165.9786	664.18
66	2.8	6.5	0.311	151.7436	709.46
67	2.65	5.5	0.262	131.5926	820.30
68	2.7	8	0.382	190.2286	547.63
69	3.35	5	0.240	110.7192	930.13
70	2.8	8	0.382	188.2700	564.23
71	3.1	5.5	0.263	123.9622	831.88
72	3.05	5	0.239	113.5320	949.97
74	2.65	7	0.334	168.7762	639.72
75	3.45	8	0.385	179.3320	592.74
76	2.6	6.5	0.310	155.7388	683.51
77	3.35	8	0.384	179.6684	568.45
78	2.8	5	0.239	117.0556	936.57
79	2.6	6	0.286	143.4202	750.97
81	3.1	5	0.239	112.8802	950.84
82	2.85	7.5	0.359	176.0798	609.46
83	3.45	5.5	0.264	121.6964	874.99
84	3.2	7.5	0.360	169.6968	605.81
85	3.4	5.5	0.264	120.9196	842.07
86	3.25	6	0.288	127.4910	867.76
88	3.2	6.5	0.312	145.9830	708.69
89	3.3	6.5	0.312	144.1444	707.61
90	2.6	7	0.334	168.1842	632.60
91	2.5	7.5	0.358	182.3114	585.19
92	2.8	5.5	0.263	127.7550	839.06
93	3.5	7.5	0.361	166.8786	631.00
94	3.25	7	0.336	156.7768	659.22
96	3.5	5.5	0.264	119.6324	847.45
97	3.25	7.5	0.360	168.4784	613.11
98	2.95	8	0.383	187.7454	547.73
99	3.2	7	0.336	157.9402	651.55
100	3.3	8	0.384	179.7242	592.71
101	3.3	6	0.289	132.7306	775.78
103	3	5.5	0.263	128.1936	855.21
104	2.65	6.5	0.310	156.2832	691.61
105	2.9	5.5	0.263	126.8298	872.15
106	3.45	5	0.240	110.3502	961.80
108	2.85	6.5	0.311	151.7378	708.15
109	3.4	7	0.336	155.9114	691.56
111	2.55	6.5	0.310	157.3218	670.40
112	3.4	7.5	0.360	167.5320	643.57
113	2.7	5.5	0.263	129.0918	819.55
114	3.15	7	0.336	158.8250	671.77
115	2.55	5.5	0.262	132.4640	791.97
116	3.45	6.5	0.312	142.5400	743.79
118	2.95	7.5	0.359	175.5990	594.09
119	2.55	8	0.382	195.1596	531.04
120	3.5	5	0.240	114.6010	916.62
121	3.15	6.5	0.312	148.4546	667.42
122	3.2	5	0.240	111.6532	926.66
124	3.05	7	0.335	160.6122	668.79
125	2.55	7	0.334	169.8920	620.46
126	2.85	6	0.287	139.7592	766.89

127	3.15	6	0.288	135.4476	728.40
128	3.1	6	0.287	135.5906	761.93
131	2.9	5	0.239	115.1720	870.20
132	2.75	7.5	0.358	178.3474	617.10
133	3.15	5.5	0.264	123.8326	795.67
135	3	5	0.239	116.2438	940.54
136	3.3	7	0.336	158.4448	680.26
138	2.7	5	0.239	117.9100	936.89
139	3.4	6	0.288	132.9708	805.09
140	2.95	6.5	0.311	150.5810	733.17
141	3.2	6	0.288	134.4294	776.03
142	2.75	6.5	0.311	152.5750	707.95
144	2.85	7	0.335	163.8770	655.53
145	3.35	7.5	0.360	168.0420	615.99
146	2.6	8	0.382	193.2456	550.79
147	2.85	5.5	0.263	127.7622	837.32

Validation Data 3

Run	R4	E	Mass	Stiffness	von Mises stress
4	3.4	6.5	0.312	143.8114	746.29
17	3.05	7.5	0.359	172.9914	622.02
33	2.7	6	0.286	141.2240	749.90
38	3.1	8	0.383	183.4468	583.50
49	2.6	5	0.238	118.6870	887.59
70	2.8	8	0.382	188.2700	564.23
82	2.85	7.5	0.359	176.0798	609.46
96	3.5	5.5	0.264	119.6324	847.45
111	2.55	6.5	0.310	157.3218	670.40
136	3.3	7	0.336	158.4448	680.26
142	2.75	6.5	0.311	152.5750	707.95
147	2.85	5.5	0.263	127.7622	837.32

Testing Data 4

Run	R_4	E	Mass	Stiffness	von Mises stress
5	2.95	6	0.287	138.4258	791.14
11	3.25	8	0.384	180.6200	565.70
16	3.35	6.5	0.312	145.5014	727.56
21	3.3	5	0.240	110.0384	930.75
23	2.75	5.5	0.263	128.7752	836.18
33	2.7	6	0.286	141.2240	749.90
38	3.1	8	0.383	183.4468	583.50
44	2.5	6	0.286	145.5800	762.25
49	2.6	5	0.238	118.6870	887.59
53	2.9	6.5	0.311	150.6446	740.36
59	3	8	0.383	185.8890	585.05
67	2.65	5.5	0.262	131.5926	820.30
75	3.45	8	0.385	179.3320	592.74
92	2.8	5.5	0.263	127.7550	839.06
108	2.85	6.5	0.311	151.7378	708.15
114	3.15	7	0.336	158.8250	671.77
109	3.4	7	0.336	155.9114	691.56
104	2.65	6.5	0.310	156.2832	691.61
126	2.85	6	0.287	139.7592	766.89
57	3.05	5.5	0.263	126.0264	793.82
115	2.55	5.5	0.262	132.4640	791.97
54	2.8	7.5	0.359	176.1000	610.52
29	3.3	5.5	0.264	122.0708	846.70
121	3.15	6.5	0.312	148.4546	667.42

136	3.3	7	0.336	158.4448	680.26
85	3.4	5.5	0.264	120.9196	842.07
144	2.85	7	0.335	163.8770	655.53
146	2.6	8	0.382	193.2456	550.79
47	2.65	5	0.239	118.5552	923.91
140	2.95	6.5	0.311	150.5810	733.17

Training Data 4					
Run	**R4**	**E**	**Mass**	**Stiffness**	**von Mises stress**
1	2.8	7	0.335	163.8864	656.70
2	3.4	5	0.240	110.0294	925.58
3	2.5	6.5	0.310	159.7752	706.14
4	3.4	6.5	0.312	143.8114	746.29
6	2.75	5	0.239	116.4776	920.33
7	2.5	5	0.238	120.3282	888.90
8	2.85	8	0.383	187.6808	563.18
9	3.45	7	0.336	156.9286	689.38
10	3.5	6	0.289	124.6784	771.73
12	2.55	7.5	0.358	182.9608	576.77
13	3.2	8	0.384	180.2974	567.21
14	3.45	6	0.288	133.1316	801.93
15	2.95	5	0.239	115.7516	896.07
17	3.05	7.5	0.359	172.9914	622.02
18	3.35	7	0.336	156.6476	662.24
19	2.6	5.5	0.263	130.2302	806.98
20	3.4	8	0.385	179.1174	594.38
22	2.5	5.5	0.262	134.3876	832.41
24	2.55	6	0.287	144.8926	725.11
25	3.15	5	0.240	112.3314	875.60
26	3.25	6.5	0.312	145.1746	711.84
27	3.35	6	0.288	133.3600	771.91
28	2.65	6	0.286	143.9418	750.72
30	3.25	5	0.240	110.8990	940.20
31	3.1	7	0.335	159.6730	669.58
32	2.9	7.5	0.359	174.8248	638.09
34	3	7.5	0.360	174.3716	633.74
35	2.65	7.5	0.358	181.4718	594.36
36	3.1	6.5	0.312	147.2514	693.58
37	3.45	7.5	0.360	166.1648	641.64
39	3	6	0.287	138.0014	793.47
40	3.1	7.5	0.359	171.5622	622.79
41	2.5	7	0.334	170.1458	629.84
42	2.55	5	0.238	120.1334	871.34
43	2.7	7	0.334	165.5972	639.49
45	3.05	8	0.383	184.5366	582.77
46	2.5	8	0.382	195.5856	540.94
48	3	7	0.335	161.8184	681.16
50	2.9	6	0.287	138.7382	798.88
51	3.35	5.5	0.264	121.9244	842.39
52	3.5	8	0.385	176.1510	565.61
55	2.9	7	0.335	162.6884	685.83
56	2.85	5	0.239	116.2382	960.24
58	2.75	8	0.382	190.7252	570.41
60	3.15	7.5	0.360	170.7166	624.83
61	3.5	7	0.337	153.3310	658.83
62	2.95	5.5	0.263	127.4184	814.65
63	3.15	8	0.384	182.4752	585.42
64	2.75	7	0.334	165.9786	664.18
65	3.25	5.5	0.264	122.0390	854.90
66	2.8	6.5	0.311	151.7436	709.46
68	2.7	8	0.382	190.2286	547.63

69	3.35	5	0.240	110.7192	930.13
70	2.8	8	0.382	188.2700	564.23
71	3.1	5.5	0.263	123.9622	831.88
72	3.05	5	0.239	113.5320	949.97
73	2.9	8	0.383	186.8866	589.10
74	2.65	7	0.334	168.7762	639.72
76	2.6	6.5	0.310	155.7388	683.51
77	3.35	8	0.384	179.6684	568.45
78	2.8	5	0.239	117.0556	936.57
79	2.6	6	0.286	143.4202	750.97
80	3.3	7.5	0.361	170.2522	632.74
81	3.1	5	0.239	112.8802	950.84
82	2.85	7.5	0.359	176.0798	609.46
83	3.45	5.5	0.264	121.6964	874.99
84	3.2	7.5	0.360	169.6968	605.81
86	3.25	6	0.288	127.4910	867.76
87	2.65	8	0.382	193.8756	549.98
88	3.2	6.5	0.312	145.9830	708.69
89	3.3	6.5	0.312	144.1444	707.61
90	2.6	7	0.334	168.1842	632.6
91	2.5	7.5	0.358	182.3114	585.19
93	3.5	7.5	0.361	166.8786	631.00
94	3.25	7	0.336	156.7768	659.22
95	2.7	7.5	0.358	177.9256	594.08
96	3.5	5.5	0.264	119.6324	847.45
97	3.25	7.5	0.360	168.4784	613.11
98	2.95	8	0.383	187.7454	547.73
99	3.2	7	0.336	157.9402	651.55
100	3.3	8	0.384	179.7242	592.71
101	3.3	6	0.289	132.7306	775.78
102	3.05	6	0.287	137.8424	726.61
103	3	5.5	0.263	128.1936	855.21
105	2.9	5.5	0.263	126.8298	872.15
106	3.45	5	0.240	110.3502	961.80
107	2.95	7	0.335	163.4206	639.06
110	3.5	6.5	0.312	142.1230	710.70
111	2.55	6.5	0.310	157.3218	670.40
112	3.4	7.5	0.360	167.5320	643.57
113	2.7	5.5	0.263	129.0918	819.55
116	3.45	6.5	0.312	142.5400	743.79
117	2.75	6	0.287	140.5116	765.33
118	2.95	7.5	0.359	175.5990	594.09
119	2.55	8	0.382	195.1596	531.04
120	3.5	5	0.240	114.6010	916.62
122	3.2	5	0.240	111.6532	926.66
123	2.8	6	0.287	139.7514	768.44
124	3.05	7	0.335	160.6122	668.79
125	2.55	7	0.334	169.8920	620.46
127	3.15	6	0.288	135.4476	728.40
128	3.1	6	0.287	135.5906	761.93
129	3	6.5	0.311	149.7670	735.31
130	2.6	7.5	0.358	182.8158	588.19
131	2.9	5	0.239	115.1720	870.20
132	2.75	7.5	0.358	178.3474	617.10
133	3.15	5.5	0.264	123.8326	795.67
134	3.2	5.5	0.264	122.8984	847.08
135	3	5	0.239	116.2438	940.54
137	2.7	6.5	0.310	153.3264	691.45
138	2.7	5	0.239	117.9100	936.89
139	3.4	6	0.288	132.9708	805.09
141	3.2	6	0.288	134.4294	776.03
142	2.75	6.5	0.311	152.5750	707.95
143	3.05	6.5	0.312	149.6866	665.70
145	3.35	7.5	0.360	168.0420	615.99

147	2.85	5.5	0.263	127.7622	837.32

Validation Data 4					
Run	**R4**	**E**	**Mass**	**Stiffness**	**von Mises stress**
2	3.40	5	0.240	110.0294	925.58
9	3.45	7	0.336	156.9286	689.38
24	2.55	6	0.287	144.8926	725.11
77	3.35	8	0.384	179.6684	568.45
88	3.20	6.5	0.312	145.9830	708.69
95	2.70	7.5	0.358	177.9256	594.08
123	2.80	6	0.287	139.7514	768.44
131	2.90	5	0.239	115.1720	870.20
133	3.15	5.5	0.264	123.8326	795.67
135	3.00	5	0.239	116.2438	940.54
137	2.70	6.5	0.310	153.3264	691.45
102	3.05	6	0.287	137.8424	726.61

Testing Data 5					
	R_4	**E**	**Mass**	**Stiffness**	**von Mises stress**
6	2.75	5	0.239	116.4776	920.33
14	3.45	6	0.288	133.1316	801.93
17	3.05	7.5	0.359	172.9914	622.02
18	3.35	7	0.336	156.6476	662.24
26	3.25	6.5	0.312	145.1746	711.84
30	3.25	5	0.240	110.8990	940.20
36	3.1	6.5	0.312	147.2514	693.58
40	3.1	7.5	0.359	171.5622	622.79
43	2.7	7	0.334	165.5972	639.49
48	3	7	0.335	161.8184	681.16
52	3.5	8	0.385	176.1510	565.61
58	2.75	8	0.382	190.7252	570.41
61	3.5	7	0.337	153.3310	658.83
71	3.1	5.5	0.263	123.9622	831.88
72	3.05	5	0.239	113.5320	949.97
77	3.35	8	0.384	179.6684	568.45
91	2.5	7.5	0.358	182.3114	585.19
96	3.5	5.5	0.264	119.6324	847.45
101	3.3	6	0.289	132.7306	775.78
106	3.45	5	0.240	110.3502	961.80
112	3.4	7.5	0.360	167.5320	643.57
118	2.95	7.5	0.359	175.5990	594.09
119	2.55	8	0.382	195.1596	531.04
125	2.55	7	0.334	169.8920	620.46
127	3.15	6	0.288	135.4476	728.40
131	2.9	5	0.239	115.1720	870.20
138	2.7	5	0.239	117.9100	936.89

Training Data 5					
	R4	**E**	**Mass**	**Stiffness**	**von Mises stress**
1	2.8	7	0.335	163.8864	656.70
2	3.4	5	0.240	110.0294	925.58
3	2.5	6.5	0.310	159.7752	706.14
4	3.4	6.5	0.312	143.8114	746.29
5	2.95	6	0.287	138.4258	791.14
7	2.5	5	0.238	120.3282	888.90
8	2.85	8	0.383	187.6808	563.18
9	3.45	7	0.336	156.9286	689.38
10	3.5	6	0.289	124.6784	771.73
11	3.25	8	0.384	180.6200	565.70
12	2.55	7.5	0.358	182.9608	576.77
13	3.2	8	0.384	180.2974	567.21
15	2.95	5	0.239	115.7516	896.07
16	3.35	6.5	0.312	145.5014	727.56
19	2.6	5.5	0.263	130.2302	806.98
20	3.4	8	0.385	179.1174	594.38
21	3.3	5	0.240	110.0384	930.75
22	2.5	5.5	0.262	134.3876	832.41
23	2.75	5.5	0.263	128.7752	836.18
24	2.55	6	0.287	144.8926	725.11
25	3.15	5	0.240	112.3314	875.60
27	3.35	6	0.288	133.3600	771.91
28	2.65	6	0.286	143.9418	750.72
29	3.3	5.5	0.264	122.0708	846.70
31	3.1	7	0.335	159.6730	669.58
32	2.9	7.5	0.359	174.8248	638.09
33	2.7	6	0.286	141.2240	749.90
34	3	7.5	0.360	174.3716	633.74
35	2.65	7.5	0.358	181.4718	594.36
37	3.45	7.5	0.360	166.1648	641.64
38	3.1	8	0.383	183.4468	583.50
39	3	6	0.287	138.0014	793.47
41	2.5	7	0.334	170.1458	629.84
42	2.55	5	0.238	120.1334	871.34
44	2.5	6	0.286	145.5800	762.25
45	3.05	8	0.383	184.5366	582.77
46	2.5	8	0.382	195.5856	540.94
47	2.65	5	0.239	118.5552	923.91
49	2.6	5	0.238	118.6870	887.59
50	2.9	6	0.287	138.7382	798.88
51	3.35	5.5	0.264	121.9244	842.39
53	2.9	6.5	0.311	150.6446	740.36
54	2.8	7.5	0.359	176.1000	610.52
55	2.9	7	0.335	162.6884	685.83
56	2.85	5	0.239	116.2382	960.24
57	3.05	5.5	0.263	126.0264	793.82
59	3	8	0.383	185.8890	585.05
60	3.15	7.5	0.360	170.7166	624.83
62	2.95	5.5	0.263	127.4184	814.65
63	3.15	8	0.384	182.4752	585.42
64	2.75	7	0.334	165.9786	664.18
65	3.25	5.5	0.264	122.0390	854.90
66	2.8	6.5	0.311	151.7436	709.46
67	2.65	5.5	0.262	131.5926	820.30
68	2.7	8	0.382	190.2286	547.63
69	3.35	5	0.240	110.7192	930.13
70	2.8	8	0.382	188.2700	564.23
73	2.9	8	0.383	186.8866	589.10
74	2.65	7	0.334	168.7762	639.72
75	3.45	8	0.385	179.3320	592.74
76	2.6	6.5	0.310	155.7388	683.51

78	2.8	5	0.239	117.0556	936.57
79	2.6	6	0.286	143.4202	750.97
80	3.3	7.5	0.361	170.2522	632.74
81	3.1	5	0.239	112.8802	950.84
82	2.85	7.5	0.359	176.0798	609.46
83	3.45	5.5	0.264	121.6964	874.99
84	3.2	7.5	0.360	169.6968	605.81
85	3.4	5.5	0.264	120.9196	842.07
86	3.25	6	0.288	127.4910	867.76
87	2.65	8	0.382	193.8756	549.98
88	3.2	6.5	0.312	145.9830	708.69
89	3.3	6.5	0.312	144.1444	707.61
90	2.6	7	0.334	168.1842	632.6
92	2.8	5.5	0.263	127.7550	839.06
93	3.5	7.5	0.361	166.8786	631.00
94	3.25	7	0.336	156.7768	659.22
95	2.7	7.5	0.358	177.9256	594.08
97	3.25	7.5	0.360	168.4784	613.11
98	2.95	8	0.383	187.7454	547.73
99	3.2	7	0.336	157.9402	651.55
100	3.3	8	0.384	179.7242	592.71
102	3.05	6	0.287	137.8424	726.61
103	3	5.5	0.263	128.1936	855.21
104	2.65	6.5	0.310	156.2832	691.61
105	2.9	5.5	0.263	126.8298	872.15
107	2.95	7	0.335	163.4206	639.06
108	2.85	6.5	0.311	151.7378	708.15
109	3.4	7	0.336	155.9114	691.56
110	3.5	6.5	0.312	142.1230	710.70
111	2.55	6.5	0.310	157.3218	670.40
113	2.7	5.5	0.263	129.0918	819.55
114	3.15	7	0.336	158.8250	671.77
115	2.55	5.5	0.262	132.4640	791.97
116	3.45	6.5	0.312	142.5400	743.79
117	2.75	6	0.287	140.5116	765.33
120	3.5	5	0.240	114.6010	916.62
121	3.15	6.5	0.312	148.4546	667.42
122	3.2	5	0.240	111.6532	926.66
123	2.8	6	0.287	139.7514	768.44
124	3.05	7	0.335	160.6122	668.79
126	2.85	6	0.287	139.7592	766.89
128	3.1	6	0.287	135.5906	761.93
129	3	6.5	0.311	149.7670	735.31
130	2.6	7.5	0.358	182.8158	588.19
132	2.75	7.5	0.358	178.3474	617.10
133	3.15	5.5	0.264	123.8326	795.67
134	3.2	5.5	0.264	122.8984	847.08
135	3	5	0.239	116.2438	940.54
136	3.3	7	0.336	158.4448	680.26
137	2.7	6.5	0.310	153.3264	691.45
139	3.4	6	0.288	132.9708	805.09
140	2.95	6.5	0.311	150.5810	733.17
141	3.2	6	0.288	134.4294	776.03
142	2.75	6.5	0.311	152.5750	707.95
143	3.05	6.5	0.312	149.6866	665.70
144	2.85	7	0.335	163.8770	655.53
145	3.35	7.5	0.360	168.0420	615.99
146	2.6	8	0.382	193.2456	550.79
147	2.85	5.5	0.263	127.7622	837.32

Validation Data 5					
	R4	**E**	**Mass**	**Stiffness**	**von Mises stress**
3	2.5	6.5	0.310	159.7752	706.14
8	2.85	8	0.383	187.6808	563.18
15	2.95	5	0.239	115.7516	896.07
25	3.15	5	0.240	112.3314	875.60
35	2.65	7.5	0.358	181.4718	594.36
39	3	6	0.287	138.0014	793.47
51	3.35	5.5	0.264	121.9244	842.39
94	3.25	7	0.336	156.7768	659.22
105	2.9	5.5	0.263	126.8298	872.15
117	2.75	6	0.287	140.5116	765.33
120	3.5	5	0.240	114.6010	916.62
144	2.85	7	0.335	163.8770	655.53

APPENDIX B

K-FOLD CROSS VALIDATION RESULTS OF THE NEURO-REGRESSION MODEL FOR MASS

Models	R^2 training	R^2 training Adjusted	R^2 testing	R^2 validation	Maximum	Minimum
L1	0.999999	0.999999	0.999942	0.999917	0.384793	0.237745
L2	0.999999	0.999999	0.999933	0.999941	0.385148	0.237448
L3	0.999999	0.999999	0.999942	0.999938	0.384804	0.237737
L4	0.999999	0.999999	0.99995	0.999926	0.385172	0.237456
L5	0.999999	0.999999	0.999942	0.999968	0.384796	0.237731
LR1	0.999999	0.999999	0.999995	0.999925	0.385649	0.238027
LR2	0.999999	0.999999	0.999945	0.999932	0.385883	0.238074
LR3	0.999999	0.999999	0.999936	0.999943	0.385086	0.238157
LR4	0.999999	0.999999	0.999951	0.99993	0.386165	0.237987
LR5	0.999999	0.999999	0.999943	0.999976	0.386625	0.23805
SON1	0.999999	0.999999	0.999941	0.999914	0.400630	0.235062
SON2	0.999999	0.999999	0.999994	0.999922	0.399337	0.235338
SON3	0.999999	0.999999	0.999941	0.999952	0.395234	0.237626
SON4	0.999999	0.999999	0.999958	0.999938	0.394482	0.236526
SON5	0.99999	0.99999	0.999933	0.999977	0.389162	0.236269
SONR1	0.999999	0.999999	0.999921	0.999922	0.398438	0.225608
~~**SONR2**~~	~~0.999999~~	~~0.999999~~	~~0.999931~~	~~0.999965~~	~~$3.4617*10^6$~~	~~0.23662~~
~~**SONR3**~~	~~0.999999~~	~~0.999999~~	~~0.999942~~	~~0.999948~~	~~$6.82006*10^7$~~	~~$-5.61*10^7$~~
~~**SONR4**~~	~~0.999999~~	~~0.999999~~	~~0.999947~~	~~0.999955~~	~~$6.01127*10^6$~~	~~-61440.6~~
~~**SONR5**~~	~~0.999999~~	~~0.999999~~	~~0.999948~~	~~0.999979~~	~~$6.37747 *10^8$~~	~~0.234656~~
FOTN1	0.999587	0.999512	0.981026	0.97782	0.384420	0.239835
FOTN2	0.999579	0.999503	0.981347	0.977508	0.383857	0.239658
FOTN3	0.999582	0.999506	0.978664	0.984523	0.386688	0.238188
FOTN4	0.999582	0.999505	0.980025	0.979306	0.384452	0.235742
FOTN5	0.999595	0.999523	0.97872	0.97805	0.387336	0.233994
FOTNR1	0.999999	0.999999	0.999934	0.999916	0.38917	0.229502
FOTNR2	0.999999	0.999999	0.999942	0.999907	0.387093	0.231509
~~**FOTNR3**~~	~~0.991208~~	~~0.989609~~	~~0.658886~~	~~0.55314~~	~~180.696~~	~~0.22007~~
FOTNR4	0.999999	0.999999	0.999941	0.999927	0.38798	0.232181
FOTNR5	0.999999	0.999999	0.999908	0.999967	0.38796	0.230908
~~**SOTN1**~~	~~0.999996~~	~~0.999981~~	~~0.999513~~	~~0.99973~~	~~5.6729~~	~~-4.68107~~
~~**SOTN2**~~	~~0.999995~~	~~0.999979~~	~~0.999714~~	~~0.999047~~	~~5.39699~~	~~-4.28576~~
~~**SOTN3**~~	~~0.999996~~	~~0.999982~~	~~0.999552~~	~~0.999776~~	~~9.50243~~	~~-8.46073~~
~~**SOTN4**~~	~~0.999995~~	~~0.99998~~	~~0.999597~~	~~0.999801~~	~~5.50219~~	~~-0.75209~~
~~**SOTN5**~~	~~0.999995~~	~~0.999982~~	~~-12.2377~~	~~0.999759~~	~~2.69464~~	~~-3.24823~~
~~**SOTNR1**~~	~~1~~	~~0.999999~~	~~0.999789~~	~~0.99995~~	~~$2.35075*10^6$~~	~~$-3.05*10^7$~~
~~**SOTNR2**~~	~~1~~	~~0.999998~~	~~0.999895~~	~~0.999964~~	~~$2.4691*10^8$~~	~~$-1.18*10^9$~~
~~**SOTNR3**~~	~~1~~	~~0.999999~~	~~0.989102~~	~~0.999992~~	~~$1.0058*10^7$~~	~~$-4.4*10^7$~~
~~**SOTNR4**~~	~~1~~	~~0.999998~~	~~0.997525~~	~~0.999985~~	~~$1.59807*10^9$~~	~~$-1.42*10^9$~~
~~**SOTNR5**~~	~~1~~	~~0.999998~~	~~0.997483~~	~~0.999989~~	~~0.402975~~	~~$-7.62*10^8$~~
FOLN1	0.999894	0.999884	0.995201	0.994795	0.383486	0.230465
FOLN2	0.999891	0.999881	0.99531	0.995809	0.380905	0.232341
FOLN3	0.999892	0.999882	0.994632	0.995418	0.380084	0.232210
FOLN4	0.999897	0.999887	0.994261	0.994775	0.382104	0.231715
FOLN5	0.999894	0.999885	0.995481	0.994894	0.383315	0.230110
FOLNR1	0.999999	0.999999	0.999947	0.999924	0.385488	0.237966
FOLNR2	0.999999	0.999999	0.999945	0.999932	0.385849	0.238023
FOLNR3	0.999999	0.999999	0.99994	0.999933	0.385040	0.238075
FOLNR4	0.999999	0.999999	0.999946	0.999937	0.386026	0.23800
FOLNR5	0.999999	0.999999	0.999943	0.999976	0.386625	0.23805
SOLN1	0.999999	0.999998	0.999924	0.999909	0.399425	0.235905
SOLN2	0.999999	0.999998	0.999928	0.999908	0.396206	0.235799

SOLN3	0.999999	0.999998	0.99992	0.999955	0.393494	0.238034
SOLN4	0.999999	0.999998	0.999949	0.999919	0.392505	0.236782
SOLN5	0.999999	0.999998	0.999914	0.999965	0.390886	0.237346
SOLNR1	~~0.999999~~	~~0.999999~~	~~0.999909~~	~~0.999925~~	~~$1.70795*10^6$~~	~~0.236077~~
SOLNR2	0.999999	0.999999	0.999942	0.999933	0.388172	0.233767
SOLNR3	~~0.999999~~	~~0.999999~~	~~0.999934~~	~~0.999952~~	~~69793.2~~	~~-230245~~
SOLNR4	~~0.999999~~	~~0.999999~~	~~0.999934~~	~~0.999949~~	~~0.384861~~	~~-114978~~
SOLNR5	~~0.999999~~	~~0.999999~~	~~0.999295~~	~~0.999977~~	~~684111~~	~~0.229529~~

APPENDIX C

K-FOLD CROSS VALIDATION RESULTS OF THE NEURO-REGRESSION MODEL FOR STIFFNESS

Models	R^2 training	R^2 training Adjusted	R^2 testing	R^2 validation	Maximum	Minimum
L1	0.999937	0.999931	0.992763	0.997713	194.749	106.052
L2	0.999912	0.999904	0.995187	0.991430	193.979	106.807
L3	0.999900	0.999891	0.997358	0.998608	193.933	106.689
L4	0.999894	0.999884	0.998327	0.997175	194.122	106.833
L5	0.999907	0.999899	0.996349	0.990546	196.138	105.961
LR1	0.999961	0.999957	0.994454	0.999048	196.019	107.559
LR2	0.999944	0.999938	0.996320	0.991364	199.157	109.12
LR3	0.999933	0.999927	0.998143	0.998914	199.017	109.069
LR4	0.999931	0.999924	0.998543	0.997308	199.128	109.265
LR5	0.999931	0.999925	0.998265	0.994745	198.989	108.216
SON1	0.999969	0.999959	0.994417	0.999011	201.566	61.6211
SON2	0.999948	0.99993	0.996656	0.991199	210.14	88.7842
SON3	0.999940	0.99992	0.998398	0.998792	199.801	72.5332
SON4	0.999937	0.999916	0.998765	0.998245	201.777	80.3779
SON5	0.999937	0.999916	0.995514	0.995368	201.052	79.6734
~~**SONR1**~~	~~0.999976~~	~~0.999967~~	~~0.994678~~	~~0.99913~~	~~$1.1991*10^{7}$~~	~~$-3.4124*10^{8}$~~
~~**SONR2**~~	~~0.999978~~	~~0.99997~~	~~0.968899~~	~~0.999329~~	~~200.891~~	~~$-1.5082*10^{8}$~~
~~**SONR3**~~	~~0.999972~~	~~0.999963~~	~~0.991636~~	~~0.999238~~	~~$1.07212*10^{9}$~~	~~$-4.317*10^{10}$~~
~~**SONR4**~~	~~0.999968~~	~~0.999956~~	~~0.996834~~	~~0.999051~~	~~$2.2644*10^{10}$~~	~~$-1.7984*10^{9}$~~
~~**SONR5**~~	~~0.999961~~	~~0.999949~~	~~0.910433~~	~~0.999323~~	~~200.896~~	~~$-2.5931*10^{8}$~~
FOTN1	0.999546	0.999464	0.983277	0.968752	201.518	102.459
FOTN2	0.999535	0.999451	0.980785	0.97756	200.37	103.853
FOTN3	0.999554	0.999473	0.97805	0.983021	201.396	103.309
FOTN4	0.999549	0.999467	0.977797	0.983653	200.609	103.458
FOTN5	0.999563	0.999486	0.975739	0.985449	199.358	102.294
FOTNR1	0.999945	0.999934	0.992463	0.997256	203.540	80.1590
FOTNR2	0.999922	0.999908	0.994731	0.988181	202.456	88.4577
FOTNR3	0.999910	0.999844	0.99665	0.998141	205.021	79.9946
~~**FOTNR4**~~	~~0.976531~~	~~0.972264~~	~~0.186057~~	~~0.109471~~	~~26460.6~~	~~$-5.812*10^{11}$~~
~~**FOTNR5**~~	~~0.999908~~	~~0.999892~~	~~0.997039~~	~~0.995671~~	~~198.4430~~	~~46.2563~~
~~**SOTN1**~~	~~0.999974~~	~~0.999887~~	~~0.966364~~	~~0.999678~~	~~33548.3~~	~~-10402.8~~
~~**SOTN2**~~	~~0.999962~~	~~0.999835~~	~~0.996938~~	~~0.989484~~	~~13569~~	~~-20055.1~~
~~**SOTN3**~~	~~0.999962~~	~~0.999835~~	~~0.996891~~	~~0.999133~~	~~18829.2~~	~~-23916.7~~
~~**SOTN4**~~	~~0.999956~~	~~0.999809~~	~~0.998225~~	~~0.998597~~	~~11331.9~~	~~-16770.4~~
~~**SOTN5**~~	~~0.999958~~	~~0.999833~~	~~-161.548~~	~~0.998321~~	~~9665.02~~	~~-2425.93~~
~~**SOTNR1**~~	~~0.999993~~	~~0.999968~~	~~0.986052~~	~~0.999602~~	~~$2.08035*10^{9}$~~	~~$-2.126*10^{11}$~~
~~**SOTNR2**~~	~~0.999981~~	~~0.999918~~	~~0.994054~~	~~0.999314~~	~~269.098~~	~~-3.40837~~
~~**SOTNR3**~~	~~0.999993~~	~~0.999968~~	~~0.970092~~	~~0.999292~~	~~$1.93599*10^{11}$~~	~~$-7.6815*10^{9}$~~
~~**SOTNR4**~~	~~0.999989~~	~~0.999953~~	~~0.993240~~	~~0.999292~~	~~$7.41799*10^{11}$~~	~~$-3.0239*10^{9}$~~
~~**SOTNR5**~~	~~0.999989~~	~~0.999954~~	~~-2.334101~~	~~0.999797~~	~~201.991~~	~~$-1.0579*10^{9}$~~
FOLN1	0.999809	0.999792	0.98443	0.994508	193.534	103.392
FOLN2	0.999767	0.999745	0.987697	0.985022	191.972	104.597
FOLN3	0.999746	0.999722	0.991532	0.994622	191.298	104.677

FOLN4	0.999736	0.999711	0.992996	0.988297	193.005	104.011
FOLN5	0.999758	0.999736	0.991266	0.979791	0.194.463	103.179
FOLNR1	0.999961	0.999958	0.994242	0.999033	196.409	107.244
FOLNR2	0.999942	0.999937	0.996316	0.991230	198.949	109.002
FOLNR3	0.999932	0.999926	0.998171	0.998907	198.563	108.684
FOLNR4	0.999929	0.999922	0.998636	0.997517	198.494	108.851
FOLNR5	0.99993	0.999923	0.998451	0.994337	198.495	107.792
SOLN1	~~0.99997~~	~~0.99996~~	~~0.994691~~	~~0.998992~~	~~201.42~~	~~61.2381~~
SOLN2	0.99995	0.999932	0.996816	0.991521	209.902	94.0656
SOLN3	0.999943	0.999923	0.998395	0.998909	199.36	73.0173
SOLN4	0.999941	0.99992	0.998706	0.998232	200.622	81.2128
SOLN5	0.999994	0.99992	0.996905	0.996107	190.068	89.3166
SOLNR1	~~0.999976~~	~~0.999968~~	~~0.994701~~	~~0.999168~~	~~$2.66892*10^7$~~	~~$-1.6384*10^8$~~
SOLNR2	~~0.999978~~	~~0.99997~~	~~0.957503~~	~~0.999317~~	~~$8.6615*10^7$~~	~~$-8.8411*10^6$~~
SOLNR3	~~0.999977~~	~~0.999969~~	~~0.990501~~	~~0.999239~~	~~$4.35845*10^8$~~	~~108.286~~
SOLNR4	~~0.999968~~	~~0.999956~~	~~0.998956~~	~~0.998742~~	~~$2.03025*10^7$~~	~~$-1.3808*10^8$~~
SOLNR5	0.99996	0.999946	0.993389	0.999218	205.671	70.6748